FSL Forum

Forecast Systems Laboratory, Boulder, Colorado December 2003

Cycled Snow Variables in the RUC Coupled Data Assimilation System – *By Tatiana Smirnova, Stanley Benjamin, John Brown, and Dongsoo Kim*

Introduction

Accurate estimation of snow water equivalent over the U.S. and adjacent areas is critical for subsequent seasonal and short-range atmospheric and hydrological model forecasts. It is also essential for a variety of important water planning activities in the western U.S., including agriculture, recreation, and public use in cities. It is difficult to estimate precipitation in much of the western U.S. due to complex terrain. For example, quantitative precipitation estimates (QPEs) based only on observations are often deficient in the cold season, especially for orographic precipitation. Recent approaches toward development of land data assimilation systems and precipitation assimilation used in the National Centers for Environmental Prediction (NCEP) Regional Reanalysis are largely focused on improvements in the specification of the land-surface state for the warm season, but are not generally applicable to the problem of snow water equivalent initialization.

The best QPEs now available – those used to drive the current NOAA/NASA Land Data Assimilation System (LDAS) – are taken from the NOAA Climate Prediction Center's 24-hour gauge precipitation analysis. These QPEs are allocated into hourly amounts using the NCEP/National Weather Service (NWS) Stage IV hourly precipitation analysis. However, this analysis has limita-

Dr. Adrian Marroquin 1943–2003

Adrian Marroquin of the Forecast Systems Laboratory passed away on September 30, 2003, from complications of cancer. Adrian worked at FSL as a CIRA Research Scientist for the past 18 years, specializing in the areas of:

- Formulation and computer implementation of two- and three-dimensional numerical model dynamics for synoptic and mesoscale meteorological applications
- Computer implementation and verification of turbulence, convection, and radiation parameterizations and boundary layer formulations for numerical weather prediction models
- Dynamic meteorology and numerical analysis with applications to weather analysis and forecasting.

Prior to 1985, Adrian worked at NCAR, in Boulder, as a CIRES Research Associate and a Postdoctoral Fellow. He also taught undergraduate physics and mathematics, and primary school students in his home country of Colombia. His academic training included a B.S. in Mathematical Physics from the University Libre de Colombia, Bogota, Colombia in 1969; an M.S. in Physics from Florida Atlantic University, Boca Raton, Florida in 1973; and a Ph.D. in Atmospheric Sciences from the New Mexico Institute of Mining and Technology, Socorro, New Mexico in 1981.

Aside from his professional contributions, Adrian will be remembered for his goodwill and the courage he showed in the face of his terrible illness – without pessimism, fear, or resentment.

Cycled Snow Variables in the RUC CDAS *(continued from the cover)*

tions, including insufficient density of rain gauges in the mountainous areas, day-to-day variations of the reporting gauges, errors in 24-hour time variations, inaccuracies of gauge observations for frozen precipitation, and difficulties in assigning the precipitation phase.

FSL has developed a four-dimensional Coupled Data Assimilation System (CDAS) using a forward, full-physics model in which the precipitation and clouds are an optimized combination of observed and forecast fields to reduce the negative effects from the limitations of the precipitation analysis mentioned above. Based on the Rapid Update Cycle (RUC) model assimilation system, CDAS updates the precipitation and cloud fields hourly using GOES cloud-top pressure, NEXRAD radar reflectivity, lightning data, and GPS precipitable water. The RUC CDAS is designed specifically to provide improved quantitative precipitation estimates for orographic precipitation in the cold season, leading to more accurate cycling of the snow state over the U.S.

Description of the RUC CDAS Forecast Model

The RUC CDAS is a coupled land-surface/atmospheric model with an hourly assimilation cycle including radar reflectivity, satellite, and other remotely sensed data to update the three-dimensional hydrometeor fields evolving through explicit mixed-phase cloud microphysics in the RUC model. The RUC is the only NCEP operational model that currently provides explicit forecasts of precipitation in liquid and solid phases. Model precipitation has consistent spatial variability from day to day, and could therefore be used to mitigate the effect of missing stations. It is also likely to provide better orographic precipitation, especially if constrained by satellite, radar, and even gauges in the CDAS optimization. Because of the 1-hour updating used in the RUC, the model is also constrained by the hourly input of surface observations to have fairly accurate short-term forecasts of low-level temperatures. The explicit microphysics and representation of the near-surface thermal structure of the atmosphere in the RUC may be expected to provide better information on precipitation type than that available from an estimate of surface temperature alone.

Precipitation Physics

Explicit Mixed-Phase Cloud Microphysics – The RUC CDAS uses the improved version (Thomspon et al. 2003) of the level 4 mixed-phase bulk microphysics scheme of Reisner et al. (1998). This scheme was originally developed for MM5, and has been used operationally in the RUC for the past 5 years (Brown et al. 2000). The mixing ratios of 5 hydrometeor species are explicitly predicted: cloud water, rain water, cloud ice, snow and graupel (the latter formed by riming of ice or snow, or by freezing of rain drops, in which circumstance it might be regarded as ice pellets or sleet); the number concentration of cloud ice particles is also predicted. The explicit prediction of these hydrometeors allows direct feedback between simulated clouds and long- and short-wave radiation. The RUC/MM5 explicit microphysics also allows an explicit forecast of snow and snow water equivalent, rather than a diagnostic for precipitation phase type based on temperature.

The original version of the scheme used in the RUC tended to strongly overpredict graupel under certain conditions, leading to unrealistic distributions of surface-precipitation type. The new version, now operational in the RUC, exhibits much improved predictions of supercooled liquid water, as well as of precipitation type at ground level. Continued enhancements to the RUC microphysics scheme are expected, with a focus on ice nucleation and explicit prediction of freezing drizzle in weakly forced synoptic situations.

Ensemble Cumulus Parameterization – A new convective parameterization of Grell and Devenyi (2002) is now used in the RUC. The original scheme was first expanded to include lateral entrainment and detrainment, including detrainment of cloud water and ice to the microphysics scheme mentioned above. In addition, the scheme draws on uncertainties in convective parameterizations by allowing an ensemble of various closure and feedback assumptions (related to how the explicitly predicted flow modifies the parameterized convection, which in turn modifies the environment) to be used every time the parameterization is called.

The four main groups of closures that are used in the

RUC application are based on removal of convective available potential energy (CAPE), destabilization effects, moisture convergence, and low-level vertical velocity. These four groups are then perturbed by 27 sensitive parameters related to feedback as well as strength of convection, which give a total of 108 ensemble members that contribute to the convective scheme. Output from the parameterization may be the ensemble mean, the most probable value, a probability density function, as well as other statistical values. Currently, only the ensemble mean is fed back to the dynamic model. The application of the Grell/Devenyi convective scheme in the RUC model also includes a removal of the negative buoyancy capping constraint at the initial time of each model forecast in areas where the GOES sounder's effective cloud amount indicates that convection may be present. This technique can aid the initiation of modeled convection at grid points where positive CAPE is observed, although it cannot create positive CAPE. In addition, an upstream dependence is introduced through relaxation of static stability (convective inhibition) constraints at adjacent downstream points based on 0–5 km mean wind, and through allowance of the downdraft mass flux at the previous convective timestep to force convection at the downstream location.

Land-Surface Model in the RUC

The sophistication of the RUC/MAPS land-surface model (LSM, Smirnova et al. 2000, 1998) has also grown in the past few years, and is now used in the operational RUC at NCEP, in experimental real-time RUC runs at FSL, and in regional climate versions of the RUC and MM5 models. The RUC LSM has also made a strong performance in the Program for Intercomparison of Land-surface Process Models (PILPS, Schlosser et al. 1999) and in the intercomparison of the snow models (SNOWMIP, Etchevers et al. 2003). The RUC LSM contains multilevel soil and snow models, and treatment of vegetation (Figure 1), all operating on the same horizontal grid as the atmospheric model. Heat and moisture transfer equations are solved at six levels for each soil column together with the energy and moisture budget equations for the ground surface, and an implicit scheme is used for the computation of the surface fluxes. The energy and moisture budgets are applied to a thin layer spanning the ground surface and including both the soil and the atmosphere with corresponding heat capacities and densities. The RUC frozen soil parameterization considers latent heat of phase

In This Issue

Forecast Systems Laboratory
A.E. MacDonald, Director
FSL Website – *http://www.fsl.noaa.gov/*

Nita Fullerton, Writer/Editor
E-mail – *Nita.Fullerton@noaa.gov*
Phone: 303-497-6995

The *FSL Forum* is an occasional bulletin that orginates with NOAA's Forecast Systems Laboratory. Comments on published articles and suggestions for future articles are welcome from any interested individual or group. Forward all inquiries and address/subscription changes to Nita Fullerton at the above E-mail address or by using the last page of this issue (no additional postage is needed within the United States).

Cycled Snow Variables in the RUC CDAS *(continued)*

changes in soil by applying an apparent heat capacity, augmented to account for phase changes inside the soil, to the heat transfer equation in frozen soil in place of the volumetric heat capacity for unfrozen soil. The effect of ice in soil on water transport is also considered in formulating the hydraulic and diffusional conductivities.

Accumulation of precipitation at the surface, as well as its partitioning between liquid and solid phases, is provided by the mixed-phase cloud microphysics routine. In the RUC, the convective parameterization also contributes to the snow accumulation if the surface air temperature is at or below 0°C. With or without snow cover, surface runoff occurs if the rate at which liquid phase becomes available for infiltration at the ground surface exceeds the maximum infiltration rate. The solid phase in the form of snow or graupel (treated identically by the LSM) is accumulated on the ground/snow surface to subsequently affect soil hydrology and thermodynamics of the low atmosphere.

In the most recent version of the LSM implemented in the RUC, a number of improvements were achieved in the treatment of snow cover and frozen soil physics. These improvements include the allowance of the evolution of snow density as a function of snow age and depth, the potential for refreezing of melted water inside the snowpack, and simple representation of patchy snow through reduction of the albedo when the snow depth is small. If the snow layer is thinner than a 2-cm threshold, it is combined with the top soil layer to permit a more accurate solution of the energy budget. This strategy gives improved prediction of nighttime surface temperatures under clear conditions and melting of shallow snow cover. Another feature of the RUC LSM is an improved algorithm for frozen soil physics for spring thaw conditions.

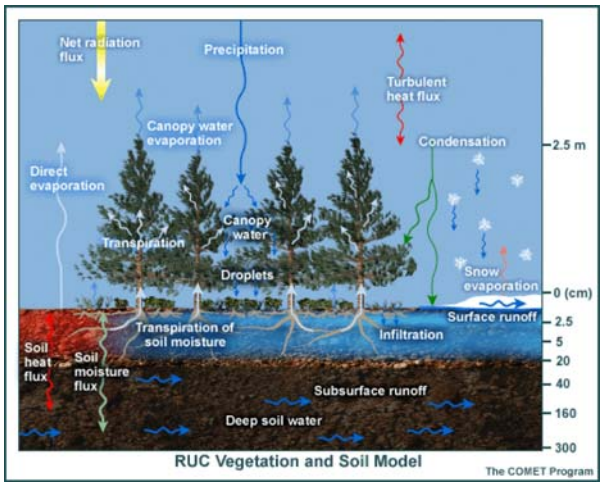

Figure 1. RUC/MAPS land-surface model.

These changes were tested off-line in a one-dimensional setting with the dataset from Valdai, Russia, and showed positive impact on the model performance. The evolution of snow density provides a more realistic representation of processes in snow, especially when fresh snow is falling onto the bare soil or an existing snowpack, and improves simulation of the snow-melting season (Figure 2). The effects of patchy snow cover were tested in the experimental version of RUC and improved prediction of the nighttime surface temperatures under clear conditions as well as melting of shallow snow cover.

More accurate predictions of the surface temperature have positive effects on the verification of 2-m temperature (Figure 3). We will also investigate adding improvements to the vegetation treatment such as interactive vegetation in the RUC land-surface model to improve its capability for regional climate prediction and simulation.

In applications of the RUC LSM in current and previous versions of the RUC, volumetric soil moisture and soil temperature are cycled at the six soil model levels, as well as canopy water, snow depth, and snow temperature. Cycling of the snow temperature of the second layer (where needed) is also performed. The RUC continues to be unique among operational models in its specification of snow cover and snow water content through cycling (Smirnova et al. 2000). The 2-layer snow model in the RUC improves the evolution of these fields, especially in springtime, more accurately depicting the snow melting season and spring spike in total runoff.

Evaluation of the RUC CDAS

The RUC CDAS has a 20-km resolution, with high-resolution fixed surface fields from the USGS land-use

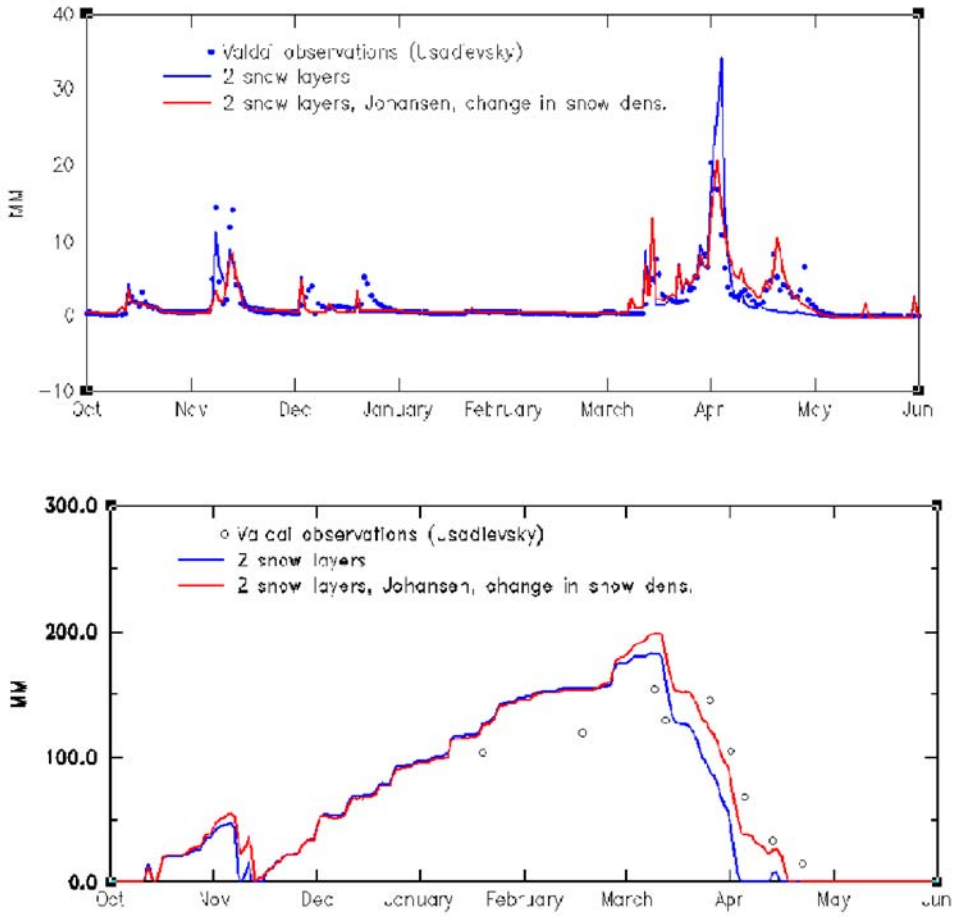

Figure 2. Results from one-dimensional simulations with the RUC/MAPS land-surface model for winter 1980–1981 for Valdai, Russia (PILPS 2D experiment, 18-year simulation). Results show improvement from allowing variability of snow density and adding the Johansen formulation for thermal conductivity. (a, above) Total runoff (millimeters) from top 1 meter of soil; (b, below) snow water equivalent (millimeters).

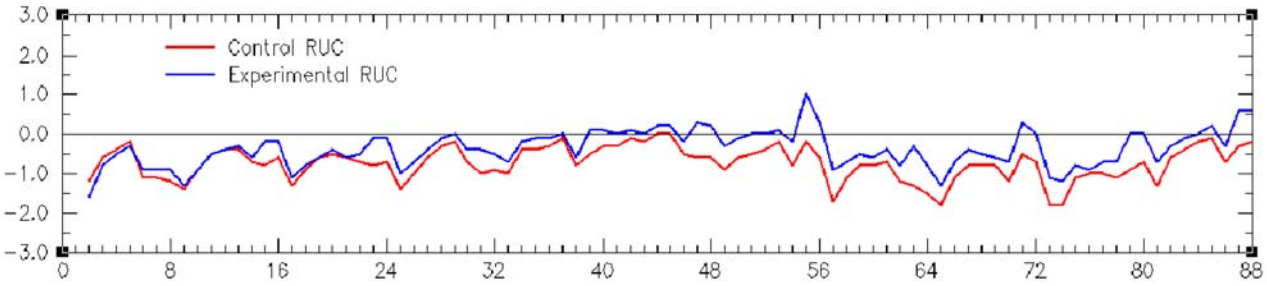

Figure 3. Surface temperature biases (°C) from 3-hour forecasts for stations with the snow depth less than 10 centimeters averaged for the period 4–14 February 2001.

Cycled Snow Variables in the RUC CDAS *(continued)*

and STATSGO (State Soil Geographic database) soil types. This system has run in real time since April 2002. The RUC/MAPS system made a transition to a three-dimensional variational (3DVAR) analysis (Devenyi and Benjamin 2003) in spring 2003 replacing the previous optimal interpolation atmospheric analysis scheme. The primary reason for this change is because of the flexibility and rigor of the variational approach in assimilating data not directly forecast by the model (such as satellite radiances and radar radial winds). The RUC CDAS currently assimilates hourly data wind profiler data from the NOAA Profiler Network and the 915-MHz Boundary Layer Network, commercial aircraft (growing rapidly in volume over the U.S. and worldwide), surface stations and buoys, available radiosonde data, and GOES satellite-estimated cloud drift winds, precipitable water measurements, and cloud-top pressure. Assimilation of GPS integrated precipitable water measurements has undergone testing for three years with the RUC and also has been implemented operationally. The most critical recent improvements in RUC assimilation were done to the cloud and moisture analysis through the assimilation of satellite and radar data.

The RUC CDAS provides refinements refinements to the 0–1 hour precipitation forecasts that drive a land-surface climate in the model by accounting for errors in both observations and model precipitation forecasts. As a result, cycled soil moisture and snow water equivalent are improved compared to the operational RUC without assimilation of the radar, lightning, and GPS data. Most improvements occur from more accurate placement of predicted precipitation.

The impact of using the radar assimilation technique to modify 3D hydrometeor fields from the national mosaic 2-km resolution maximum reflectivity data has been regularly monitored and evaluated. The operational RUC20 – without radar reflectivity assimilation – is used as the control experiment.

The NCEP Stage II hourly QPE is used to verify the 3-hour accumulated precipitation, and quality controlled Stage IV is used for the verification of 24-hour accumulations. The Stage IV precipitation data, derived from NEXRAD reflectivity and gauge observations, are at 4-km resolution and include quality control. The original 4-km resolution Stage IV precipitation data are remapped to the RUC grid by taking the maximum value in the grid box to represent the grid point. The verification of accumulated forecast precipitation from eight 3-hour forecasts in RUC assimilation cycles over a 24-hour period is performed daily (see the example in Figure 4.)

A spatial correlation field was computed as a measure of precipitation verification. The spatial cross-correlation is a function of x-y displacement between two fields, QPF and QPE within a predetermined evaluation window (60 x 60 grid points on a 20-km grid, Figure 4d–f). The distance of maximum correlation to the center (zero displacement) is a measure of QPF phase error, and the maximum value of correlation coefficient provides an approximate measure of forecast accuracy modulated by spatial variability of rainfall amount. The shape of the contours gives information on the directional dependency of precipitation forecast accuracy.

The two contour fields were compared with the spatial autocorrelation field, which is computed from the QPE against itself. The preferred orientation of precipitation isopleths during this period is evident, with strong anisotropy oriented from west-southwest to north-northeast. The spatial patterns also depend on the duration of accumulation. As an overall assessment, better QPF should result in a QPF-QPE correlation pattern similar to that of the spatial auto correlation. Figure 4 shows that the maximum value of cross correlation coefficient of the parallel run (with radar reflectivity assimilation) is 0.67, better than 0.58 for the control run (without radar reflectivity assimilation), indicating that the QPF error in the parallel run is reduced from that of the control run. The contour lines of the parallel run result are better defined, suggesting that its spatial scales and directional orientations are more accurate than those of the control run in this case.

Snow State Cycling in the RUC CDAS

The RUC Control and RUC CDAS were run in parallel during the first cold season of winter 2002-

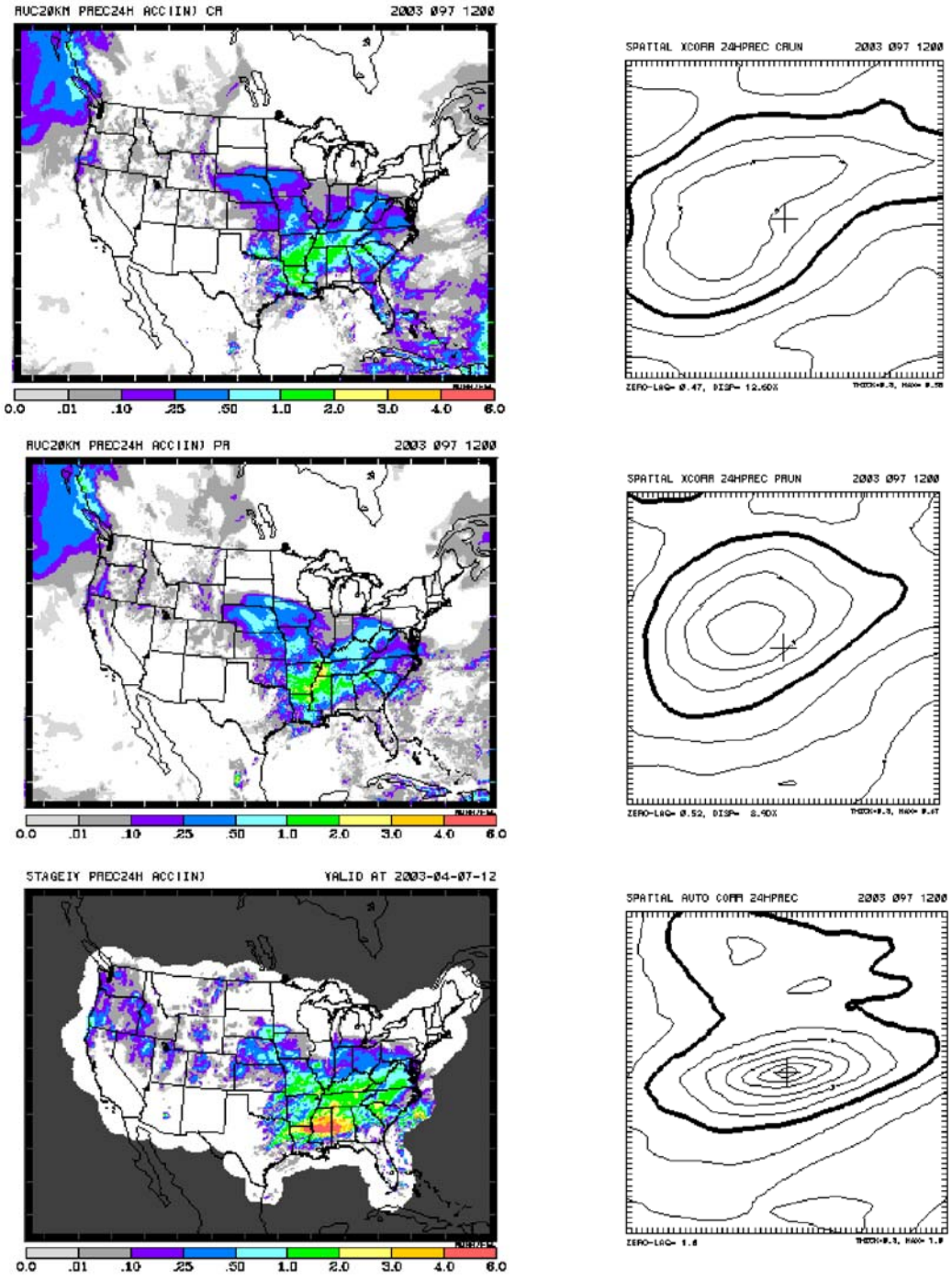

Figure 4. A 24-hour accumulation of precipitation for the period ending 1200 UTC 7 April 2003 from (a, top left) control run, without radar reflectivity assimilation, (b, middle left) from parallel run with radar reflectivity, and (c, bottom left) Stage IV precipitation amounts (sum of four 6-hour totals). Forecast amounts are for 8 consecutive 3-hour forecasts from RUC cycles. (d, e, and f, right panel) are spatial correlation functions corresponding to a), b), and c), and the maximum correlation is also shown. See text for more explanation.

Cycled Snow Variables in the RUC CDAS *(continued)*

2003. The advantages of of the RUC CDAS could be monitored in the evolution of the snow depth field driven by the 1-hour precipitation forecast. Although the atmospheric forcing from the RUC 1-hour cycle often corrects misplaced snow precipitation by providing the energy for snow melting, still the snow field is a very good indicator of the improvements in the precipitation forecasts in the RUC CDAS.

The example in Figure 5 (a–c) illustrates the comparison of snow depths from the RUC Control and RUC CDAS cycles against the NOHRSC (National Operational Hydrologic Remote Sensing Center) NSA (National Snow Analysis). The NOHRSC product combines the snow model assimilation with all available snow observations and provides one of the most reliable datasets of this variable. Although RUC CDAS improves the cycled snow state, at the same time certain deficiencies still exist in the amounts of the precipitation in the RUC CDAS, causing most often underestimation of cycled snow depth. This also has a delayed effect on the soil moisture climate and surface physics in the warm season.

Conclusion

Further improvements of the cycled snow depth could be achieved by updating the snow state fields from existing observations. This approach has been implemented at the National Operational Hydrologic Remote Sensing Center in their National Snow Analysis. Snow data used to update the model include observations from the NOHRSC's Airborne Snow Survey Program, NWS and FAA field offices, NWS Cooperative Observers, the

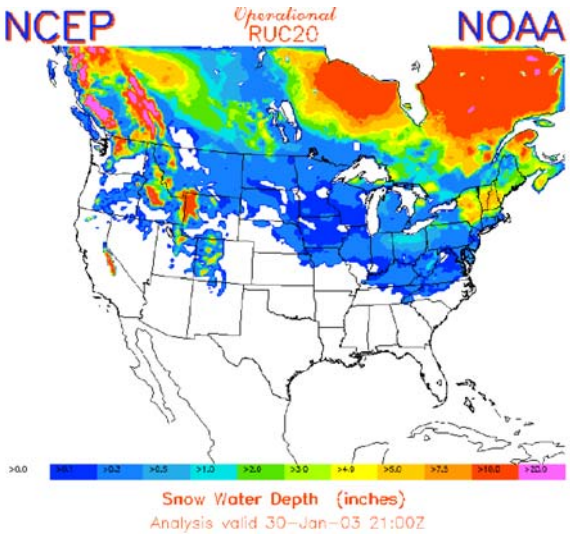

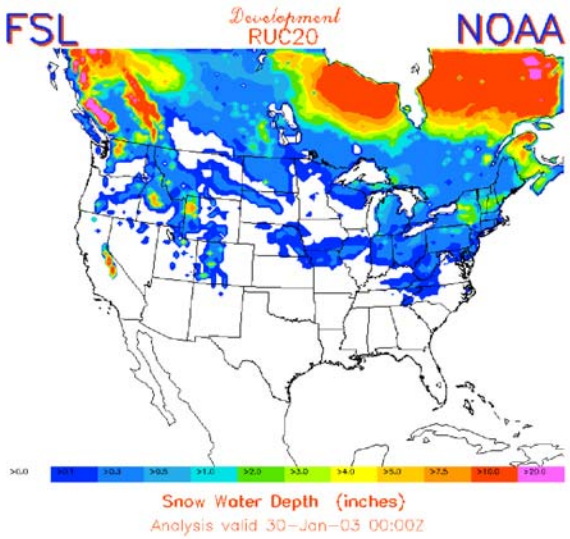

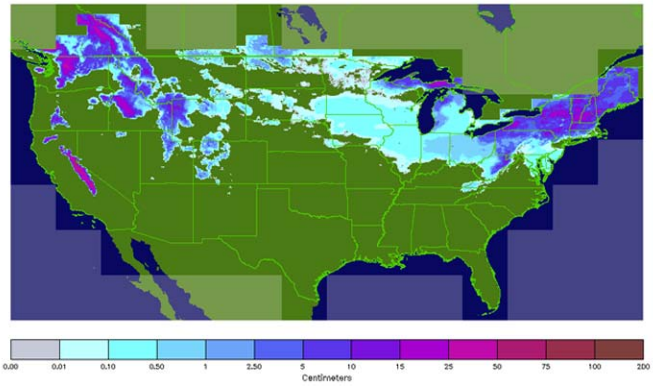

Figure 5. Snow depth from the RUC Control (a, above left) and RUC CDAS (b, above right) verified against the NOHRSC snow analysis (c, right) valid on 30 January 2003.

National Resources Conservation Service (NRCS) Snow Water Equivalent Information (SNOTEL) and snow course networks, the California Department of Water Resources snow pillow networks, and snow cover observations from NOAA's GOES and AVHRR satellites.

The first step in this direction is to compare RUC CDAS snow state variables to the NOHRSC NSA and identify the areas with the largest deficiencies. Then the technique should be developed and applied to make corrections of RUC CDAS snow variables for these areas. Improvements of the snow climate in the RUC CDAS will also be beneficial for the NOHRSC NSA, because that snow model is driven by the RUC precipitation and atmospheric forcing. An example of time series products from the NSA showing the verification of the RUC precipitation forcing as well as NSA snow depth verification for the March 2003 snow storm in Boulder, Colorado, is presented on Figure 6 (a,b). In this particular case, the RUC model was able to provide sufficiently accurate forcing for the NOHRSC snow model, and corrections of the snow analysis from observations were not needed. Similar verification of the RUC precipitation and atmospheric forcing is performed regularly at the NOHRSC for different stations, and it demonstrates that in some cases the improvements to the RUC precipitation forcing are necessary. We will continue to make more detailed comparisons between the RUC CDAS snow state variables and the NOHRSC NSA, and these results will be presented in future articles.

Note: A complete list of references and more information on this and related topics are available at the main FSL Website www.fsl.noaa.gov, by clicking on "Publications" and "Research Articles."

(Tanya Smirnova is a researcher (under CIRES contract) in the Regional Analysis and Prediction Branch, headed by Dr. Stan Benjamin. She can be reached by email at Tanya.Smirnova@noaa.gov, or by phone at 303-497-6253.)

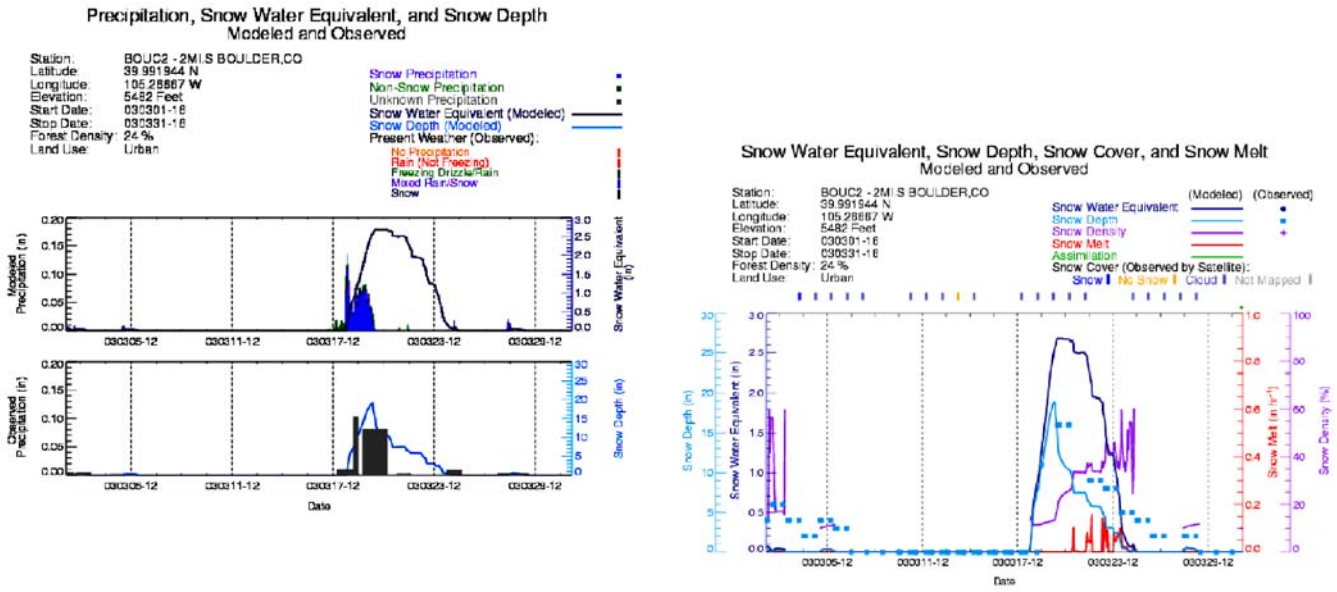

Figure 6. The precipitation forcing from RUC 1-hour forecasts (a, left top panel) for March 2003 snow storm compared to the observed precipitation (a, left bottom panel), and the National Snow Analysis snow depth (b) comparison to observations for Boulder, Colorado.

Using the Graphical Forecast Editor in NWS Forecast Operations

— *By Thomas LeFebvre and Tracy Hansen*

Introduction

FSL's role in the development of the Interactive Forecast Preparation System (IFPS) was featured in the December 2000 issue of the *FSL Forum*. Also included in these comprehensive articles was the Graphical Forecast Editor (referred to as the GFESuite), an important aspect of IFPS. Three years ago, only 15 National Weather Service (NWS) forecast offices were using this prototype software quasi-operationally to produce a small number of experimental products. Since then, GFESuite software has been installed at every NWS Weather Forecast Office (WFO), and forecasters are using it operationally around the clock to express the weather forecast digitally. This initial operating capability (IOC) represents a major milestone for the GFESuite software and the NWS.

Forecasters now interact with a suite of tools that manipulate gridded numerical representations of the forecast instead of spending most of their shift typing text products. With these useful products no longer needing to be typed by hand, forecasters can focus more on the forecast as the products are formatted automatically from digital grids that "feed" the National Digital Forecast Database (NDFD), soon to become the official representation of all WFO-generated forecasts. Much has been accomplished to reach this IOC milestone. GFESuite developers designed and implemented a new text product formatter framework that is flexible enough to accommodate local preferences ranging from simple wording issues to major changes in the text product format. The InterSite Coordination (ISC) facility allows adjacent offices to compare their forecasts graphically so that they can produce gridded forecasts that look as seamless as possible when the data are mosaicked in the NDFD. To complement implementation of the software, GFESuite developers devoted a significant amount of time preparing and presenting training material to convey critical information to NWS forecasters.

GFESuite Description

The GFESuite comprises not only the Graphical Forecast Editor, but also a collection of software (Figure 1) that permits forecasters to define the weather forecast numerically or digitally. Forecasters use the GFE interactive editor to manipulate gridded representations of the forecast. The GFE houses dozens of tools that can modify the gridded forecast in meteorologically useful ways. Three separate editors provide different views of

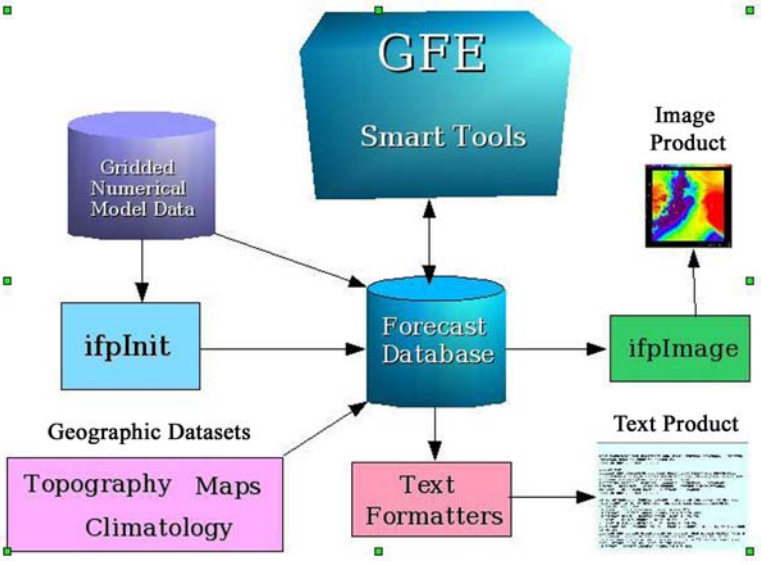

Figure 1. Diagram illustrating major components of the GFESuite software.

the forecast database (Figure 2). The Spatial Editor presents an areal perspective of the grids so that forecasters can edit the gridded data over a particular area. The Temporal Editor displays a time series view of the data over any selected area. This editor lets the forecaster modify the grids for the selected area as a function of time. The Grid Manager displays an inventory view of the database where forecasters can inject or replace grids based on numerical model output, change the time period over which grids are valid, add new grids by interpolating based on existing grids, and perform a variety of other operations.

The GFE also contains a programmable interface we call the Smart Tool framework, which is used by forecasters to implement their own tools to perform a virtually limitless number of operations. Smart Tools have access to a growing array of data sources including numerical model output, surface observations, and topography. The Smart Tool architecture is shown in Figure 3.

The other GFESuite programs are dedicated to generating forecast products or processing meteorological data that

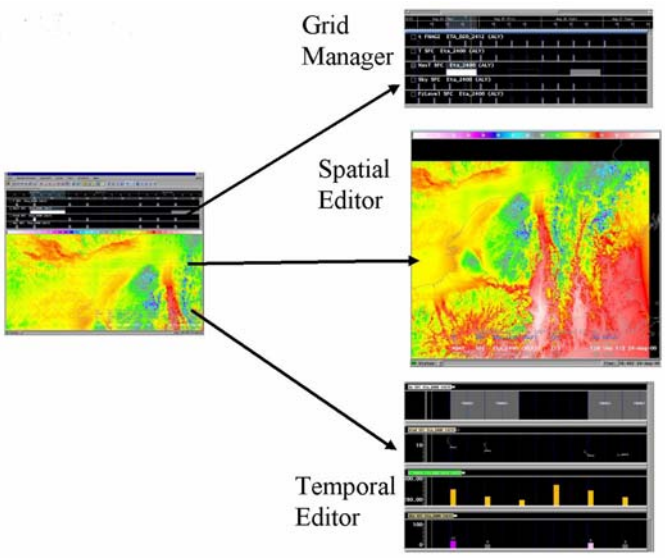

Figure 2. GFE editors include the Grid Manager (an inventory of weather elements), Spatial Editor (grids in plan view), and Temporal Editor (time series representation of weather elements).

are used by some other component of the GFE. The ifpInit facility ingests raw numerical model output and calculates various sensible weather elements at the earth's surface. These grids are sometimes used by forecasters to initialize the gridded forecast, particularly in the 5–7 day forecast period. The Daily Forecast Critique (DFC) archives surface observations and plots them in a time series format along with point forecasts extracted from the grids. This program gives forecasters the capability to compare their forecast with observations, providing insight into systematic forecast errors.

Several GFESuite programs produce forecast products based on the forecast grids. The ifpnetCDF program creates a binary representation of the forecast. This format is useful for transferring the values of the forecast to users who require the highest level of forecast detail, such as fire behavior modelers. The ifpImage program produces pictures of the forecast in Portable Network Graphics (PNG) format. Many NWS Forecast Offices use this as part of their Website to convey forecast information to the general public. GFESuite text formatters sample the gridded data over some specified location and time period and create words that represent the forecast. This suite of text formatters provides a very important function to NWS forecasters. High quality, automatically generated text products are very important to the success of IFPS, since the time that forecasters previously spent typing text products can now be better spent improving the quality of the gridded forecast.

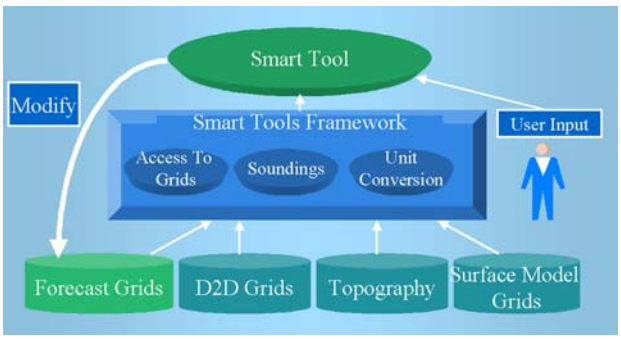

Figure 3. The Smart Tool architecture.

GFESuite Use in Forecast Operations *(continued)*

New Features

Several new features have been added to the GFESuite since our last report (*December 2000 Forum*). A new text product formatter infrastructure was designed and implemented so that local forecast offices have better control over the words derived from the forecast grids. We implemented the InterSite Coordination (ISC) facility so that forecasters can view grids from adjacent offices and more efficiently coordinate their forecasts. The Daily Forecast Critique, built in 2002, gives forecasters the opportunity to compare their forecasts to surface observations.

GFESuite Text Product Infrastructure

The task of automatically generating text products from the GFESuite forecast grids has been a major focus over the last year. We introduced an experimental prototype in 1998 at the Modernized Product Workshop as a way to create new innovative text products directly from forecast grids (Figure 4). The field forecasters quickly adopted this new approach, which uses the Python programming language, to make it extensible and easy to customize to the local site. They explored the use of this technology to create new products as well as to work with the legacy text products. The popularity of this approach prompted the NWS in August 2002 to ask FSL, in concert with field forecasters, to write a set of core products as an alternative to the existing products. This was quite an undertaking, and to set it in motion, we immediately formed a Focus Group of about 25 motivated forecasters who had been working with the text product framework.

The National Weather Service issues directives describing the content and format of text products to be issued. The core products (about 12 in all) include the Zone Forecast Product, Coastal Waters Forecast, Fire Weather Forecast as well as tables such as the Coded Cities Forecast. The directives (Figure 5) needed to be encoded into the baseline software, but that's only half the story. These directives act only as guidelines, and each local office has its own variations and preferences based on the geographic and meteorological characteristics of its domain. We began a series of 14 releases of the software to the forecasters on our team. They tested the code and made sure it could handle their local customizations, and then gave us their "bug" reports and requests for enhancements. On the surface, the idea of representing numbers as simple phrases does not seem too difficult: "Sunny. Highs in the 80s." How hard could that be?

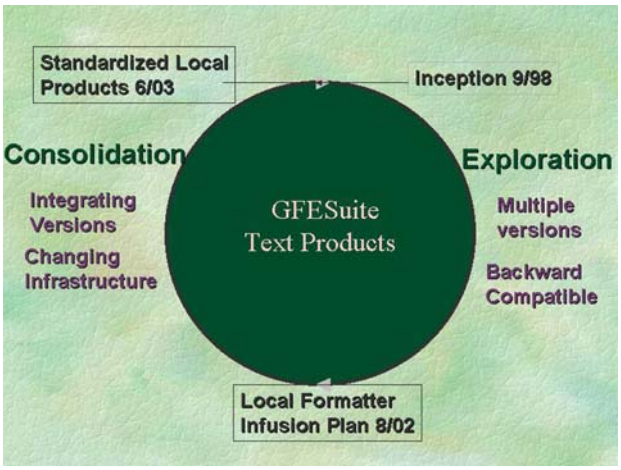

Figure 4. Events that comprise the evolution of the current text formatter infrastructure.

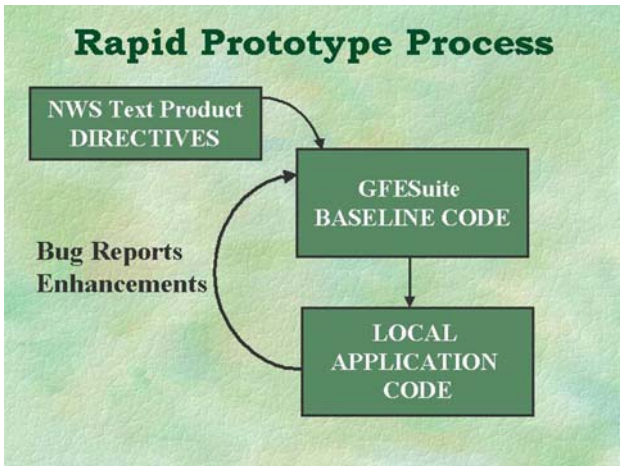

Figure 5. NWS Directives are the starting point for building a text product formatter. Code developed in the field that addresses details not mentioned in the directives are also folded into the baseline software.

However, we discovered that there are many subtleties and complexities that we did not foresee. For example, the probability of precipitation (PoP) phrase, "Chance of rain...," "Chance of snow..." depends on the current weather events. Or the snow accumulation we report in the "Today" period will contribute to the total snow amount reported in a later period. We could have "a chance of rain and fog in the morning" then "a chance of rain in the afternoon," and the formatters have to be smart enough to see that there is a chance of rain all day and fog only in the morning.

The temporal resolution of the grids can lead to more complexity with many different weather scenarios in a 12-hour period. The formatters have to be able to consolidate this digital information and produce concise yet accurate phrases. Beyond that, we needed to account for local effects and report differences between areas, such as the "coast" versus "inland," or "mountains" versus "valleys."

In order to tackle these complexities and dependencies, we invented a new way of processing, which we call "holographic." This means that the narrative components and phrases are represented in a tree-like structure in the computer memory (Figure 6). Then different dependency and logical rules can be applied to any part of the tree *before* producing the final product. The weather conditions can be examined to properly word the PoP phrase. The snow accumulation can be summed over consecutive periods to yield a total snow amount that is consistent and accurate. Phrases can be more detailed, new ones can be added, or the order of the phrases can be changed on the fly. Forecasters do not have to commit to any part of the product until all dependencies are accounted for and the whole is complete.

Once this framework was in place, we worked with our Focus Group to determine *which* rules to apply to the tree-like structure. It turns out that these are the rules forecasters have used almost intuitively over the years as they typed their text forecasts. The Rapid Prototype Process, working interactively with the users, is a very effective way of extracting this information. This approach was successful, and in June of 2003 we released the core products for national deployment. This means that if you look up the official forecast for a National Weather Service office, it is likely that the words you read were generated by software written at FSL. Similarly, if you listen to NOAA weather radio, the words you hear are likely to be a result of this system. And now this infrastructure, bolstered by our experience with the core products, can be used to create new and innovative products such as pointcasts, travelers' forecasts, and products for other programs such as Aviation and River Forecast products.

InterSite Coordination

Under the previous text-based paradigm, forecasts from several offices were rarely, if ever, presented on the same display, thus offices seldom coordinated routine forecasts. However, with the NDFD presenting a national mosaic of digital forecasts from literally dozens of offices, it became clear that forecast offices must spend more effort coordinating their forecasts. To help with this coordination effort, FSL built the ISC facility that lets forecasters look at forecast grids from surrounding offices before they commit their official grids to the NDFD.

As the gridded forecast is being developed at a local office, the forecaster has the option of sending the grids to adjacent offices over the AWIPS Wide Area Network (WAN). A few minutes later these grids are received at the adjacent offices and remapped or transformed into a format so that they can be viewed properly by the adja-

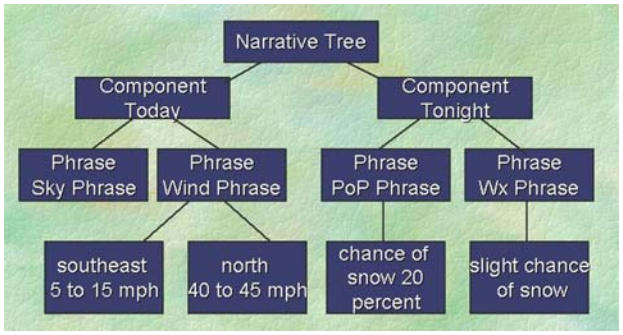

Figure 6. Text products are represented in a tree-like structure before the words are generated.

GFESuite Use in Forecast Operations *(continued)*

cent sites. The forecasters only need to select a single button on the GFE, and gridded data from surrounding sites instantly appear on the display. Forecasters can then very easily see any discrepancies between their own forecast and that of their neighbors. Figure 7 shows a GFE display with data from surrounding sites interleaved.

The capability to look at the forecast from an adjacent site is not the only advantage in using the ISC. New tools have been developed that flag forecast data discrepancies beyond a configurable threshold. Grids that exceed these thresholds are color-coded in the GFE Grid Manager so forecasters can see at a glance which grids do not meet the criteria. If the discrepancies are relatively minor, tools built into the GFE can smooth them out. Major discrepancies generally require some additional communication between the two offices. Over time, forecasters have learned that coordinating the forecast before editing the gridded forecast usually leads to better results than waiting until the forecast is complete. Many forecast offices use Internet chat software to collaborate and reach consensus on the forecast before beginning the process of editing the grids. As a result, forecasts produced at these offices usually contain fewer spatial discrepancies than those produced at offices where forecasters do not collaborate.

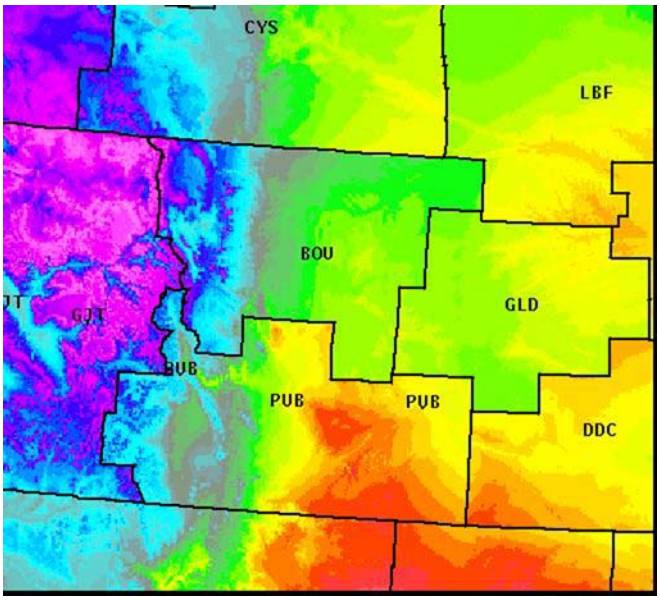

Figure 7. InterSite Coordination software performs an automatic mosaic of the gridded data from surrounding sites so forecasters can compare their forecasts with neighboring offices.

Daily Forecast Critique

The Daily Forecast Critique (DFC) permits forecasters to compare their gridded forecasts to actual observations. Since observations are collected at selected points within their forecast area, point forecasts are extracted from the grids before the comparison takes place. Forecasters use the DFC to give them a sense of forecast accuracy and to learn about any systematic errors so that they may use that knowledge to make a better forecast next time.

The DFC consists of two main programs, an archiver and display program. Since the AWIPS software saves on average only 36 hours of surface observations, a DFC archive program was developed so that offices could save as many observations as they thought useful. The archiver is started about every 15 minutes, searches the AWIPS database for any new observations, extracts them, and archives them. In addition to saving observations, the archiver also saves forecast points extracted from the official database as well as any or all numerical model databases. The model database archive lets forecasters compare the numerical model-predicted values against observations, giving insight into systematic model errors.

The display program consists of a user interface window and a display window. With the user interface, forecasters can select from various categories such as the weather element, station, data source (observations, model, official forecast), and model time, followed by a command to plot the data. Once the data are plotted, a different data source or model time can be selected and that dataset can be combineed with the previously plotted dataset. This type of interface allows users to plot any dataset against any other and have complete control over which datasets are compared. The DFC configuration files let forecasters control which stations and models are archived, as well as display preferences such as colors, plotting symbols, and line textures.

Future Work

Though the GFESuite system was judged adequate to meet IOC requirements, we will continue to develop new tools and interact with operational forecasters to create a system that makes the task of weather forecasting more efficient. Expressing the forecast as a gridded field is a very new concept for forecasters. Therefore, the methodology, or the techniques employed to edit the grids, is generally quite primitive. Many forecasters use interactive tools that require a significant amount of forecaster input to accomplish a task. This practice is both time-consuming and can lead to grids that are internally inconsistent. GFESuite needs a more sophisticated level of tools that apply changes to the forecast in a meteorologically meaningful way while keeping the database internally consistent in time, space, and across weather elements. With an eye toward that goal, we are now working to inject more science in the forecast process.

The Smart Tool framework developed several years ago has worked reasonably well thus far, but needs new enhancements that will make writing new tools less cumbersome, and injecting good science into the forecast process easier. We are developing a new set of meteorological tools that will provide the fundamental building blocks for creating scientifically sound tools. These tools include methods to perform numerical derivatives on meteorological fields, a set of atmospheric physics methods that enable tools to more easily calculate important derived quantities, and utility methods that make the job of writing new Smart Tools easier. GFE currently offers an interpolation facility that calculates new grids based on grids that have been already defined. Interpolation allows forecasters to easily and quickly fill in temporal gaps in the forecast, saving precious time. Unfortunately, this interpolation program is purely mathematical and lacks all knowledge of meteorological concepts. A new interpolation facility is needed that knows how various weather elements interact with each other. To make the results more predictable, we plan to allow user input in the interpolation process, such as the position and strength of a cold front as a function of time, so that these interpolation algorithms can make better, more intelligent decisions when filling in the temporal gaps. We are now designing a new interpolation facility that provides for this user input and also contains knowledge about how weather elements interact so that interpolated grids are more consistent with the overall forecast.

Forecasters have demonstrated strong personal preferences when creating the words that represent the forecast. We expect that the text formatter infrastructure and the text formatters themselves will require refinement as traditional products evolve and new products are developed.

Conclusion

Despite our success in the IFPS project, we still have much work ahead. GFE can be used as an effective tool for making gridded digital forecasts, but many improvements are needed to make this forecasting process more efficient and more scientific. Refinements to the product formatters will free up time spent on making products and permit forecasters to better focus on the meteorology. Better science in the forecast process will likely lead to forecasts of unprecedented detail and accuracy.

Editor's Note: A complete list of references and more information on this and related topics are available at the main FSL Website www.fsl.noaa.gov, by clicking on "Publications" and "Research Articles."

(Tom LeFebvre is a meteorologist in the Modernization Division. He can be reached at Thomas.J.LeFebvre @noaa.gov, or 303-497-6582.)

Defining Observed Fields for Verifying Spatial Forecasts of Convection

– By Jennifer Mahoney, Joan Hart, and Barbara Brown

Introduction

A variety of convective weather forecasts are produced operationally and used by the aviation community as decision aids for rerouting air traffic around convective weather. These forecasts, which include the National Weather Service (NWS) Convective Collaborative Forecast Product (CCFP) and Convective Significant Meteorological Advisories (C-SIGMETs), describe convective activity at different spatial and temporal scales and differ slightly in the characteristics that are included in the forecast area.

A critical challenge in evaluating the quality of these forecasts is determining how to appropriately match the forecasts to the observations so that statistical results are representative of the forecast characteristics, the forecast spatial and temporal scales, and the forecast's operational relevance. This process has been particularly difficult for evaluating forecasts from the CCFP and C-SIGMETs that are required to meet minimum size thresholds as well as specific criteria for coverage of convection, cloud top height, and cell movement.

Historically, observations used to evaluate the CCFP were expanded from a 4-km grid to a 40-km grid to approximately match the scale of the forecast. Matching the forecast scale was difficult to determine, since the impact of the convective activity on the operational flow of enroute air traffic was not well defined. Moreover, the coverage attribute was excluded from the verification approach because the application of the attribute was not clearly understood.

This article presents new methods for defining the observation fields used for evaluating the CCFP and C-SIGMET forecasts that consider the effects of convection on the flow of air traffic such as Convective Constraint Areas (CCAs) and incorporate the observed coverage.

Data: Forecasts and Observations

Forecasts – The CCFP forecasts are issued by the NWS Aviation Weather Center (AWC), but are produced through a collaborative process with AWC forecasters, airline and Center Weather Service Unit (CWSU) meteorologists, and MSC (Meteorological Service of Canada) meteorologists. CCFP forecasts are required for areas of intense convection and thunderstorms every 2 hours, with lead times of 2, 4, and 6 hours after the forecast delivery time. The CCFP comprises polygons that are at least 3,000 mi^2 in size and contain a coverage of at least 25% convection with echoes of at least 40 dBZ composite reflectivity, and also a coverage of at least 25% with echo tops of 25,000 feet and greater.

The C-SIGMET, generated by forecasters at the AWC, is a text forecast of convective activity that is issued hourly but valid for up to 2 hours (as outlined in the National Weather Service Operations Manual D-22). These forecasts are intended to capture severe or embedded thunderstorms and their hazards (e.g., hail, high winds) that are either occurring or forecasted to occur within 30 minutes of the valid period and cover at least 40% of the 3,000 mi^2 or larger forecast area.

Observations **–** The National Convective Weather Forecast Hazard Product (NCWF-H) is used to describe intense convection as it applies to the CCFP that is a threat to aircraft. It is defined by the video integration and processor (which contours radar reflectivity, in dBZ, into 6 VIP levels) values of 3 or greater, and/or 3 or more strokes of lightning in 10 minutes within 8 kilometers of a grid point, on a 4-km grid. For further information see *http://cdm.aviation weather.noaa.gov/ncwf/ncwf_wt/ncwf_wt_haz.htm*.

Techniques for Defining Observations

The techniques for defining the observations for evaluating the CCFP and the C-SIGMET are separated into two parts: 1) developing a definition for Convective Constrained Areas (CCA) and 2) producing observed fields that reflect the attributes of the CCFP, particularly the size and coverage criteria.

Convective Constraint Area (CCA) – This provides the basis for measuring the "scale" of convective activity that impacts the flow of enroute air traffic. Rhoda et al. (2002) determined that pilots tend to deviate around

strong precipitation until they get quite close to the arrival airport. However, they were unable to determine the typical distance of the deviations. Therefore, the CCA concept applied here follows guidance provided by the Aeronautical Information Manual (AIM), see *http://www1.faa.gov/ATPubs/AIM/index.htm*, which suggests that pilots should remain at least 20 nm away from intense convection in order to minimize safety concerns that are related to convection. However, in practice, this distance is often too large when air space becomes congested. Therefore, to take this operational consideration into account, we defined the CCA here as an area of intense convection (identified by the 4-km NCWF-H grid) plus a 10-nm radius surrounding the convection. The 10-nm radius is measured from the center of each 4-km NCWF-H grid box. Figure 1 shows the raw NCWF-H in which the green areas represent the grid boxes with intense convection. Once the 10-nm radius criterion is applied to the observations in Figure 1, the areas grow slightly (Figure 2) to represent the CCAs. The CCAs in Figure 2 should not be thought of as areas "closed" to enroute air traffic. Rather, they should be considered as areas where the flow of enroute air traffic is reduced because of the influences produced by the intense convection.

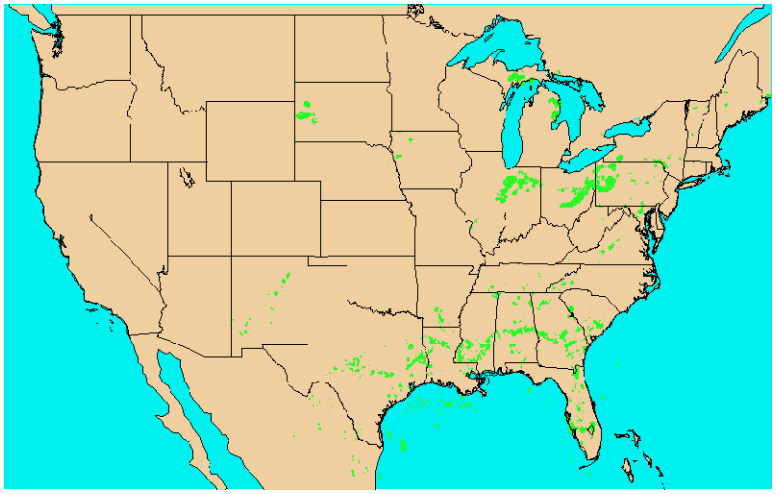

Figure 1. Raw NCWF Hazard Product at 4-km resolution at 1900 UTC on 4 July 2003. Green areas indicate VIP values that are 3 and greater and cloud tops are assumed to be 20,000 feet and greater.

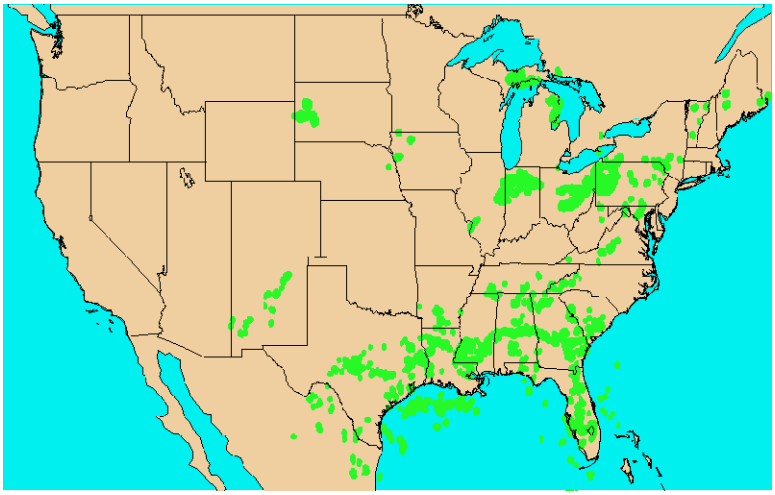

Figure 2. Map of convective activity that impacts enroute air traffic at 1900 UTC on 4 July 2003. Green areas indicate 4-km NCWF Hazard +10-nm radius.

Defining Observed Fields for Verifying Spatial Forecasts *(continued)*

Using the CCA as the area of interest, coverage is computed by evaluating the percentage of 4-km CCA boxes meeting the CCA criterion within a larger 92 x 92 km search box. This search box represents the 3,000 mi^2 minimum size required before a CCFP or C-SIGMET forecast polygon can be issued. The percent of observed coverage within the search box is assigned to the center 4-km box. The search box is moved one grid square and the coverage is recomputed and assigned to the center 4-km box. This procedure continues until each 4-km box within the forecast domain is assigned an observed coverage value. Figure 3 shows the CCA coverage for the example shown in Figure 1. Increasing coverage represents a decrease in the flow of air traffic, though exactly how much of a decrease is yet to be determined and will be the focus of future research.

Application

The application of the technique for two convective cases: a well-organized convective line on 8 June 2003 (Figure 4) and disorganized isolated convection on 5 August 2003 (Figure 5). The observed fields shown in these figures pictorially represent the "perfect" forecast, where the sizes of the fields are greater than 3,000 mi^2 and the areas contain a coverage that is greater than the minimum threshold for the CCFP, 25% (Figures 4a, 5a) and the C-SIGMETs, 40% (Figures 4b, 5b).

For the 8 June 2003 case (Figure 4), the forecasts nicely capture the main convective line over the Midwest and large convective area over the Southeast. Convection over the West and Southwest was left out of both forecasts, possibly because the impact on rerouting aircraft due to convection is generally less of a problem over the West than over the eastern half of the U.S.

In the 5 August 2003 case (Figure 5), the larger convective areas over the Northeast, Atlantic States, lower middle half of the U.S., and the upper Northwest were accurately captured by both the CCFP and the C-SIGMETs. However, the smaller convective areas were excluded from both forecasts. These results may suggest that the CCFP and the C-SIGMET forecasts are focused on main areas of convection that are typically much larger than 3,000 mi^2 and that the area requirement for the minimum forecast area should be reconsidered.

Conclusions and Future Work

Defining the observed fields for verifying spatial forecasts for convection is key to developing approaches that meet the forecast and user requirements. Here, we build a definition for a Convective Constraint Area (CCA) that is consistent with operational guidelines and is used to characterize the airspace around intense convective weather where the flow of enroute air traffic may be

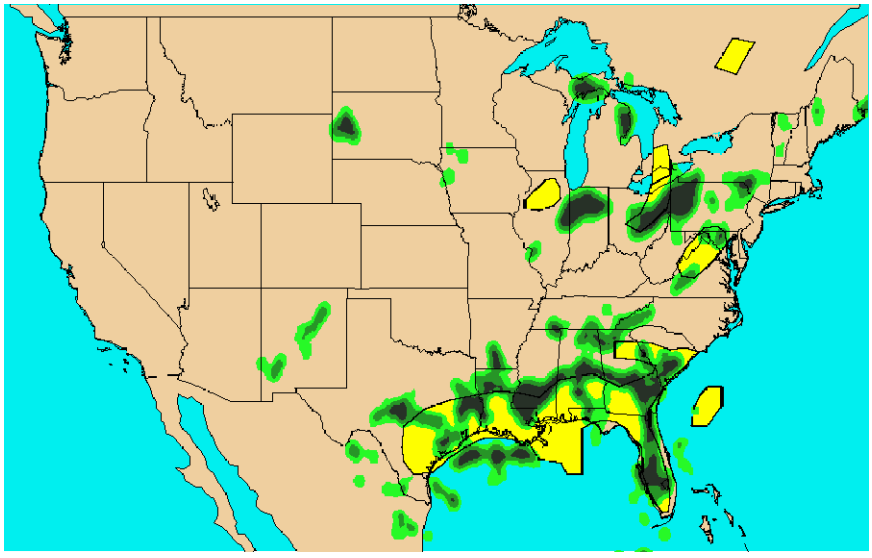

Figure 3. Map of convective constraint areas with coverage 3,000 mi^2 area that is 25–49% (light green), 50–74% (medium green) and 75% and greater (dark green), at 1900 UTC on 4 July 2003. Yellow areas indicate CCFP forecast.

obstructed or reduced. The CCA forms the basis for developing the coverage fields that are used to evaluate the quality of – and characterize the weather requirements for – the CCFP and the C-SIGMETs. Input from the user community is necessary to ensure that the size criterion of 10 nm is operationally relevant. In addition, cloud-top heights need to be added to the CCA techniques presented here to fully incorporate the CCFP weather attributes into the verification approach. Finally, the relationship between the observed coverage and the reduction in the flow of air traffic will be the focus of future research. Defining the observations in this manner sets the stage for the application of object-oriented verification approaches.

Editor's Note: A complete list of references and more information on this and related topics are available at the main FSL Website www.fsl.noaa.gov, by clicking on "Publications" and "Research Articles."

(Jennifer Mahoney is Chief of the Forecast Verification Branch in the Aviation Division. She can be reached at Jennifer.Mahoney@noaa.gov, or 303-497-6514.)

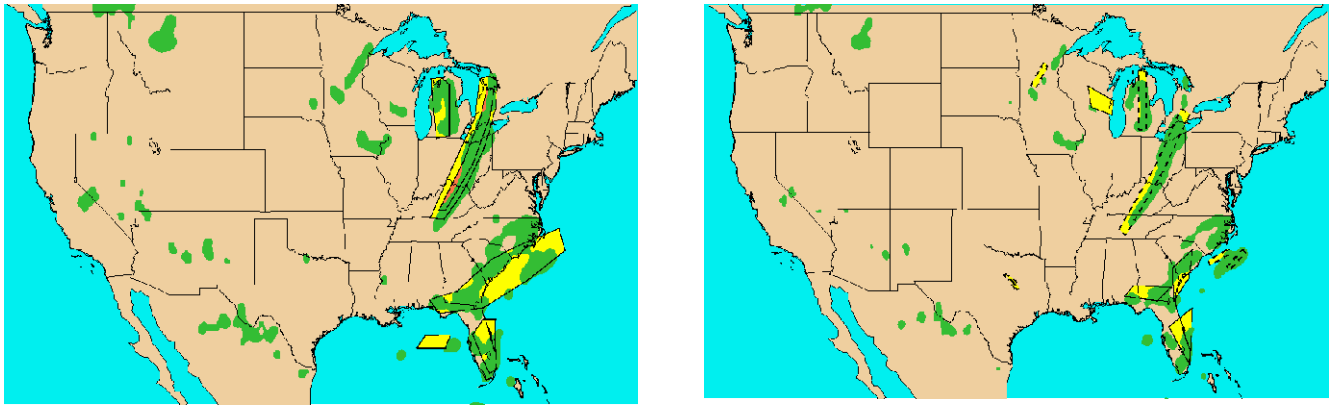

Figure 4. Organized convective line, 8 June 2003 2-hour forecasts for CCFP (a, left) and C-SIGMET(right) issued 1900 UTC. Observed CCAs, coverage 25% (a) and 40% (b). Forecasts are indicated by hatched areas.

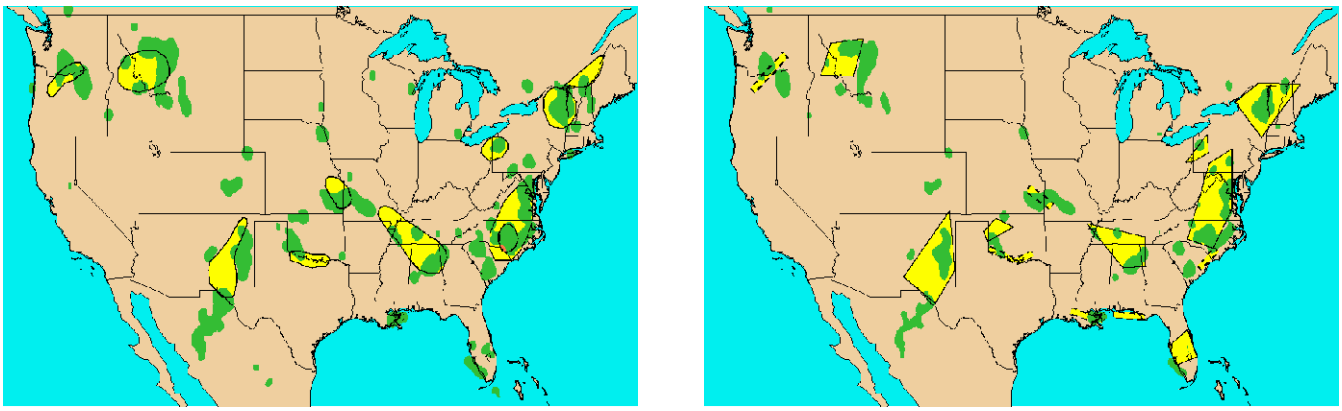

Figures 5. Disorganized convection on 5 August 2003, 2-hour forecasts from the CCFP (a, left) and C-SIGMETs (right) issued at 2300 UTC. Observed CCAs, coverage 25% (a) and 40% (b). Forecasts are indicated by yellow areas.

Using the WRF Model in National Weather Service Operations –

By Brent Shaw, Mike Kay, Jennifer Mahoney, John McGinley, and John Smart

Introduction

Under the auspices of a nationwide effort led by NOAA known as the Coastal Storms Initiative (CSI), a locally run version of the new Weather Research and Forecast (WRF) mesoscale numerical weather prediction model has been installed at the Jacksonville (JAX), Florida, National Weather Service Weather Forecast Office (WFO). CSI is a collaborative effort of various local, state, and federal organizations to lessen the impacts of storms on coastal communities. The effort to install WRF at the Jacksonville WFO is but one component of the initiative, designed to improve accuracy and detail of forecasts of coastal winds, precipitation, and visibility. This local modeling effort represents collaboration between the NWS Office of Science and Technology, the Jacksonville WFO, FSL, and the Florida State University (FSU) Department of Meteorology.

Three pertinent issues related to local modeling within the NWS WFO environment are addressed. First, can public forecast services provided by a WFO be enhanced through the use of a locally run mesoscale modeling system? Second, does the use of a data assimilation component improve local model forecasts compared to simply initializing a local model directly from the NCEP national forecast models? Third, can the new WRF model serve as the local model component in the WFO environment in a similar manner as the workstation Eta system has in other WFOs?

To address these questions, the group of collaborators designed a local configuration that would meet the operational needs while providing data and a verification method that could provide insight into these issues. In this article we provide an overview of the CSI WRF modeling system as installed at the Jacksonville WFO, including the data assimilation component, postprocessing, and limited quantitative results. Information on the perspective of the operational forecasters regarding value added by this system is contained in Welsh et al. (2004). A verification study of the operational WRF forecasts is provided in Bogenschutz et al. (2004) and in Mahoney et al. (2003).

System Description

WRF Configuration – Version 1.3 of WRF in use at the Jacksonville WFO is available to the general community for download at *http://www.wrf-model.org*. The dynamic core used for the CSI system is the third-order Runge-Kutta solver (Wicker and Skamarock 2002) formulated for the mass-based vertical coordinate. No explicit numerical filters are used during model integration (diffusion constants are set to zero).

The horizontal model domain (Figure 1) grid uses a Lambert Conformal map projection with grid spacing of 5 kilometers. This was chosen to match the resolution of the grids used to populate the National Digital Forecast Database (NDFD) via the Interactive Forecast Preparation System (IFPS; see the LeFebvre article on page 10). The analysis grid consists of 145 points in each direction. Use of an Arakawa-C stagger in the WRF results in 144 mass points in each direction, allowing an equal number of points in the grid to be distributed across

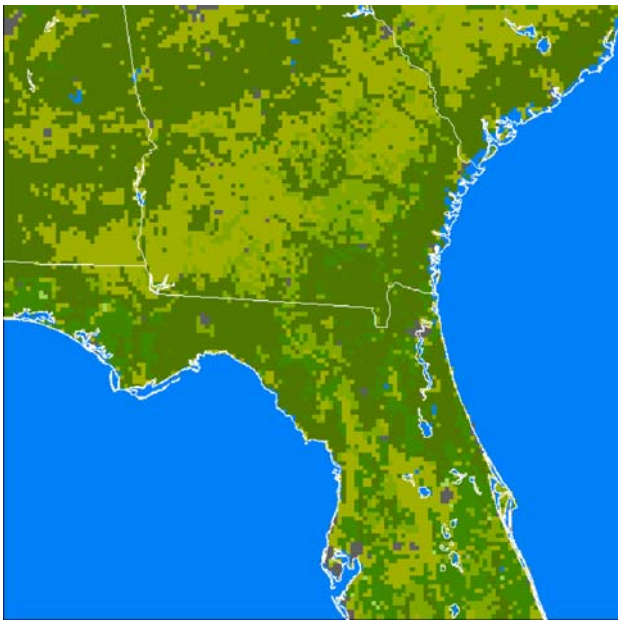

Figure 1. Horizontal model domain for the CSI JAX WRF simulations. The domain consists of 145x145 points on a 5-km non-staggered grid. Image is USGS 24-category land use class as provided via the WRF Standard Initialization package.

the 16 processors available on the computational platform. The Runge-Kutta solver allows a long time step of 30 seconds to be used despite the 5-km grid spacing.

In the vertical, 42 full levels (41 computational layers for the mass variables) are used, with a minimum vertical increment of approximately 20 meters at the lowest levels, increasing to approximately 1000 meters at the model top, which is set at 100 millibars.

Physics options employed include the NCEP 5-class version 1.3 of WRF microphysics, Dudhia shortwave radiation, RRTM longwave radiation, the MRF (Hong-Pan) PBL scheme, and the OSU Land Surface Model. No cumulus parameterization is employed.

The model initial and lateral boundary conditions are provided via the WRF Standard Initialization (WRFSI) package, version 1.3.2, also available to the public at the above Website. The WRFSI is configured to read analysis grids from the Local Analysis and Prediction System (LAPS) for the initial atmospheric conditions, and NCEP Eta grids on the 12-km NCEP grid 218 for the initial soil and sea conditions, and for the lateral boundary conditions.

Data Assimilation – For the WRF simulations used by the operational forecasters, the initial conditions are provided by LAPS, using the diabatic initialization technique (Shaw et al. 2001). LAPS is able to use a wide variety of observational data, including GOES imagery, GOES soundings, WSR-88D reflectivity and radial velocity data, wind profilers, RASS temperature profiles, METAR and maritime surface observations, mesonet observations, GPS-Met total precipitable water, and ACARS data. In the Jacksonville WFO implementation, the availability on the NOAAPORT data feed and what is available via the Local Data Acquisition and Distribution (LDAD) feed. For now, this consists primarily of surface observations, satellite imagery, and single-level radar reflectivity data. For the surface observations, there are typically between 100 and 150 surface observations available from the combination of METAR reports, mesonet sites, and marine observations. As communication and LDAD issues are addressed, we anticipate additional datasets becoming readily available, such as ACARS, GPSMet, and wideband WSR-88D radial velocity and full-volume reflectivity.

The unique diabatic initialization relies on the LAPS three-dimensional cloud analysis, which includes a cloud model to partition the condensate into the various species and determine cloud-type information. Using the cloud-type information, a vertical motion profile is derived, and these profiles are used as "observations" in a final three-dimensional variational (3DVAR) adjustment to ensure that the mass and momentum fields are in balance with the analyzed cloud field. The 3DVAR balance step is fully described in McGinley and Smart (2001), and the details of the cloud analysis and vertical profile assignment are discussed in Schultz and Albers (2001). Note that LAPS is under continuous development, and the version described here is much newer than the versions currently fielded within the AWIPS platform. The forecasters at Jacksonville have reconfigured the standard AWIPS version to match the CSI domain, and they are able to view the analyses from the standard AWIPS LAPS as well as the advanced CSI LAPS.

Hardware Platform and WFO Integration – The computer used for LAPS and WRF is a Linux cluster consisting of 9 nodes. Each node contains dual Athlon 2-GHz processors, and interprocessor communication is handled via the Gigabit Ethernet interface. LAPS and all model pre- and postprocessing are performed on the master node. The WRF model runs on 16 processors, spanning the remaining 8 nodes, using the MPI version of the model. The model configuration described earlier is able to complete a 24-hour forecast in approximately 2.5 hours.

The cluster interacts with the Advanced Weather Interactive Processing System (AWIPS) via the LDAD system. LDAD is used to transfer observational data and national model grids to the cluster for ingest by LAPS. Output from LAPS and WRF is transferred back to AWIPS via the same LDAD exchange mechanism. The WRF model is post-processed incrementally by a model postprocessor that is provided with LAPS. The output is destaggered onto

Using the WRF Model in NWS Operations *(continued)*

the analysis grid, vertically interpolated to isobaric levels, and written into GRIB files that are sent to AWIPS as the model is running. Thus, forecasters are able to view each output hour of the forecast as they are produced rather than waiting for the entire simulation to be completed. The postprocessor also provides tabular text forecasts for a list of points specified by the Jacksonville WFO. By sending the grids to AWIPS, forecasters are able to use and evaluate the forecasts on their operational workstations, which allow overlay of other data such as observations, satellite and radar imagery, and other grids. Additionally, sending the data to AWIPS provides the opportunity to import the WRF grids into the Interactive Forecast Preparation System.

Experiment Design and Verification – The computing capacity at the WFO and the model configuration allow for multiple model cycles per day. The schedule of runs was configured to best meet the needs of the local forecast operations while providing meaningful data to study the impact of adding a local data assimilation component and/or the value of local modeling compared to the national products. All simulations discussed below are run out to a 24-hour output increment (i.e., 25 frames per forecast cycle).

Each day, two cycles with a 0600 UTC initial time are produced. Both simulations are identical in every aspect except for the initial conditions. Both simulations utilize the 0000 UTC NCEP Eta on a 12-km Lambert Conformal grid for lower and lateral boundary conditions. The "operational" run (hereafter referred to as WRF-LAPS) is initialized with LAPS and is started at 0645 UTC and completed by 0815 UTC. The second "comparison" simulation (hereafter referred to as WRF-Eta) begins when the operational run is complete, and uses the 6-hour forecast from the 0000 UTC Eta as the initial condition instead of LAPS. Since the first-guess used for LAPS in the operational run is also the 6-hour forecast from the 0000 UTC Eta, these two runs serve the purpose of determining the value of adding additional local data and performing a reanalysis in the context of the LAPS diabatic initialization. Furthermore, since they have a 0600 UTC initial time, they can be directly compared to the 0600 UTC Eta run from NCEP to see what if any value is added by local models compared to the national guidance.

In addition to the 0600 UTC runs, two more WRF-LAPS runs are performed each day at 1500 UTC and 2100 UTC to meet the needs of the Jacksonville WFO. These two runs provide updated, high-resolution model output between the national Eta and GFS runs using the LAPS diabatic initialization. The 1200 UTC and 1800 UTC runs of the operational NCEP Eta model provide the boundary conditions for these runs.

For all four runs each day, a subset of the postprocessed model output in GRIB is transferred back to FSL for processing through the Real-Time Verification System (RTVS, Mahoney et al. 2002). RTVS verifies the forecasts of surface temperature, humidity, wind speed and direction, and precipitation against surface observations within the domain. Standard statistical measures of accuracy for continuous variables such as bias and root mean square error are provided for temperature, humidity, and wind parameters.

In addition to the CSI WRF runs, the 12-km national Eta model is also processed through RTVS using the same algorithms and observations. When comparing more than one model run, RTVS provides "equalization" to ensure that only those model cycles for which all models being compared were available are used in the statistics. Finally, RTVS provides a Web-based interface to view the results of the verification interactively at *http://www-ad.fsl.noaa.gov/fvb/rtvs/csi/*. A detailed analysis of the RTVS results is contained in Mahoney et al. (2003).

In addition to the quantitative validation being provided via RTVS, the GRIB data retrieved by FSL is also provided to Florida State University, where detailed case studies and mesoscale feature-based assessments are being performed (Bogenschutz et al. 2004).

Results

Successes **–** The most important measure of success when testing a new application in a WFO environment is whether or not the forecasters find the application use-

ful. Making the WRF grid available on AWIPS provided the incentive for the forecasters to look at the model forecasts, and over time, more and more of the forecasters have become comfortable with the WRF model and have begun to rely on it in various situations. In particular, early in the experiment, forecasters discovered that WRF forecasts of visibility reductions due to fog were very accurate. One of the first area forecast discussions issued by the Jacksonville WFO referencing the WRF actually indicated a change in their thinking for the visibility forecast based solely on the WRF forecast and its previous performance in similar situations.

The surface winds forecast parameter is also important within the Jacksonville WFO area of responsibility. The CSI project specifically calls for improved forecasts of wind speed and direction for input into a new wave model being developed under CSI. Quantitative verification of the WRF wind speed forecasts using the RTVS show that the WRF forecasts significantly outperformed the NCEP Eta forecasts at all hours of the 24-hour forecast period. Figure 2 shows the root mean square error (RMSE) and bias of the surface wind forecasts for the 0600 UTC run of Eta, WRF-LAPS, and WRF-Eta.

The southeast U.S. and adjacent coastal areas are dominated by convective activity during much of the year. Quantitative precipitation forecasts (QPFs) via numerical methods are traditionally poor for these types of events due to lack of model resolution and the inherent chaotic nature of air mass thunderstorm development and evolution. The LAPS diabatic initialization attempts to improve explicit short-range QPFs by initializing the NWP models with active clouds and precipitation. This experiment provides further evidence that finer scale models coupled with advanced techniques using satellite and radar information can provide improvements. Figure 3 depicts the ESS and frequency bias scores for the 0–6 hour QPF for various thresholds of precipitation from the 0600 UTC run of the NCEP Eta, the WRF-Eta, and the WRF-LAPS.

The WRF-LAPS demonstrates better ESS and a more consistent bias across all thresholds of precipitation than either the NCEP Eta or the WRF-Eta run. This figure also shows the benefit of adding local data to the initialization using the LAPS diabatic method, as the WRF-Eta forecasts had a low bias for all thresholds, indicative of the typical model "spin-up" problem for precipitation processes. The Eta suffers much less from the spin-up problem, likely due to its advanced 3DVAR data assimilation cycle, but is still outperformed in the 0–6 hour forecast period by WRF-LAPS.

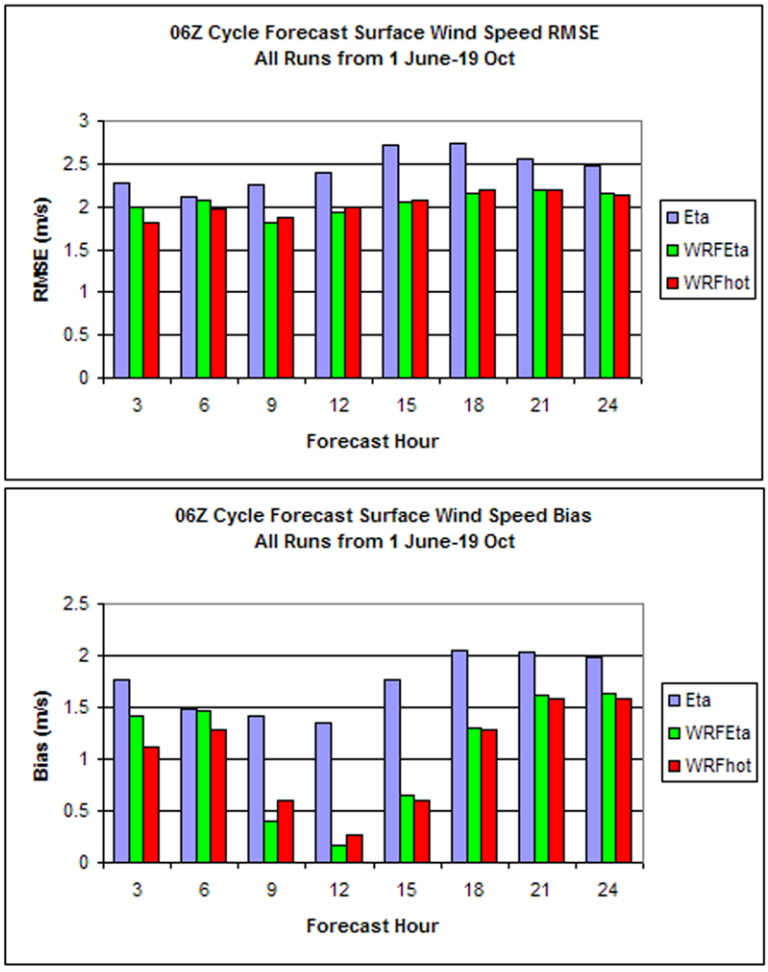

Figure 2. RMSE and bias for all 0600 UTC Eta, WRF-Eta, and WRF-LAPS forecasts of wind speed.

Using the WRF Model in NWS Operations *(continued)*

Challenges **–** Several challenges presented themselves during this project. First and foremost, network security requirements and lack of bandwidth between the Jacksonville WFO and the rest of the NWS network made it difficult to engineer an optimum solution to ensure timely availability of all required input data. The first-guess grids and observational data, including radar and satellite, are made available via the LDAD system, whereas the Eta tiles for the lateral and lower boundary conditions are obtained via FTP from either the NWS Southern Region Headquarters in Fort Worth, Texas, or from the NCEP anonymous FTP server. Many of the run failures during the experiment were due to slow or incomplete data transfers, either due to network performance or unanticipated impacts when router configurations were changed while applying security patches.

Network bandwidth available to a WFO varies by location, and JAX happens to be more limited than most in the Southern Region. Plans for the LAPS analysis included the acquisition of multiple wideband WSR-88D radar feeds from within the region by making use of the CRAFT network. Unfortunately, at the time of writing, this was still not possible. To mitigate this, FSL has been performing the radar data ingest at FSL using narrowband radar from multiple sites and transferring the LAPS intermediate file to the JAX cluster. It is expected that the LAPS diabatic initialization will benefit greatly from multiple wideband radar sites as demonstrated in the International H_2O Project (Shaw et al. 2004).

Planned upgrades to AWIPS during the experiment provided additional challenges, as various changes and additions made to allow ingest of the local model, as well as custom scripts to provide data to the cluster via LDAD, were overwritten during the upgrades and had to be recovered. Support for custom configurations on AWIPS will likely improve as local modeling within the WFOs becomes more prevalent.

Difficulties arose in the initial integration of the Linux cluster because of how it was configured by the vendor, which was more suited to "high availability" computing rather than "high performance" computing. This required some time to learn and reconfigure the system for use with parallelized software. Lessons learned from the CSI project are valuable in preventing this in future WFO offices. Additionally, minor hardware failures, including a failed network card and a failed main processor, were responsible for a few mode failures during the project. These were generally discovered and repaired quickly by the Jacksonville WFO Information Technology Officer.

Meteorologically, the WRF forecasts did not perform as well as the Eta model and other national guidance for surface temperature (Figure 4). Both the WRF-LAPS and WRF-Eta runs exhibit a negative temperature bias (too cool) during the afternoon hours (at peak heating) and a positive temperature bias (too warm) at night. This is fairly typical for many models, including the Eta, but was much more exaggerated for the WRF forecasts.

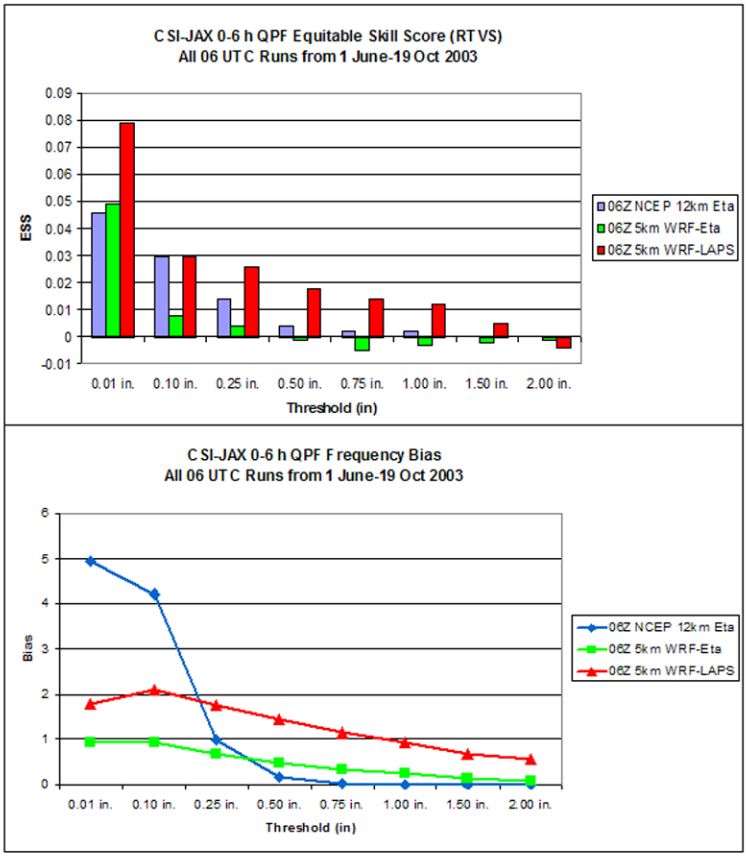

Figure 3. ESS and bias for the 0–6 hour forecast period from the NCEP Eta, CSI WRF-Eta, and CSI WRF-LAPS.Statistics are from RTVS for 1 June–19 October 2003.

However, it is important to remember that the Eta model and its associated postprocessed fields (e.g., 2-m temperature) has undergone extensive tuning since its implementation several years ago, whereas the WRF model is new and was used in an "off-the-shelf" configuration. Officially, WRF is not yet considered to even be a research-grade model. Despite the deficiencies in forecasting surface temperatures, its performance in other categories is still quite encouraging given the state of its development. The problems with the temperature forecasts warrant some investigation into the implementation of the PBL, land surface, and radiation schemes and their interactions within the WRF model.

Conclusions and Future Work

Despite the challenges faced in implementing the WRF model as a quasi-operational tool within the Weather Forecast Office, this project has made progress in answering the questions posed in the Introduction. The quantitative statistics and anecdotal evidence show that local models can and do add value in the local forecast process, particularly in the area of QPF and wind forecasts. For short-term forecasts (0–6 hours), initializing these models using additional local data appears to provide even more value. For longer term forecasts, lateral boundary conditions tend to dominate the source of forecast error for such small domains as the Coastal Storms Initiative area, but in some cases (e.g., wind speed), the additional resolution of the model appears to still provide advantages.

Finally, even though it is in the early stages of development, the performance of the WRF model is very encouraging. Groundwork laid by the CSI project may serve as a foundation for developing a standardized WRF-based local numerical weather prediction package suitable for use in all NWS WFOs. We hope to continue upgrades to the Jacksonville WFO system, including the addition of the wideband WSR-88D reflectivity and radial velocity data from Jacksonville and surrounding offices, GPS total precipitable water retrievals, ACARS data, and local wind profilers, all of which are currently supported by the version of LAPS being used but are unavailable to the cluster at the time of writing. A second evaluation period during the winter may also provide useful verification data to assess WRF performance in a different weather regime.

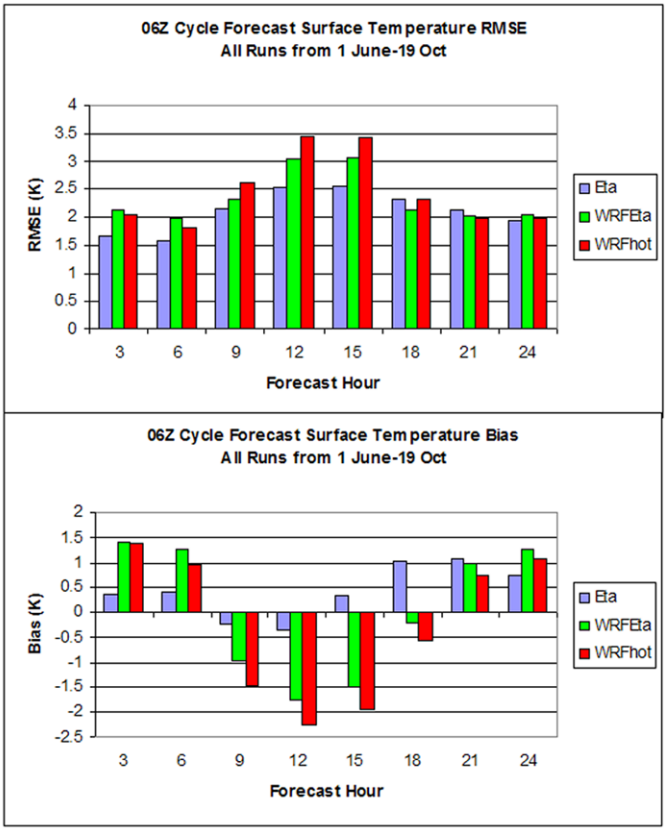

Acknowledgments *– Special thanks to the following collaborators in this project: P. Welsch and A. Wildman, NOAA NWS Weather Forecast Office, Jacksonville, FL.; J. Savadel, NOAA NWS Office of Science and Technology, Silver Spring, MD; and P. Bogenschutz and P. Ruscher, Florida State University, Department of Meteorology, Tallahassee, FL.*

Editor's Note: A complete list of references and more information on this and related topics are available at the main FSL Website www.fsl.noaa.gov, by clicking on "Publications" and "Research Articles."

(Brent Shaw is a researcher in the Local Analysis and Prediction Branch headed by Dr. John McGinley. He can be reached at Brent.Shaw@noaa.gov, or 303-497-6100.)

Figure 4. RMSE and bias for the Eta, WRF-Eta, and WRF-LAPS surface temperature forecasts for all forecast hours of the 06 UTC runs from 1 June through 13 October 2003.

The Value of Wind Profiler Data in U.S. Weather Forecasting –

By Steven E. Koch, Stanley G. Benjamin, Barry E. Schwartz, and Edward J. Szoke

Introduction

FSL has operated a network of 404-MHz full tropospheric profilers within the NOAA Profiler Network (NPN) since 1992. The Profiler Program was inaugurated in 1986 with a congressional initiative for a Wind Profiler Demonstration Network. The mission was "to develop, deploy, and operate a network of 30 wind profilers in the central United States and, in cooperation with the National Weather Service (NWS) and other agencies, conduct an assessment of that network." These profilers operate today over the central United States, with the exception of a few in Alaska and elsewhere (Figure 1).

Wind measurements are produced at 36 range gates along each of three orthogonal beams (zenith and 16.3 degrees off-zenith in the east and north directions) in both a low mode pulse width with 320-m resolution below 9.25 km and in a high mode from 7.5 to 16.25 km with 1000-m resolution. These data are then combined to produce wind profiles every 6 minutes with a reporting increment of 250 m. After the application of additional quality control and averaging measures, hourly wind profiles are obtained. These data are then assimilated into the Rapid Update Cycle (RUC), Eta, and Global Forecast System (GFS) models at the National Centers for Environmental Prediction (NCEP).

The delivery rate of wind profiler data from FSL to the NWS has steadily increased since 1992, with rates currently approaching 97% (Figure 2). Such a high level of reliability is required for operational numerical weather prediction. The blueprint for high data availability includes redundant hardware and communications links to the profilers, the installation of remote breaker resets to power cycle the site, and monitoring of profiler status after hours.

This article presents a comprehensive assessment of the value of profiler data from the NPN in both numerical weather prediction and subjective weather forecasting. A series of experiments using the RUC model was conducted for a 14-day period. Data from profilers and from ACARS (Aircraft Communication

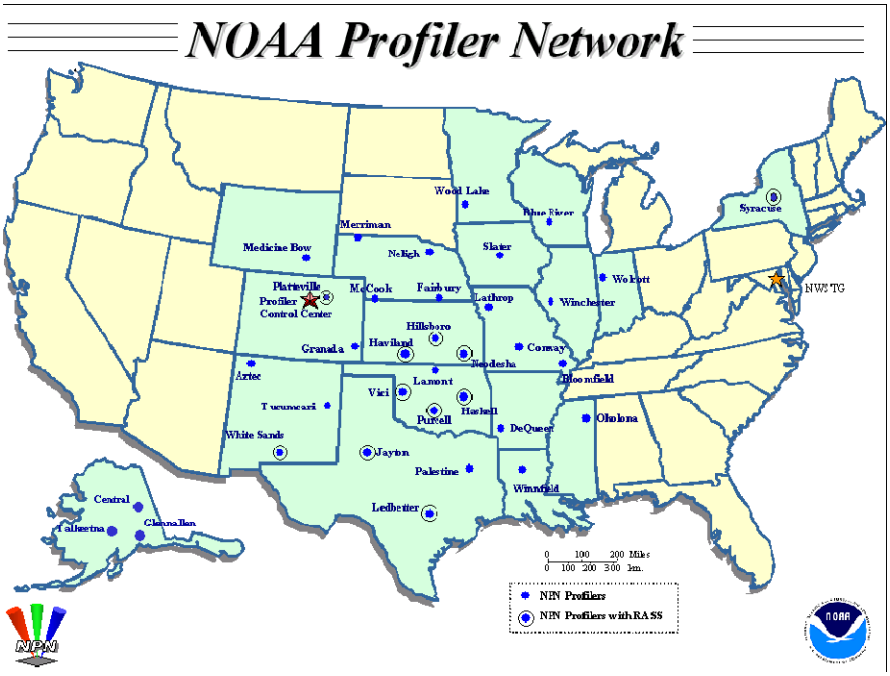

Figure 1. The NOAA Profiler Network as of August 2003. All sites are 404 MHz systems, with the exception of Platteville, Colorado; Syracuse, New York; and the three Alaska sites (449 MHz). Circled sites also have a Radio Acoustic Sounding System (RASS).

and Reporting System) reports were separately denied in the RUC in order to assess the relative importance of the profiler data for short-range wind forecasts. A more drastic data denial experiment in which all observational data were withheld was also performed as a "worst case" calibration. The value of the data on the forecasts was determined by comparing the forecasts to radiosonde observations.

Two case studies are presented that illustrate the value of the profiler observations for improving weather forecasts. The first case study assesses the importance of profiler data in the RUC model runs for the 3 May 1999 Oklahoma tornado outbreak. The second examines the impact of profiler data in RUC forecasts associated with a severe snow and ice storm that occurred over the Central Plains on 8–9 February 2001. We also summarize an analysis on how NWS forecasters use profiler data to see whether operational use of these data support the results from the two case studies and the statistical model impact study.

RUC Numerical Weather Prediction Impact Study

The 20-km operational RUC model with 50 hybrid isentropic-sigma vertical levels was used in the model impact experiment. The RUC uses an hourly intermittent assimilation cycle, allowing full use of hourly profiler (and other high-frequency) observational data in the RUC three-dimensional variational system (3DVAR). The 14-day experiment began at 0000 UTC 4 February 2001 with the background provided from a 1-hour RUC forecast initialized at 2300 UTC 3 February. Lateral boundary conditions were specified from the NCEP Eta model initialized every 6 hours and available with 3-hour output frequency. The high-frequency observations used in the RUC experiments described here include those from wind profilers, commercial aircraft, Doppler radar velocity azimuth display (VAD) wind profiles, and surface stations.

Verification was performed using conventional 12-hourly radiosonde data over the three domains: the

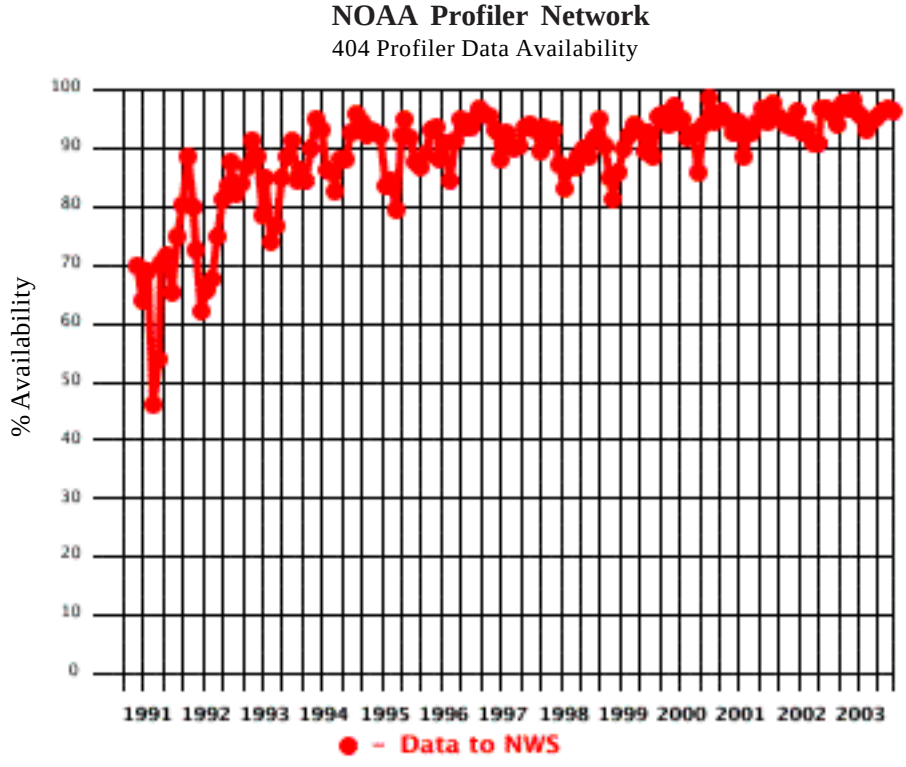

Figure 2. Hourly rate of availability of profiler data plotted on a monthly basis from 1991–2000. Data provided by the NPN hub at FSL to the National Weather Service.

The Value of Wind Profiler Data in NWS Operations *(continued)*

RUC model domain, a "profiler domain," and a "downstream domain" (Figure 3). The black box outlining the profiler domain includes most of the Midwest profilers and contains 22 radiosonde sites. The area defined by the red box, referred to as the downstream domain, was chosen to depict an area that might be affected by forecasts initialized in the profiler domain due to downstream advection of information originating from the profiler data. For each experiment, RMS vector differences between forecasts and observations were computed at all radiosonde sites located within each of the three domains. These scores were then averaged over the 14-day test period. In many of the figures that follow, the statistic displayed is a difference between these average scores: the control (RUC run with all data, referred to as CNTL) minus the experiment (no profiler or no aircraft, referred to as EXP-P and EXP-A). In addition, the Student's t-test was performed on the differences between the CNTL and EXP runs to determine statistical significance of the results.

The average 3-, 6-, and 12-hour wind forecast impacts (EXP-P–CNTL) for the profiler domain show positive values from 850 to 150 hPa (Figure 4). Similar analyses for the other two domains (not shown) also exhibited positive impact of profiler data at all levels at 3 hours, but the greatest impact occurred over the profiler domain. In general, for all 3 domains, the impact decreased with increased forecast projection and fell to negligible levels by the 12-hour forecast.

A breakdown of profiler impact results by time of day over the profiler domain (Figure 5) shows that the impact is stronger at 1200 UTC than at 0000 UTC, especially above 500 hPa. This is likely the result of a lower volume of aircraft data in the 0600–0900 UTC nighttime period than the 1800–2100 UTC daytime period. This breakdown also shows that the profiler data can contribute strongly to improving wind forecasts even at jet levels and that the accuracy of 3-hour jet-level wind forecasts valid at 1200 UTC over the United States is strengthened by wind profiler data.

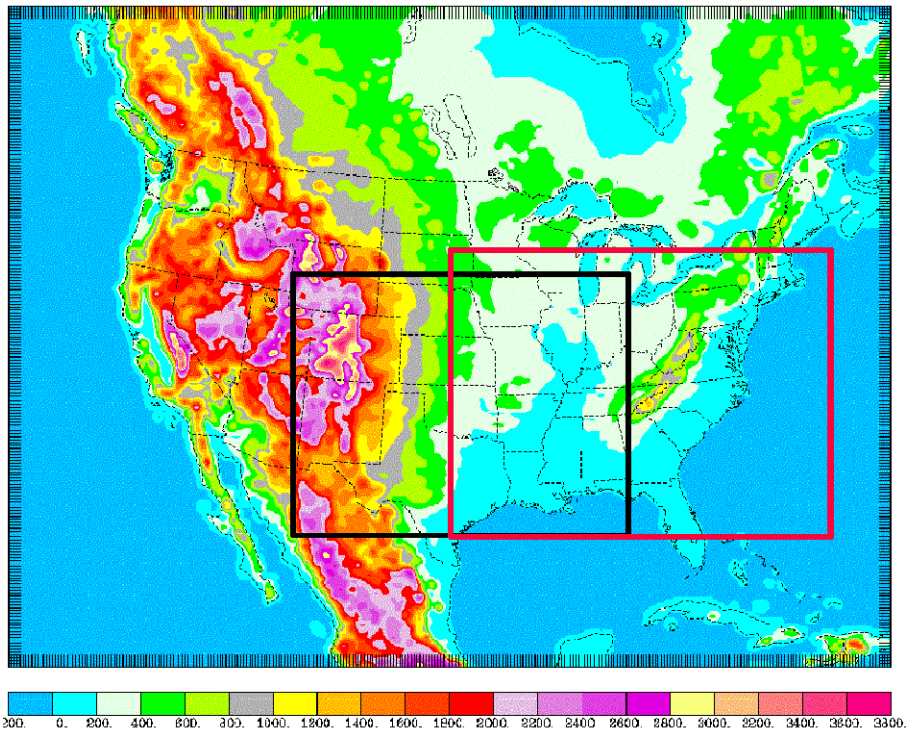

Figure 3. The full RUC20 domain with model terrain elevation (meters), profiler verification domain (black box), and downstream verification domain (red box).

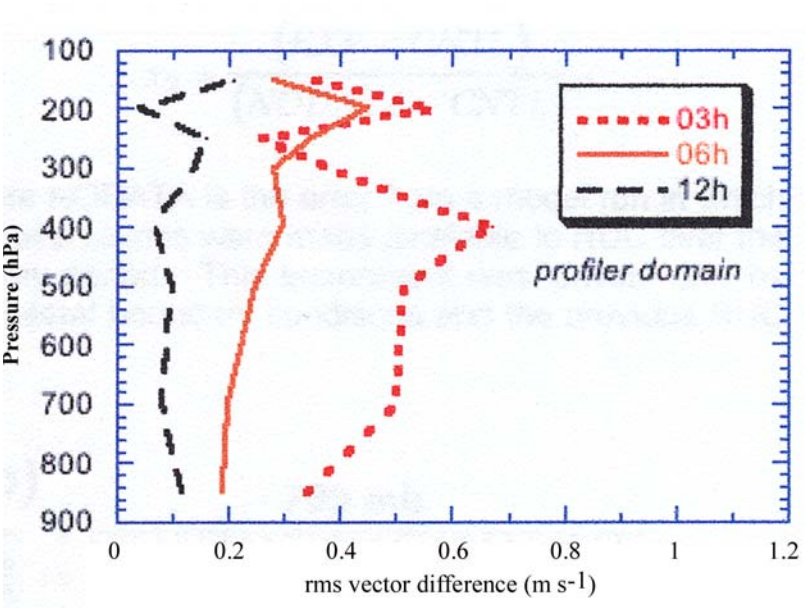

Figure 4. Effects of profiler data denial on RMSE vector errors (meters per second) over the profiler domain from RUC 3–12-hour forecasts for the 4–16 February 2001 period. Errors resulting from denying profiler data are largest for the 3-hour model forecasts and diminish with time.

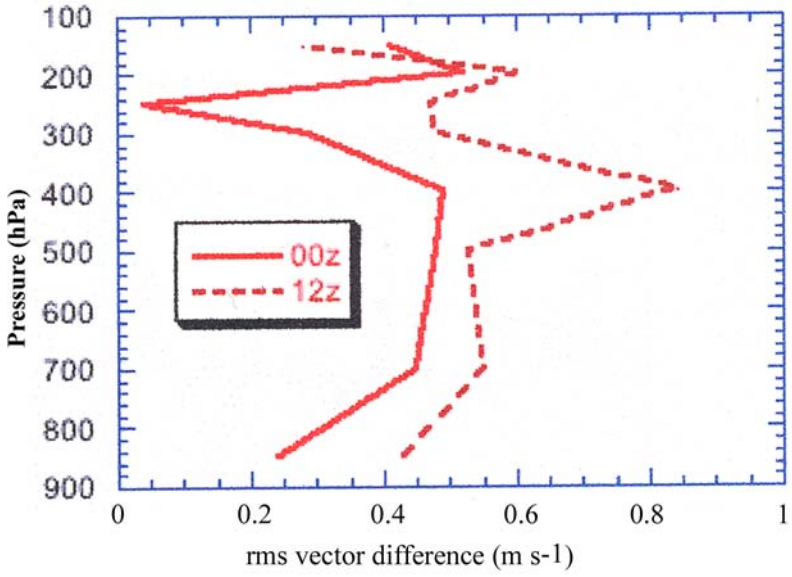

Figure 5. Diurnal variability of profiler impact (EXP-P–CNTL) on RMSE 3-h wind forecast vector error in profiler domain for 0000 UTC and 1200 UTC.

The Value of Wind Profiler Data in NWS Operations *(continued)*

Time series of profiler impact at selected mandatory pressure surfaces at each 12-hour verification time are displayed in Figure 6. Clearly, the impact from profiler data is more often than not positive from one time to the next, especially below 250 hPa. However, it also is apparent that significant day-to-day variations occur in the amount of impact. On several days, the impact is quite a bit larger than on most other days. This behavior suggests that the influence of profiler data on weather prediction depends upon the situation and underscores the importance of performing case studies to understand the manner in which these data actually influence NWP models. Two case studies are discussed below.

Automated observations from commercial aircraft over the U.S. (mostly reported through ACARS) constitute another important source of asynoptic wind data. In order to calibrate the relative impact of profiler and ACARS data on RUC short-range forecasts, the impact of data denial can be expressed in terms of percentage of forecast error. We first calculated percentage impact as

$$x_1 = \frac{(EXP - CNTL)}{CNTL},$$

where EXP is the average score for profiler or aircraft data denial experiments, and CNTL is the average forecast error score for the control experi-

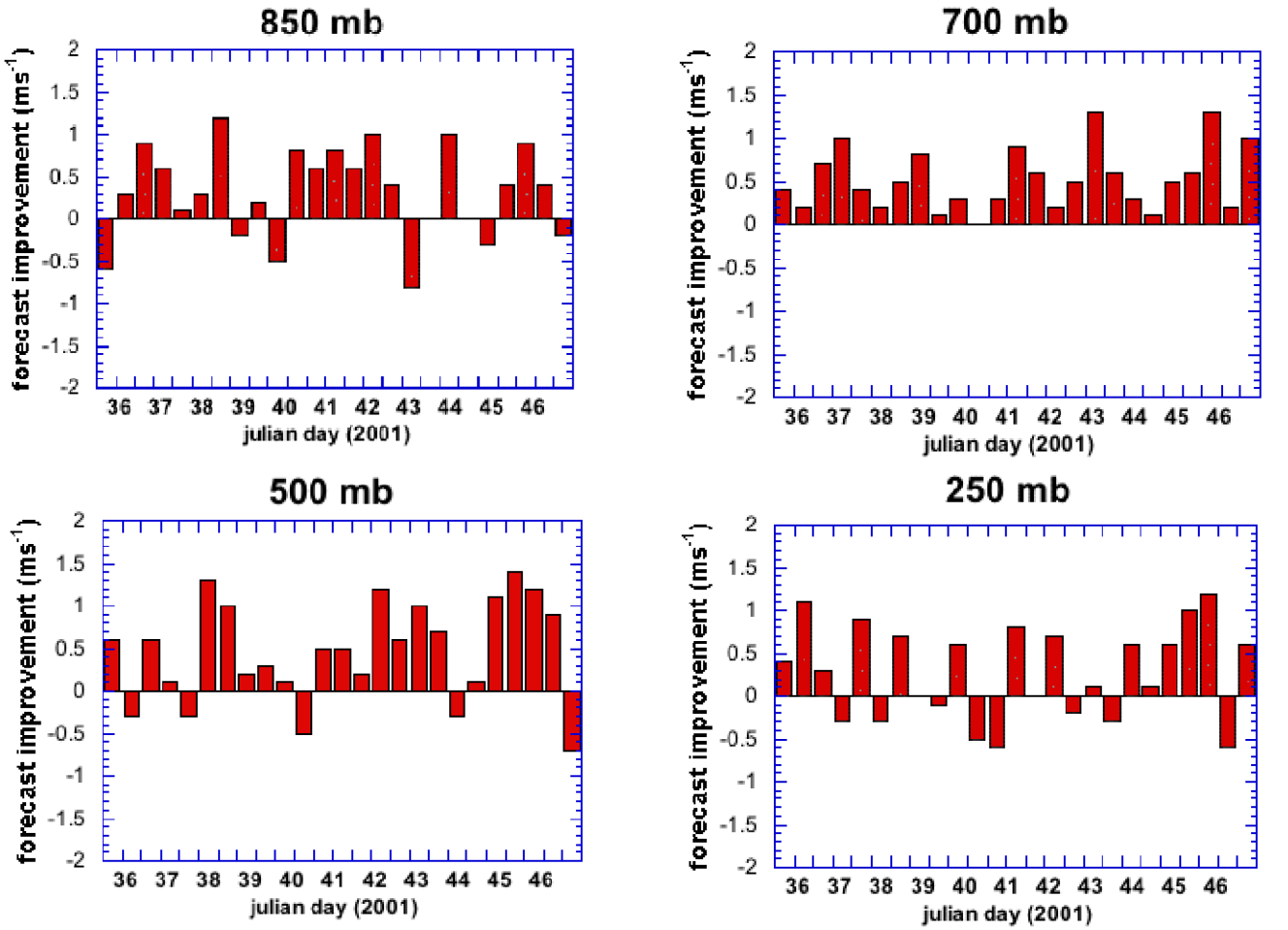

Figure 6. Difference in 3-hour wind forecast rms vector error score between EXP-P (no profiler) and CNTL (all data) from every 12-hour verification time during 4–16 February 2001 test period at indicated mandatory isobaric levels.

ment with all data used. With this normalization, profiler data were found to reduce 3-hour wind forecast error by 12–20% in the 400–700 hPa layer (Figure 7).

To determine the data impact, a second normalization – the percentage of the total observational data impact provided by a single observation type – was computed as

$$x_2 = \frac{(EXP-CNTL)}{(NODATA-CNTL)},$$

where NODATA is the error from a model run in which no observations were made available to RUC over the 14-day period. This experiment was "driven" only by the lateral boundary conditions and the previous RUC hourly analysis. Normalizing the errors as such revealed that the profiler data accounts for up to 30% (at 700 hPa) of the total reduction of wind forecast error from assimilating all observations. ACARS and profiler data offer trade-offs and are complementary to each other. The inclusion of aircraft data accounts for significant upper level forecast improvements in a shallower layer as much as 20% of the total 3-hour forecast improvement at 250 hPa. Aircraft data provide high resolution data at flight levels, generally between 300–200 hPa, and a lesser but still significant number of ascent/descent profiles. Profilers provide hourly (and even 6-minute) wind profiles, and, of course, they are not dependent on flight schedules and route structures.

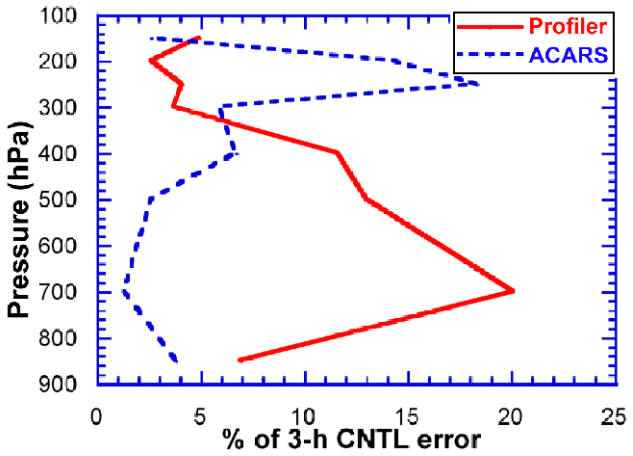

Figure 7. Normalized impact from profiler and ACARS data denial experiments for RUC 3-hour forecasts averaged for the 4–17 February 2001 test period over the profiler domain using the equation for x_1.

Regardless of how the impact is normalized, *these results show that a large proportion of the short-range wind forecast skill over the central U.S. in the RUC model is due to its use of wind profiler data and strongly suggest that similar benefits could be realized over much of the CONUS if a national network of profilers existed*. Short-range forecasts of other variables (geopotential height, relative humidity, temperature) also benefit from the assimilation of wind profiler data (error reduction of 10–18%). The improvement in such forecasts (not shown) is an outcome of multivariate effects of the RUC 3DVAR and subsequent interaction in the model.

Case Studies

Here we highlight two case studies performed with the RUC20 model (see note at end of this article for more details on these and other case studies).

3 May 1999 Tornado Outbreak – Forecasters at the Storm Prediction Center in Norman, Oklahoma, typically use profiler data to monitor evolving vertical wind shear and to issue both Convective Outlooks and Watches. Studies have shown that profiler data are often critical in determining the level of thunderstorm severity expected. The case of the Oklahoma-Kansas tornado outbreak of 3 May 1999 offers a prime example. In this event, forecasters observed considerably stronger winds at the Tucumcari, New Mexico, profiler site in the late morning of 3 May than were forecasted by any of the models. Extrapolation of these winds to the afternoon tornado threat area gave the forecasters confidence that the risk of tornadic storms with organized supercell storms would be the main mode of severe weather. Because of the likelihood of stronger vertical wind shear, the risk would be greater than the earlier forecasts based on numerical model forecast winds. With the knowledge gained from the profiler observations, the Storm Prediction Center first increased the threat in the Day One Convective Outlook from "Slight Risk" to "Moderate Risk" by late morning, and then to "High Risk" by early afternoon. Response groups such as emergency managers regard such changes seriously, and the elevated risk levels result in a more dramatic level of response to a potential tornado threat.

The Value of Wind Profiler Data in NWS Operations *(continued)*

Having these risk levels forecast in advance by the Storm Prediction Center likely resulted in increased preparedness that made it easier to handle the severe outbreak of tornadoes that followed. The NWS NOAA Service Assessment Report for the 3 May 1999 tornadoes noted the critical role that the profiler data had in improving the Convective Outlooks from the Storm Prediction Center, and recommended that the existing profiler network be supported as a reliable operational data source.

The 20-km RUC with a 1-hour assimilation cycle, excluding VAD (velocity azimuth display) winds from WSR-88D radars, was rerun for the 24-hour period 0000 UTC 3 May though 0000 UTC 4 May with (CNTL) and without (EXP) the profiler data to assess their impact on forecasts of preconvective environment parameters and precipitation over Oklahoma. The 300-hPa winds in the RUC 6-hour forecasts initialized at 1800 UTC were stronger in the CNTL experiment than the no-profiler run over a broad area including western Oklahoma and north-central Texas. In addition, the CNTL run produced ~ 50 $m^2 s^{-2}$ greater helicity values compared to the EXP run in central Oklahoma (values in the verifying analysis at 0000 UTC 4 May exceeded 250 $m^2 s^{-2}$). The tornadic storms formed in southwestern Oklahoma and propagated into the central part of the state as they matured, into an environment more favorable for supercell development according to the CNTL run.

CAPE (Convective Available Potential Energy) forecasts derived from the CNTL run experiment were also more conducive to tornadic storm activity than in the EXP no-profiler run. Forecast CAPE differences between the CNTL and EXP runs valid at 2100 UTC are displayed in Figure 8 (top and middle), and the control analysis (below). Observed CAPE values are quite large (>4,000 J kg^{-1}) in the area where the first storms formed in southwestern Oklahoma. However, the forecast error for the EXP run indicates an area of strongly underforecast CAPE from west-central Texas into southwestern Oklahoma. The CNTL run did not differ nearly as much from the analysis as the EXP run; the large improvement (by ~1,000 J kg^{-1}) is primarily the result of a northwestward shift in the location of the axis of maximum CAPE (i.e.,

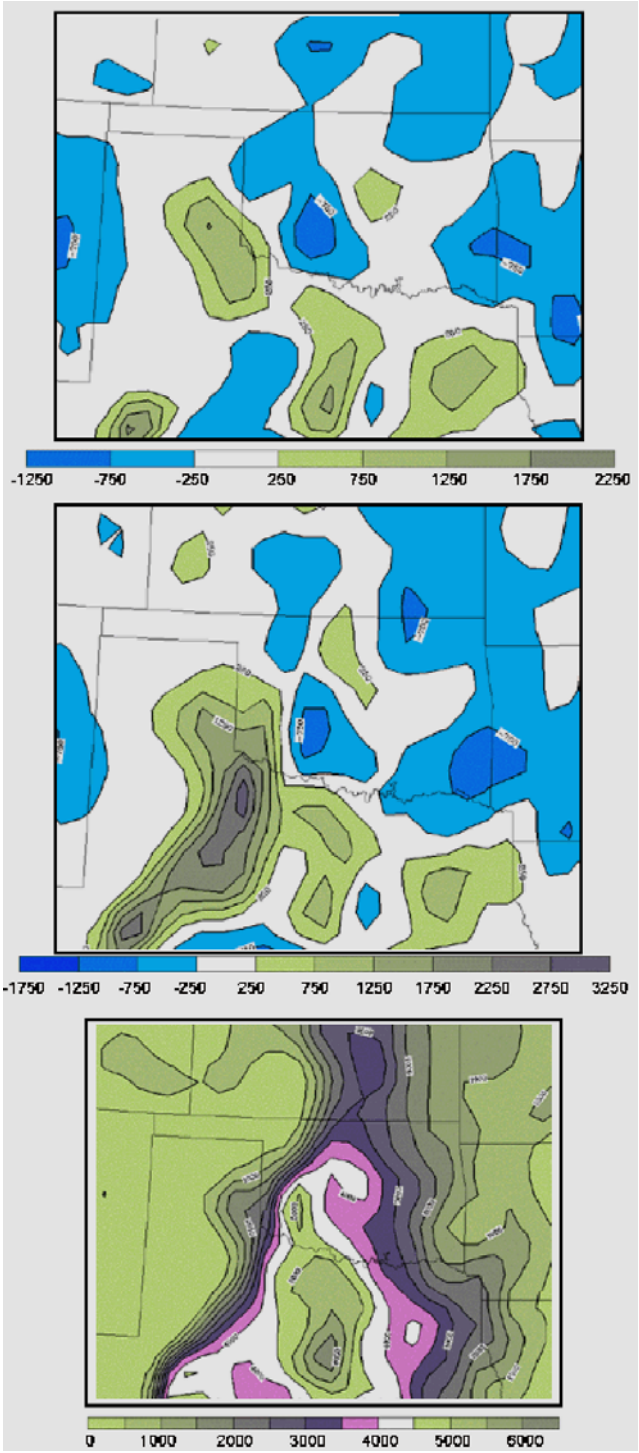

Figure 8. Three-hour CAPE forecast-analysis fields for CNTL (top) and EXP-P (middle). Analysis valid at 2100 UTC 3 May 1999 (bottom).

reduced phase error). Dewpoint temperatures in the area of the underforecast CAPE in the EXP run were as much as 3ºC lower than in the CNTL run as the result of weaker southeasterly flow in central Texas. The resulting phase shift of the maximum CAPE in the control run with profiler data brought it closer in agreement with the region where the storms initiated, which resulted in a better forecast of convective precipitation over southwestern Oklahoma.

8–9 February 2001 Winter Storm – The 20-km RUC was also used to examine the impact of profiler data for forecasts of a winter storm that brought sleet and freezing rain to south-central and eastern Kansas, and heavy snow in central and northern Kansas over the two-day period of 8–9 February 2001. This event fell within the retrospective test period used for the data denial experiments described earlier. Although this storm system was typical of winter storms in this area, some locations experienced 25–40 cm (10–16 inches) total snowfall. Snow is a prognostic quantity explicitly predicted in the RUC via mixed-phase cloud microphysics.

The synoptic situation at 0000 UTC 9 February consisted of a region of substantial upper-level forcing ahead of an approaching trough moving out of the Rockies and strong southerly flow at the surface south of a sharp, slow-moving cold front located from Kansas City to just west of Oklahoma City, stretching back to a surface low in western Texas. At this time, a band of heavy snow was moving east across west-central Kansas, while sleet and freezing rain were intensifying over south-central Kansas. RUC precipitation forecasts for the period 0000 – 0300 UTC from the CNTL experiment were more intense over the region in south-central Kansas than in the no-profiler EXP-P experiment (not shown).

A comparison of the 3-hour forecasts from the two experiments showed that the location and curvature of the front was slightly different, with a northward bulge near the Kansas-Oklahoma border in CNTL, and a fairly uniform front about 100 km southward of this location in EXP. Although these differences are not exceptional, they were important enough to result in heavier forecast frozen precipitation to the north of the front in southern Kansas than in the CNTL experiment, resulting in better overall agreement with the observations. Vertical cross sections oriented north-south across the front displayed strong southerly cross-frontal flow of 25–30 meters per second ascending upward over the front in Kansas in both experiments. However, the slantwise ascent was both sharper and deeper in the CNTL experiment, resulting in heavier precipitation about 200 kilometers north of the surface front over southern Kansas. These differences within the frontal zone appeared to be responsible for the improved precipitation forecast in the CNTL experiment. Results from these comparisons will be presented in later publications.

Profiler Data in NWS Operations

The frequent use of profiler data by NWS forecasters is indisputable. Mention of features seen using profiler displays on AWIPS (Advanced Weather Interactive Processing System) is common in the Area Forecast Discussions issued by NWS Weather Forecast Offices (WFOs). Forecasters typically use a time series display of hourly profiler winds on AWIPS, and also display overlays of profiler winds on satellite and/or radar images to better discern mesoscale detail. In addition, profiler data are often used to help verify analyses and short-range forecasts from the models, enabling forecasters to judge the reliability, in real time, of the model guidance.

Profilers are located near many WFOs in the Central and Southern Regions of the NWS. In a study conducted for a presentation at the National Weather Association's Annual Conference in October 2002, the NWS Southern Region Scientific Services Division sent a survey to WFOs within the Profiler Network to inquire how the profiler data are used in operations. The examples given of profiler use are typical of those seen over the years. An additional part of the survey asked each WFO to characterize the integration of profiler data into operations on a scale of 1 to 10, with "10" meaning all forecasters know when and how to use the data and do so when appropriate, and "1" meaning, "What's a profiler?" The average response was 9, indicating very high understanding of the potential for and use of profiler data in forecaster operations.

The Value of Wind Profiler Data in NWS Operations *(continued)*

Even though the NOAA Profiler Network does not extend to the NWS Eastern Region, forecasters there have recently begun using data from a number of boundary layer profilers that have been deployed by other agencies. Data from these profilers are not available on AWIPS, but forecasters can access these boundary layer datasets through the Internet and have found them to be quite useful.

The 3 May 1999 case discussed earlier may be the most dramatic example of profiler impact cited by the Storm Prediction Center, but it by no means represents an isolated example of profiler use. Profiler data are not only frequently used at the SPC, but they are considered to be critical to their operations. Profilers are needed to reliably diagnose changes in vertical wind shear at lower levels as well as through a deep layer (through 6 km AGL), both critical to determining potential tornado severity. Profiler data are also used to better determine storm motion, critical in distinguishing stationary thunderstorms that produce flooding from fast moving severe thunderstorms that produce severe weather. Profilers help forecasters to better determine storm relative flows and, consequently, the character of supercells.

Profiler winds are critical for monitoring the low-level jet life cycle, an important factor in mesoscale convective system development, and therefore the threat for flooding and/or severe weather. It is worth mentioning that profilers are unique in their ability to provide high-frequency full-tropospheric winds compared to radiosonde and VAD data. Though Doppler radar-derived VAD winds also provide such resolution, they cannot monitor deeper level vertical wind shear, information that the Storm Prediction Center deems critical to performing its forecast tasks. The SPC has added use of the 6-minute profiler data since 2000 to better monitor conditions with rapidly evolving severe weather.

Conclusions

Average verification statistics from a 14-day test period indicate that the profiler data have a positive impact on short-range (3–6-hour) forecasts over a central U.S. domain that includes most of the profiler sites as well as immediately downwind of the profiler observations. Averaged over time of day, the profiler data most strongly reduce the overall vector error in the troposphere below 300 hPa, where there are relatively few automated aircraft observations. At night when fewer commercial aircraft are flying, profiler data also contribute strongly to more accurate 3-hour forecasts at jet levels. For the test period, the profiler data contributed up to 30% (at 700 hPa) of the overall reduction of 3-hour wind forecast error by all data sources combined.

Comparisons made between experiments in which profiler data were withheld and a second experiment in which all aircraft data were withheld show the complementary nature of the two types of observations. The picture that emerges from this study is a composite high-frequency observing system, with profiler observations contributing more to improvement through the middle and lower troposphere, and aircraft observations contributing more strongly at jet levels. Profiler observations fill gaps in the ACARS/aircraft observing system, with automated, continuous profiles 24 hours per day with no variations over time of day or day of week (package carriers operate on a much reduced schedule over weekends). Profiler data are available (or could be) when aircraft data may be more drastically curtailed, owing to national security, as in the 11–13 September 2001 terrorist event, or as occurred in such severe weather events as the East Coast snowstorm of 15–17 February 2003. Profiler observations also allow improved quality control of other observations from aircraft, radiosonde, radar, or satellite.

Although the average statistical NWP impact results are compelling evidence that the profiler data do add value to short-range (0–6-hour) NWP forecasts, the value ranges from negligible (often on days with benign weather), to much higher, usually on days with more difficult forecasts and active weather. This day-to-day difference was evident in breakdowns of profiler impact statistics to individual days and to peak error events. These breakdowns were made to accompany the conglomerate statistics that generally mask the stronger impact that occurs when there is active weather and a more accurate

forecast is most important, and suggest the need to conduct case studies of profiler impact. Two case studies were presented that illustrate the value of the profiler observations for improving weather forecasts.

The first case study indicates that inclusion of profiler data in the RUC model runs for the 3 May 1999 Oklahoma tornado outbreak improved model guidance of convective available potential energy (CAPE), 850–300 hPa wind shear, 0–3 km helicity, and precipitation in southwestern Oklahoma prior to the outbreak of the severe weather. In the second case study, inclusion of profiler data on 8–9 February 2001 improved RUC precipitation forecasts associated with a severe snow and ice storm that occurred over the Central Plains of the United States. Assimilation of profiler data resulted in a better forecast of the strength of the lower level southerly flow overrunning a strong cold front, resulting in a narrow band of strong postfrontal upward motion. The outcome of this improved depiction of the transverse circulation in the frontal zone was a more accurate forecast of sleet and snow in Kansas, 200 kilometers north of the surface front. More case studies of this kind would likely provide more understanding of the ways in which wind profiler data affect atmospheric predictability.

Summaries of NWS forecaster use of profiler data in daily operations support the results from these two case studies and the statistical forecast model impact study. Profiler data are widely used and have become an important part of the forecast preparation process. Profilers produce the only full-tropospheric wind data available on a continuous basis over the U.S., and as discussed above, could possibly be the only data that would be available during extreme weather events or a national security event that would ground commercial aircraft. The critical improvements provided to short-range model forecasts and subjective forecast preparation from wind profiler data have been available only over the central U.S. and, to a lesser extent, downstream over the eastern part of the country. These benefits for forecast accuracy and reliability could be extended nationwide by implementation of a national profiler network, strengthening this recommendation made by the NWS Service Assessment Report for the 3 May 1999 tornado case. The interests that would obtain a national-scale benefit from such a profiler network include not only severe weather forecasting but also aviation, energy, space flight, and homeland security.

Editor's Note: A complete list of references and more information on this and related topics are available at the main FSL Website www.fsl.noaa.gov, by clicking on "Publications" and "Research Articles."

(Dr. Steven Koch is Chief of the Forecast Research Division. He can be reached at 303-497-5487 or Steven.Koch@noaa.gov.)

Evaluating Convective Forecasts During IHOP – *By Edward J. Szoke, John Brown, and Brent Shaw*

Introduction

From 13 May to 25 June 2002, FSL scientists were involved in the International H_2O Project (IHOP), an extensive field study covering the Southern Plains and based in Oklahoma. More than 100 people participated in the campaign to determine primarily how to improve the characterization of the four-dimensional distribution of water vapor and its application to better understand and predict convection. The four main components of the program included quantitative precipitation forecasts (QPFs), convective initiation (CI), atmospheric boundary layer processes, and instrumentation. FSL ran experimental versions of local and national scale models during IHOP to assist with nowcasting and short-range forecasting and to determine whether such models could provide useful forecast and nowcast guidance for convective weather.

FSL's Rapid Update Cycle (RUC) model, a national scale model, and the Local Analysis and Prediction System (LAPS), a smaller scale model, were used during IHOP. LAPS was designed to run onsite at a National Weather Service Forecast Office (WFO), using local analyses that take advantage of locally available data. LAPS is currently running in AWIPS at WFOs on an hourly cycle with a 10-km grid spacing. LAPS was run at a 12- and 4-km horizontal grid resolution and used to initialize some of the models that FSL ran during IHOP.

One goal of a short-range model is to provide better prediction of precipitation without a spin-up period. To aid in this goal a "Hot Start" scheme was developed using the LAPS cloud analysis to prescribe a vertical velocity profile where sufficiently deep clouds are present at initialization time. The three-dimensional dynamical relationship between mass and momentum is adjusted by the LAPS balance algorithm to force consistency with the diagnosed cloud vertical motions and allow for a smooth model start. During IHOP, a 12-km horizontal resolution MM5 hotstart initialized with LAPS was run, with a nested 4-km version covering the IHOP experimental domain (Figure 1). LAPS also was used to initialize a similar 12-km setup for the Weather Research and Forecast (WRF) model. In addition to these models initialized with LAPS, FSL ran a 10-km version of the RUC model. The RUC model employs a three-dimensional variational (3DVAR) analysis for the mass fields, and initial RUC hydrometeor fields are adjusted to correspond to base scan reflectivity patterns at the initial time, but without any modification of the initial vertical velocity field (in contrast to the hotstart method). The models run by FSL for IHOP are summarized in Table 1. (These experimental model runs are archived by UCAR at *http://www.joss.ucar.edu/ihop*.)

Evaluation of Model Performance

One of our goals during IHOP was to compile a fairly extensive subjective evaluation of the various models in real time. Objective model evaluation was done within FSL (see Brent Shaw's article on page 20). In order to perform subjective evaluation, an online evaluation form was designed that allowed the forecaster/nowcaster to document what the model was forecasting, the relationship of various forcing features to the subsequent convection forecast by the model, and the forecaster's confidence in

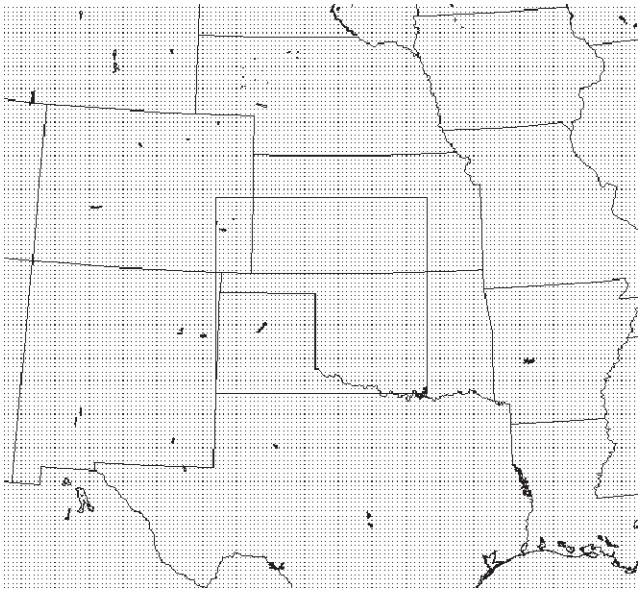

Figure 1. The 12-km and inner 14-km IHOP domains for LAPS MM5 and WRF runs (points every 12 km).

Table 1. FSL Real-Time Models in IHOP (*except LAPS-WRF, available after IHOP)

Model	Delta x km	Number Vertical Levels	Runs Every x Hour	Forecast Duration (Hours)	Convective Scheme	Microphysics
MM5hot	4	34	3	12	None	Schultz
MM5hot	12	34	3	12	Kain-Fritsch	Schultz
LAPS-WRF*	12	34	3	12	Kain-Fritsch	NCEP-5
RUC	20	34	3	6–24	Grell-Devenyi	RUC/MM5 Mixed Phase
RUC	10	50	3	6–24	Grell-Devenyi Ensemble-Closure	

the forecast. The forecasters also made many freeform comments that give insight into how the models performed with the various short-range forecast problems during IHOP. A summary of these comments follow:

• The MM5 models using LAPS for the initial state did an excellent job of initializing ongoing convection, but often this convection was lost in the first hour of simulation. Adjustments were made to the Hot Start scheme for a set of post-IHOP reruns of both MM5 and the WRF model, and our preliminary evaluation of some of these reruns indicates some improvement with this problem. The most easily "lost" convection involved elevated storms (nonsurface-based convection), while very strong individual storms and lines were much better retained from the initialization.

• Outflows tended to be easily produced from convection in the MM5 model, especially so in the 4-km run, whereas the RUC tended to be more conservative in producing outflows but was able to do so.

• The most difficult storms to forecast were elevated convection, which usually formed in the very early morning (presunrise) hours and could persist for up to 6 hours after sunrise. Coincidentally, this type of convection is also among the most challenging for forecasters, as it can occur without any obvious surface forcing feature present. Though seldom producing severe storms (at least during IHOP), elevated convective events were often of the "surprise" category. There were often indications in the model of possible activity, for example in the form of midlevel echo but without precipitation reaching the surface, so an underforecasting of the convection. Convection associated with a warm front (on the cool side of the warm front) also tended to be an area where the models were deficient. This type of convection often was not surface-based, sharing that characteristic with the elevated storms noted above.

• Some of the forecasts of convective initiation along drylines were quite good. For a few cases the model beat the forecasters, particularly when temperatures both at the surface and aloft were quite hot. In these cases, forecasters overestimated the time it would take to break the cap, while the model more correctly forecast convective initiation earlier.

• Other good forecasts occurred with well-defined surface-based forcing features, such as cold fronts.

• As noted earlier, there was some skill in the model's ability to forecast storm type and evolution, with several events during IHOP that featured upscale growth into organized lines that often accelerated much faster than indicated in the precipitation fields from conventional models (for example, the Eta model).

Selected Case Studies From IHOP

Two cases are examined using both model runs during IHOP and the reruns that occurred after IHOP. The reruns provided a series of model runs from the WRF model, which was actually run during IHOP but not able to display in real time. As a result of the real-time experiences during IHOP, we decided to apply improvements to the hotstart method to the reruns. A significant improvement involved removal of a warm bias that existed in the LAPS initialization, and was likely

Evaluating Convective Forecasts During IHOP *(continued)*

responsible for overprediction of convective precipitation during IHOP from the MM5.

2 June 2002: Dryline Case – On this day the western half of the IHOP domain was dominated by very hot temperatures, reaching the low 100s (°F) during the afternoon. A well-defined dryline was not seen initially, but was sharpened in the early afternoon, as shown by the LAPS analysis of wind and dewpoint along with low-level reflectivity in Figure 2. This sharpening first appeared as a surge of westerly surface flow that emerged out of eastern Colorado that then pushed into Kansas. On this day, the IHOP forecasters predicted that a dryline would become better defined during the afternoon (somewhat later than what occurred) but they thought convective initiation along it would occur fairly late in the afternoon as they waited for the dryline to sharpen and temperatures to break the significant cap that was in place. As it turned out, the presence of the very hot surface temperatures and a somewhat stronger and earlier dryline push than expected allowed the cap to be broken and convective initiation to occur over 2 hours ahead of the IHOP forecasters' prediction. It was noted in IHOP that the MM5 model did a good job indicating this convection earlier than expected, particularly the run initialized at 1500 UTC. Some of the runs from that day are examined and the somewhat different forecasts are contrasted for this relatively "tricky" case. With the expense of some of the resources in IHOP, in particular the aircraft, timing of convective initiation was a critical forecast issue. In this case, even a forecast error of 2 hours for convective initiation from a midmorning forecast was critical and resulted in an aborted mission, since convection was well underway before the aircraft (leaving Norman, Oklahoma) could reach the dryline target.

We first examine some forecasts initialized at 1200 UTC since reruns of both MM5 and WRF are available at this time. A forecast from the MM5 run initialized at 1200 UTC and valid at 2100 UTC is shown in Figure 3. In this and subsequent figures, when no contours are present, the model is forecasting reflectivity aloft with no precipi-

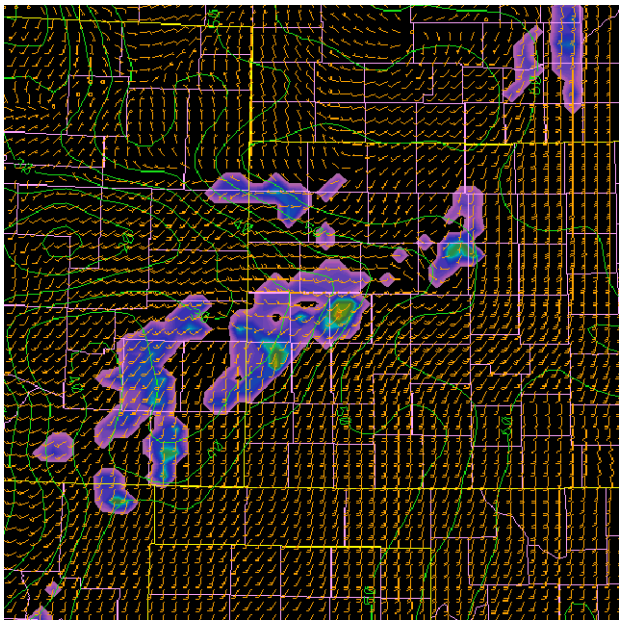

Figure 2. LAPS analysis of surface wind, dewpoint, and low-level reflectivity at 2100 UTC 2 June. The western portion of Kansas is in the center.

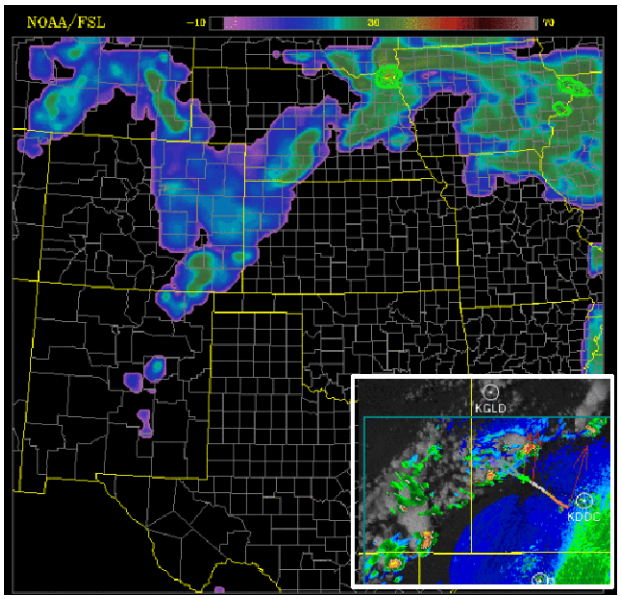

Figure 3. MM5 12-km IHOP run of 9-hour forecasat valid at 2100 UTC 2 June 2002. Image is a composite reflectivity, with contours indicating model durface reflectivity. Inset shows a composite low-level radar image at this time over western Kansas.

tation reaching the surface. For the most part, the reflectivity values for the image in Figure 3 are 30 dBZ or less. Some stronger cells are forecast for which these surface reflectivity contours are depicted (e.g., in extreme northeastern Nebraska and along the Iowa/Illinois border). The insert shows a composite low-level reflectivity image overlaid with a visible satellite image (white areas) over a region centered on western Kansas. This indicates that storms were really producing rain by 2100 UTC, with maximum reflectivities exceeding 50 dBZ. Thus, the MM5 12-km run was forecasting high-based convection that would not produce precipitation, so it correctly indicated that storms would be produced along the dryline, but was underforecasting development. For comparison, the post-IHOP rerun of the MM5 12-km model for the same time is shown in Figure 4, and for the WRF 12-km model in Figure 5. The MM5 rerun is very similar to the original MM5 12-km run during IHOP, and the WRF forecast from the 1200 UTC run valid at the same time is also very similar. All the runs indicate convective development with reasonable timing but only forecast virga-producing storms. The forecasts from these same runs valid 3 hours later at 0000 UTC on 3 June (WRF is shown in Figure 6) were very similar to the 2100 UTC forecasts, in that there continued to be no indication of storms that would produce precipitation. In reality, the line of broken storms advanced slowly to the east, and by 0000 UTC extended all the way from north-central Kansas south-southwest to the far western Texas Panhandle.

The MM5 4-km run initialized at 1200 UTC produced higher values of composite reflectivity, but still no surface reflectivity (and therefore no precipitation reaching the ground). On the other hand, the MM5 4-km run initialized 3 hours later at 1500 UTC did produce well-defined surface storms, although slower than what actually occurred and by 0000 UTC with a line of storms not far enough east (Figure 7). The MM5 12-km run for this same time made during IHOP (Figure 8) was not as bodacious with storm development as the 4-km run, but it did indicate a surface echo in the Oklahoma Panhandle,

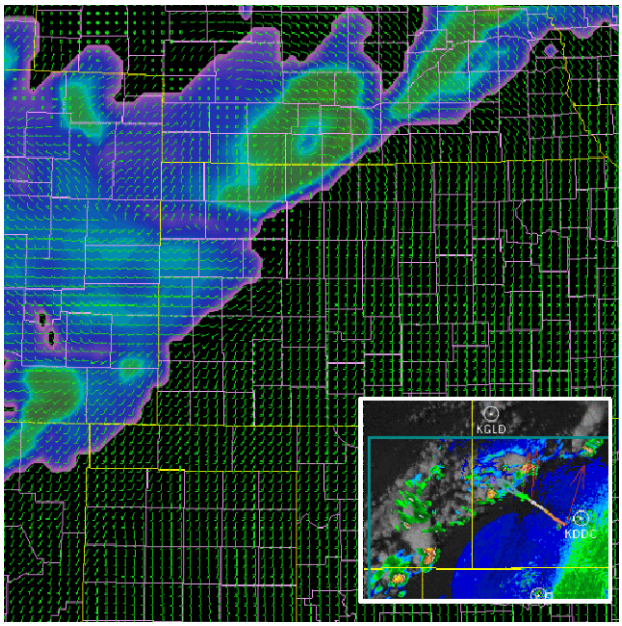

Figure 4. Same as Figure 3 except for a 9-hour forecast from the MM5 12-km rerun valid at 2100 UTC.

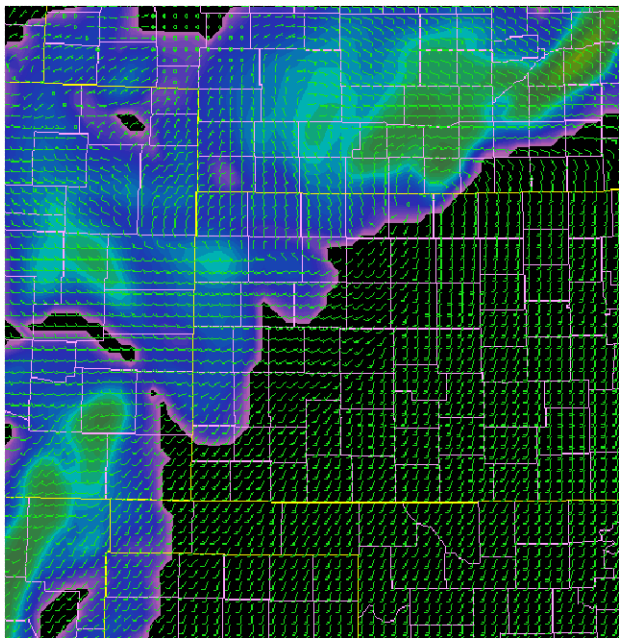

Figure 5. Same as Figure 3 except for a 9-hour forecast from the WRF 12-km rerun valid at 2100 UTC.

The color scale runs from -10 to 70 dBZ and is similar for all model figures of this type.

Evaluating Convective Forecasts During IHOP *(continued)*

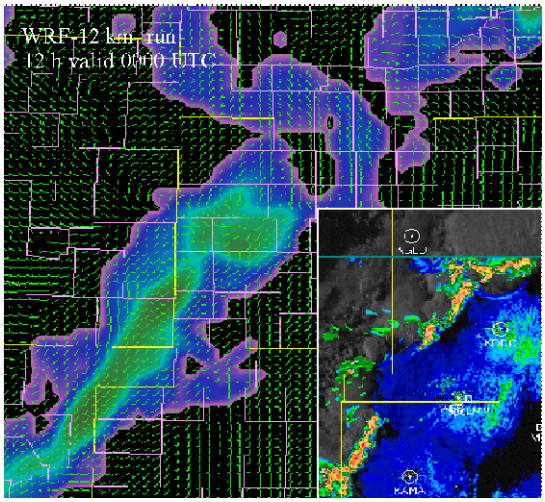

Figure 6. As in Figure 5 except a 12-hour forecaast from WRF 12-km rerun valid 0000 UTC on 3 June. The insert depicts the actual radar reflectivity at this time.

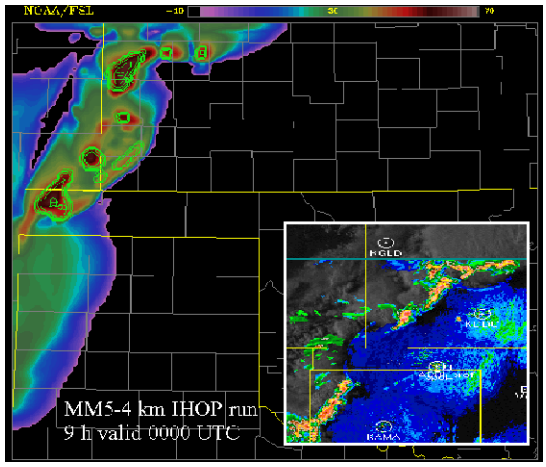

Figure 7. MM5 4-km 1500 UTC IHOP run 9-hour reflectivity forecast (as in Figure 3) valid 0000 UTC 3 June.

Figure 8. (right) As in Figure 7 except for the MM5 12-km 1500 UTC IHOP run 9-hour reflectivity forecast valid 0000 UTC 3 June.

and another much farther north along the line. The actual reflectivity at 0000 UTC is shown in Figure 9. Though the forecasts (especially the 4-km runs) that were initialized at 1500 UTC were better than the 1200 UTC ones, for some reason this improving trend did not continue with the 1800 UTC runs. The 6-hour forecasts from the various models (MM5 4-km, MM5 12-km IHOP run, MM5 12-km rerun, and WRF 12-km rerun) are shown in Figure10 (a–d). The MM5 4-km run still correctly produces a surface echo, but there is less an of echo than was in the forecast from the 1500 UTC run, and the line of echoes is even farther west. The MM5 12-km runs (Figures 10b and c) are quite similar to each other, and neither predicts any surface echo. Recall that the 1500 UTC 12-km IHOP run (Figure 8) actually did predict an echo reaching the surface by 0000 UTC, so the forecast initialized 3 hours later is not as good, similar to the behavior of the 4-km run. Note that the WRF 12-km rerun (Figure 10d) is actually a little drier than the MM5 12-km rerun and similar to the WRF 12-km rerun from 1200 UTC.

In summary, for this case the models showed a dryline moving into western Kansas more or less as occurred. The main message from the model runs is that convection would be initiated by the dryline, but the storms would be weak without any surface rain, typical of high-based, mostly dry convection that might occur on such a hot day with marginal moisture. The 4-km MM5 runs accurately indicated that more substantial storms could occur that would produce surface precipitation, and in particular the rerun initialized at 1500 UTC was the closest to reality. In real time during IHOP forecasters saw the 4-km run but

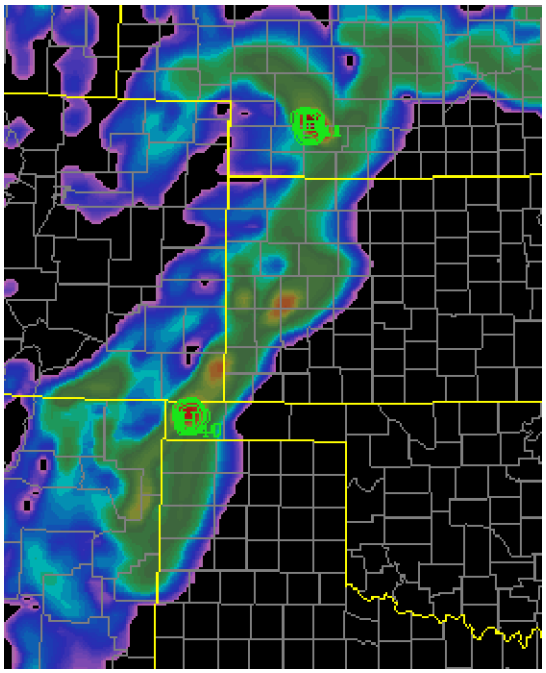

doubted that such echoes could develop with the environment that appeared to be in place, opting for a forecast of later and weaker storm development than indicated by the model (or than actually occurred). We are not certain at this stage of our research why the runs initialized at 1800 UTC did not perform as well as those initialized 3 hours earlier.

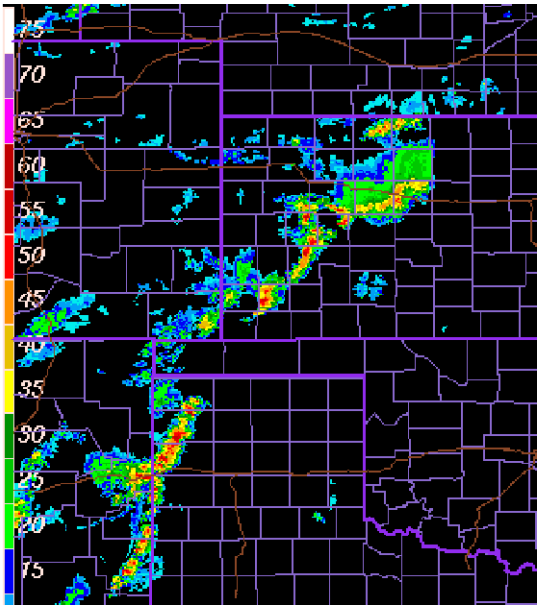

Figure 9. Observed low-level radar reflectivity at 0000 UTC 3 June.

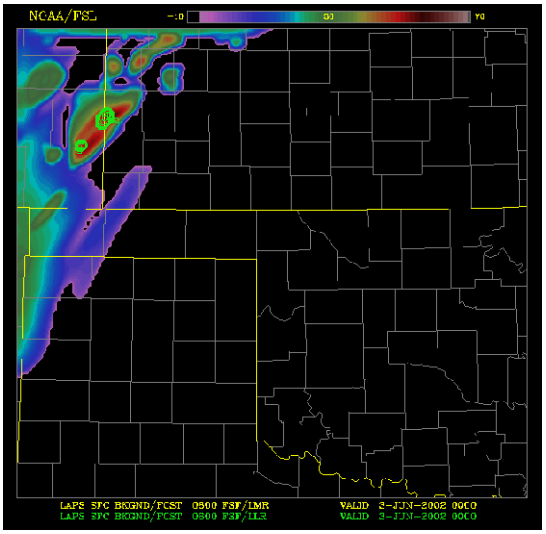

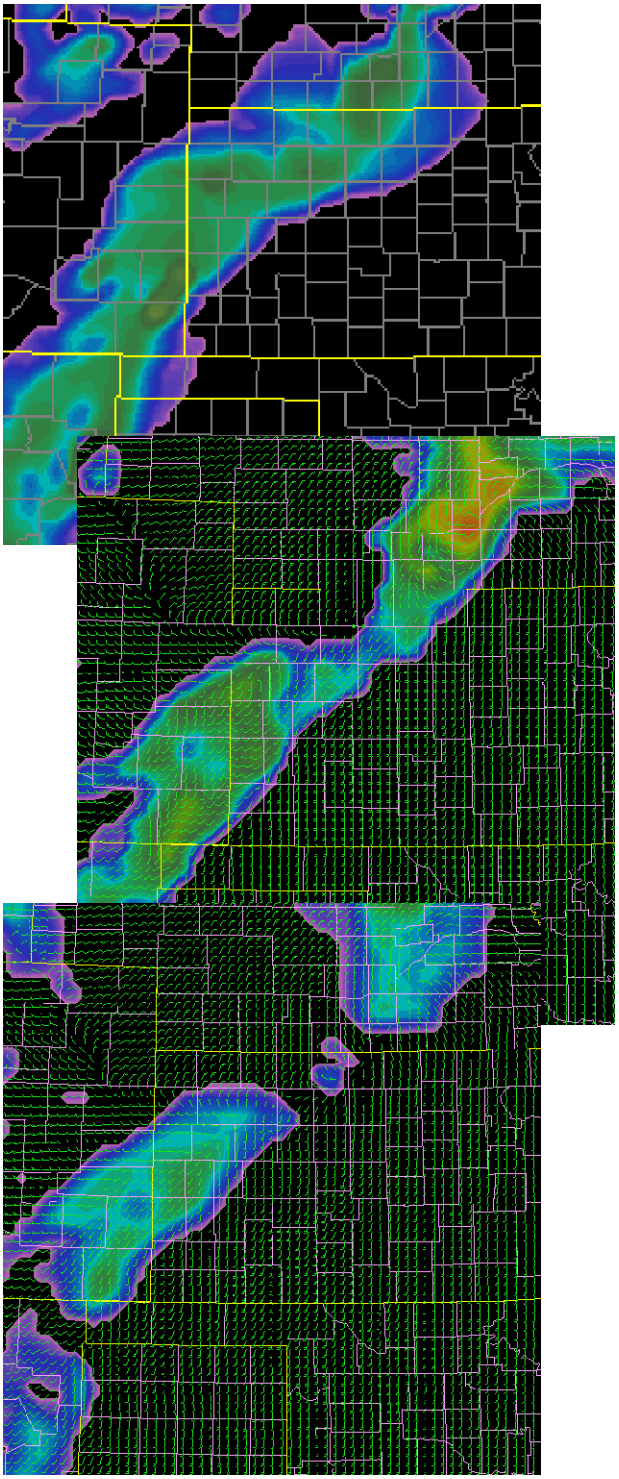

Figure 10. a, left bottom) MM5 4-km 1800 UTC IHOP run 6-hour reflectivity forecast (as in Figure 7) valid 0000 UTC 3 June. b, right top) As in 10a except for MM5 12-km run. c, right center) As in 10a except for MM5 12-km rerun. d, right bottom) As in 10a except for WRF 12-km rerun.

Evaluating Convective Forecasts During IHOP *(continued)*

15 June 2002: Complex Case – All forms of convection were evident in the 15 June 2002 IHOP case. This single day began with early morning elevated storms, evolving into a supercell storm that eventually produced a tornado, moving to upscale growth of strong cells into an organized line that bowed and accelerated southward out of the domain. The actual focus of IHOP operations on this day concerned where convective initiation would occur along a dryline feature, which, like the rest of this case, was a fairly complex feature with a double structure.

In examining the performance of the various models, we will concentrate here on the convective types that occurred rather than specifics of the dryline. Widespread development of elevated convection over the Texas Panhandle between 0800–0900 UTC was a forecast issue for an early IHOP flight to investigate a low-level jet. The storms eventually exceeded reflectivities of 50 dBZ at low levels, and persisted well into the daytime hours (until around 1600 UTC). Fortunately, as forecast by the Storm Prediction Center, the storms did dissipate, allowing the rest of the day to become a very interesting IHOP case. However, the development of the storms was not anticipated by IHOP forecasters, and as is typical in cases of elevated nighttime convection, was a difficult forecast problem. A radar overview of the storms is presented in Figure 11. The model simulations from the 0600 UTC runs are depicted in Figure 12.

At 0600 UTC (not shown) a couple of surface-based storms formed at the southern end of the Texas Panhandle, developing earlier in New Mexico and moving eastward. These storms (shown in Figure 11) continue to move southward with time. It is interesting that the Hot Start method nicely initialized the LAPS runs (MM5 and WRF) correctly with an echo at 0600 UTC, but the echo was mostly lost within the first hour. Although loss of the initial echo was a problem for other 0900 UTC cases during IHOP and is the subject of ongoing work with the Hot Start procedure, it appears particularly acute in situations like this, where nighttime surface conditions would not support surface-based storms. The area of elevated storms developed north of the longer lived echoes, and remained more or less in the same area, peaking around 1200 UTC and diminishing rapidly after 1600 UTC. All three of the model simulations shown in Figure 12 that were initialized at 0600 UTC do develop some mid-level echo, but for the most part, it is not in the Texas Panhandle specifically, and is certainly slow to develop (for example, note the lack of any echoes at

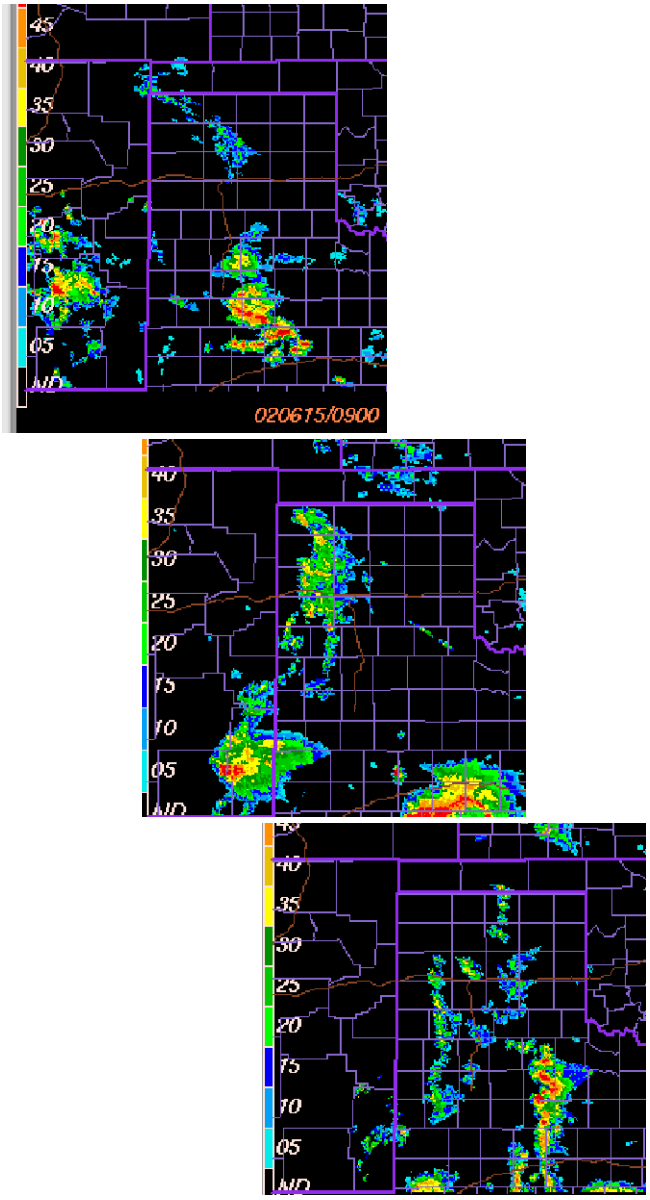

Figure 11. Low-level reflectivity composites. Two strong surface-based storms are shown at the south end of the area (top and middle, 0900 UTC), as elevated convection develops to the north over the Texas Panhandle (bottomm 1500 UTC).

0900 UTC). There are contrasting forecasts among the three models, though, and apparent attempts at forecasting the elevated storms. The MM5 12-km run shows some significant surface echoes, though the southernmost storm moved out of New Mexico apparently in the same manner as the earlier strong storms. The more northern cells develop in southeast Colorado and may well be the models' forecast of elevated type storms. The MM5 4-km run also shows these more northern storms extending in a broken line from northwest to southeast. It is not certain what forced this line, but it could be more of a development along a warm frontal type boundary that was actually positioned somewhat farther east and north. The WRF 12-km model appears to come closest to positioning the mid-level echo correctly in the Texas Panhandle, although it underpredicts the strength of the storms with only limited surface reflectivity. (For the WRF model the image shows surface reflectivity of 20 dBZ and above, with the white contours showing values below 20 dBZ.)

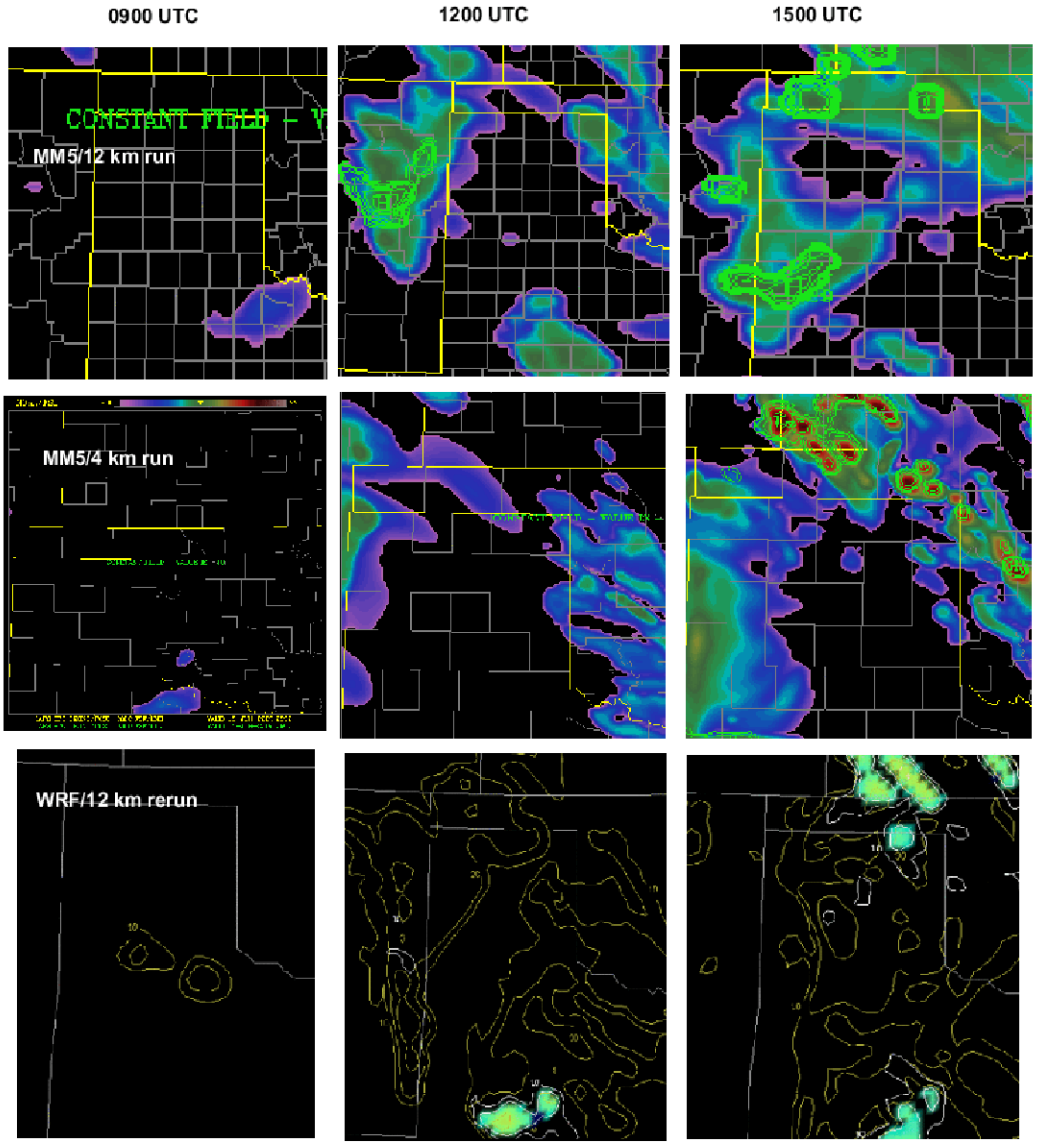

Figure 12. Model simulations from the 0600 UTC 15 June runs of the MM5 12-km (top row), MM5 4-km (middle), and WRF 12-km (bottom) for the elevated convection in the Texas Panhandle. Reflectivity is displayed as before for the MM5 models, while the WRF contours show a composite and image surface reflectivity.

Evaluating Convective Forecasts During IHOP *(continued)*

The next feature of interest is whether the models could predict a long-lived echo that formed from a group of small cells east of Denver (near Limon) at 1500 UTC that gradually grew as they moved east, with more or less one main storm by 1800 UTC that then turned to the right as it moved into western Kansas (see the reflectivity images in Figure 13). This storm became supercellular but did not produce a tornado until 2100 UTC after it intersected a pre-existing north-south dryline (the IHOP focus) and then moved southward along it. Although the resolution of the model runs at 12 km (and to a lesser extent, 4 km) would appear to be too coarse to successfully forecast an individual storm, some surprisingly excellent forecasts have been made with a 10-km version of the MM5, so we were interested to examine the models for this event.

For this case the storm formed beyond the domain of the MM5 4-km model, and shown in Figure 13 are forecasts from the MM5 and WRF 12-km models rerun after IHOP using some improvements to the hotstart method. The runs are both initialized at 0600 UTC so the forecasts shown begin 15 hours into the run. Both runs seem to develop storms by 1500 UTC in the correct location in eastern Colorado, strengthening the storm and moving it at about the right speed to near the Colorado/Kansas border by 1800 UTC. The model then continues to strengthen the echo and turns it to the right, in pretty good agreement with the actual behavior. The MM5 rerun tends to have a more concentrated and stronger surface echo then the WRF, but both have fairly impressive forecasts considering the one valid at 2100 UTC is a 21-hour forecast. The IHOP MM5 12-km run (which extended to 12 hours) from 0600 UTC was not as successful as the MM5 rerun, but had a weaker echo in about the same location. For unknown reasons, the forecasts from the IHOP runs initialized for 0900, 1200, and 1500 UTC were not very good in forecasting this long-lived system. Even the IHOP MM5 12-km 1800 UTC run, with the storm already in progress, did not have a good forecast as it tended to lose the initialized storm for the most part by 1 hour into the forecast.

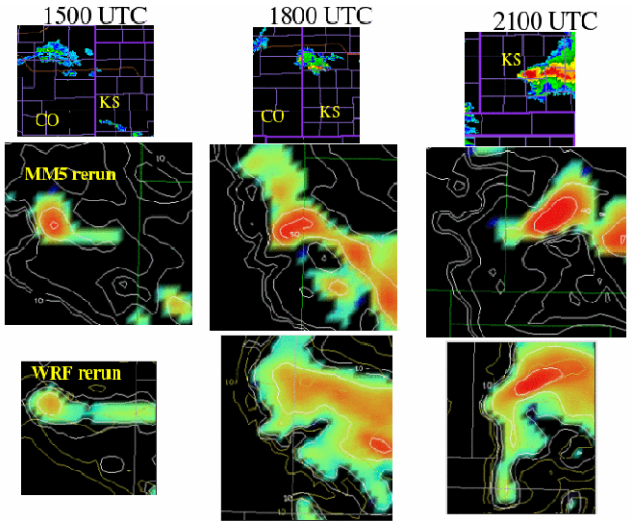

Figure 13. Comparison of the 12-km resolution MM5 and WRF model reruns initialized at 0600 UTC on 15 June with composite low-level reflectivity (top row). Model images and white contours are surface reflectivity (image is 20 dBZ and greater), with dimmer contours composite reflectivity.

In summary, results are mixed for this aspect of 15 June; on one hand the 0600 UTC runs indicate some fairly impressive predictability, but inability to repeat this predictability for the IHOP runs closer to the event is curious. We hope to compare MM5 and WRF reruns from 1200 UTC to the 0600 UTC reruns to see if the storm was still forecast for these later model runs.

The final portion of the 15 June 2002 case that is examined involves the organization of three areas of convection into a squall line by 0000 UTC on 16 June that then accelerates southward out of the IHOP domain by 0600 UTC. A radar overview of this evolution is shown in Figure 14. At 1800 UTC the organized storm discussed earlier is just crossing into western Kansas, and at 2100 UTC is at the western end of the line segment located in southwestern Kansas. By 0000 UTC a line extends from northern Oklahoma west-southwest into the Texas Panhandle, with the eastern portion developed from the area of cells that moved south out of Nebraska. After 0000 UTC, the line organizes and accelerates as it bows over western to south-central Oklahoma. The model forecasts from the 0600 UTC reruns of the MM5 12-km are shown in Figure 15 and the WRF 12-km forecasts are shown in Figure 16. The MM5 organizes a group of cells

in Kansas at 2100 UTC into a line segment close to where it is actually found at 0000 UTC, then accelerates the line southward. Although the actual line moves faster than the forecast, the track is similar and the model forecast includes a bowing line as observed. Considering that the later period of this forecast is an 18–24 hour forecast, it is fairly impressive, with the model doing a very good job of forecasting the organization into an accelerating, bowing line. This line forms in about the right place even though the MM5 essentially misses all of the storms that around 0900 UTC began to form in a north-northwest to south-southeast line from central Kansas to west-central Nebraska. These storms continued to expand in about the same place, and appear to have been, at least initially, somewhat elevated type storms that developed just ahead of a warm frontal boundary. The earlier times of this MM5 forecast never included anything but some mid-level reflectivity, and even then it was west of where the line actually occurred. The difficulty in handling convection that may not have been surface-based or forced by a distinct low-level boundary is similar to the problems that all of the models had with the elevated convection in the Texas Panhandle discussed earlier.

A similar set of forecasts from the WRF 12-km rerun is shown in Figure 16. The WRF forecasts have a little more surface reflectivity than the MM5 forecasts, but like the MM5 run also misses the warm frontal convection discussed earlier. By 0000 UTC (compare Figures 15c

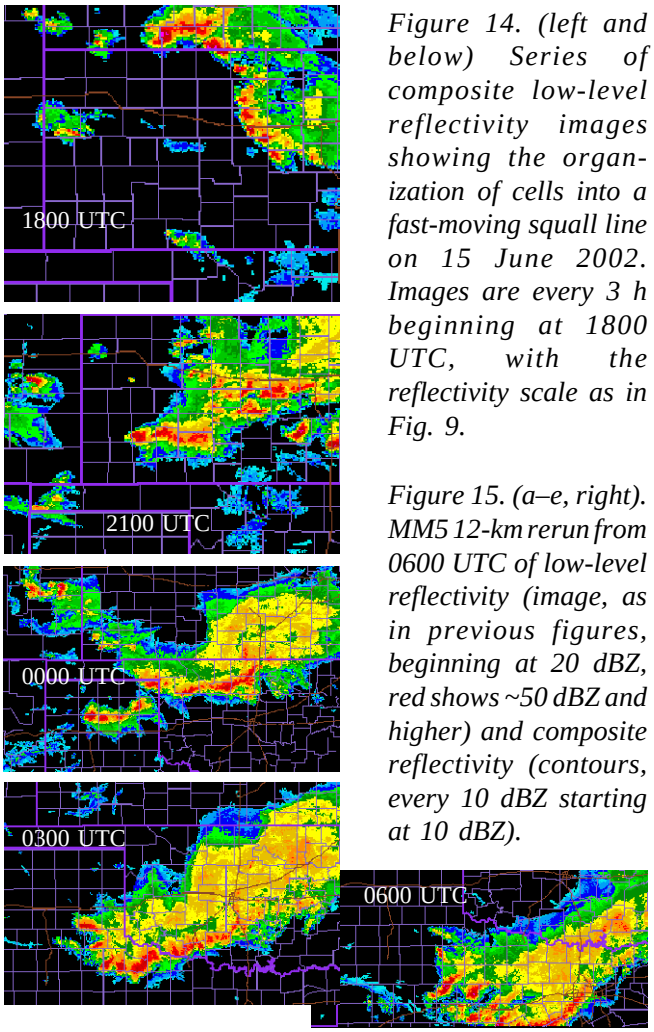

Figure 14. (left and below) Series of composite low-level reflectivity images showing the organization of cells into a fast-moving squall line on 15 June 2002. Images are every 3 h beginning at 1800 UTC, with the reflectivity scale as in Fig. 9.

Figure 15. (a–e, right). MM5 12-km rerun from 0600 UTC of low-level reflectivity (image, as in previous figures, beginning at 20 dBZ, red shows ~50 dBZ and higher) and composite reflectivity (contours, every 10 dBZ starting at 10 dBZ).

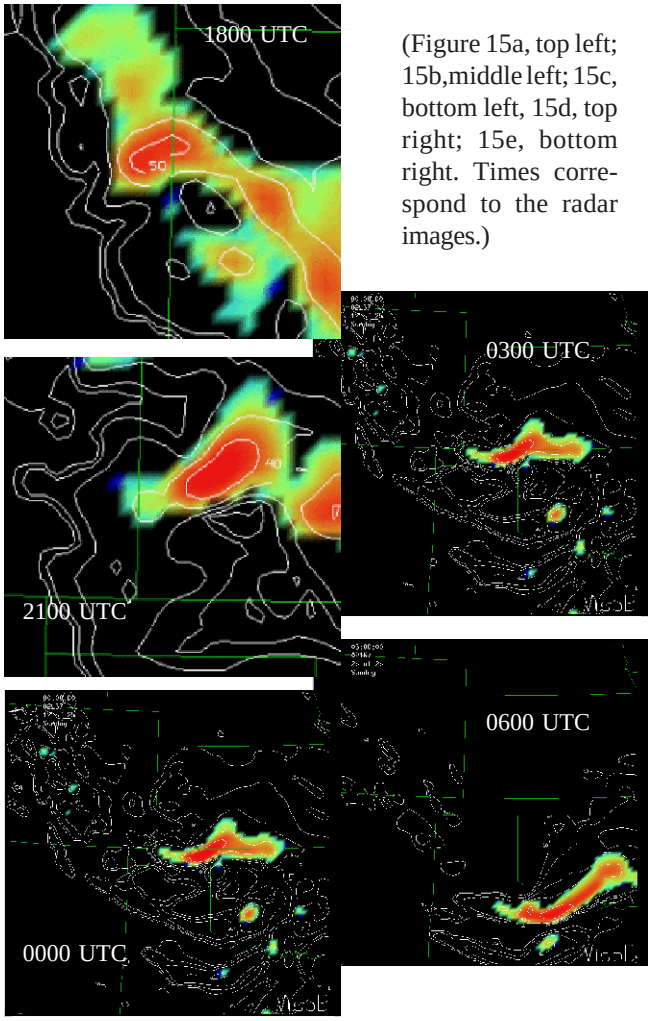

(Figure 15a, top left; 15b,middle left; 15c, bottom left, 15d, top right; 15e, bottom right. Times correspond to the radar images.)

Evaluating Convective Forecasts During IHOP *(continued)*

and 16c), the forecast for the developing line segment is similar to the MM5 and about in the same location, though the WRF continues to produce far more echo presence (and hence precipitation), with a large diffuse surface echo extending to the east-northeast of the line. This is a better forecast than the MM5 for the extent of echo if one compares it to the observed echo at 0000 UTC that shows an extensive area of moderate-strength surface echo in about the same position as the WRF forecast. After 0000 UTC the forecast is not quite as good as the MM5 run with a smaller line that is located a bit too far east. However, like the MM5 rerun, it is impressive that the WRF model was able to predict the upscale growth to a bowing line in about the right place and about when it occurred.

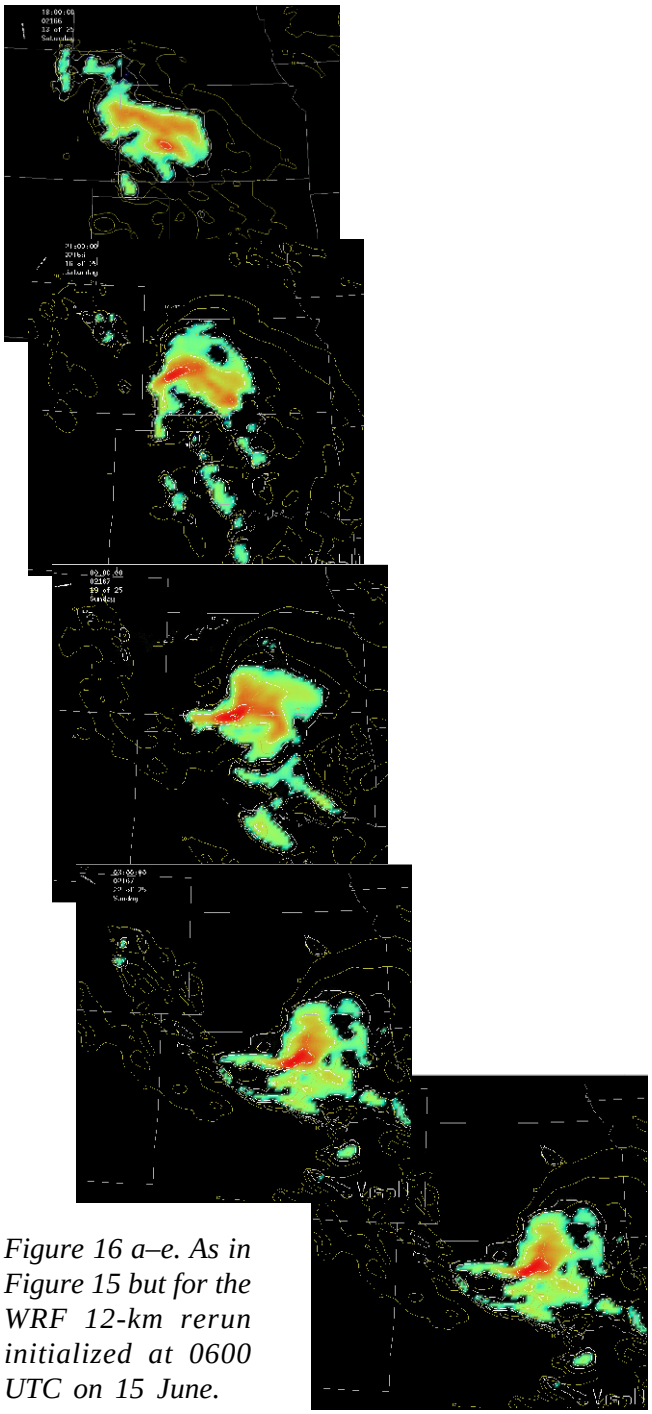

Figure 16 a–e. As in Figure 15 but for the WRF 12-km rerun initialized at 0600 UTC on 15 June.

The MM5 runs during IHOP extended out only to 12 hours, compared to 24 hours for the reruns, so for comparison, runs beginning at 1500 UTC for the 12-km MM5 and at 1800 UTC for the 4-km MM5 will be shown. The 1500 UTC MM5 12-km IHOP run is shown in Figure 17. Note how the initialization from LAPS nicely captures the ongoing convection at 1500 UTC (Figure 17a), although the storms are quickly lost, mostly in the first hour. This occurred at times with MM5 during IHOP, as noted earlier, and for this case may have been exaggerated somewhat because much of this convection near an apparent warm front may not have been surface-based. Unfortunately there is such a loss of echo that by the 3-hour forecast (valid at 1800 UTC), a composite echo is forecast but none is predicted to reach the surface. Right after 1800 UTC, however, the mid-level echo shown entering northwest Kansas in the 1800 UTC forecast strengthens rapidly, then expands to form the line segment shown in the forecast valid at 2100 UTC. This line segment then moves southward and strengthens and expands, bowing somewhat at 0000 UTC but then becoming more of a straight line by 0200 UTC. The line in this forecast does not accelerate as fast as in the 0600 UTC forecasts from the WRF and MM5 reruns shown earlier.

A comparison of the MM5 IHOP 12-km and 4-km runs initialized at 1800 UTC is shown in Figure 18. The two runs did capture the evolution to a line that accelerated and bowed with time. Organization into a stronger system with more bowing happens in the 4-km run ahead of the 12 km run, with the 4 km likely able to capture storm outflows better with its higher resolution. The 4-km run

Figure 17 a–e. As in Figure 15 except for the MM5 12-km forecast made during IHOP and initialized at 1500 UTC. Note that the 12-hour forecast was not available, so the 11-hour forecast valid at 0200 UTC is in Figure 17e.

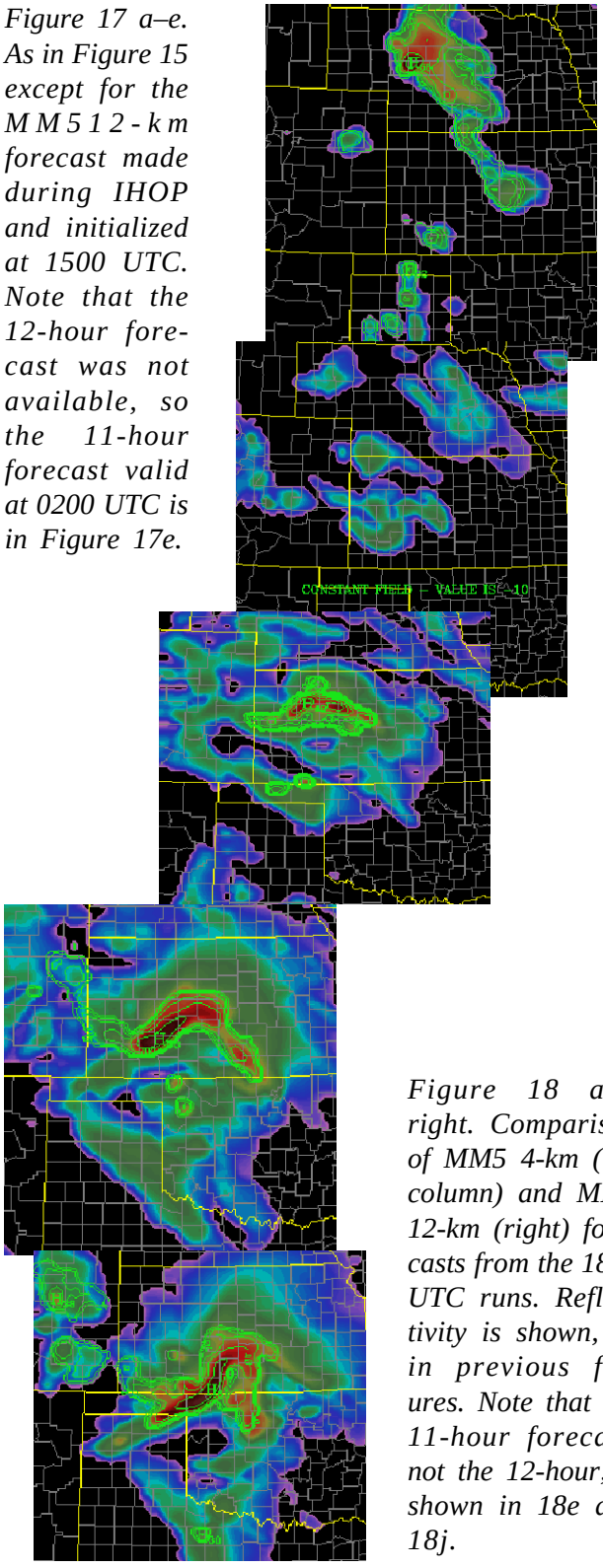

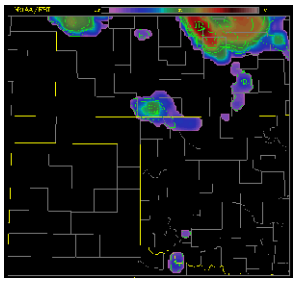

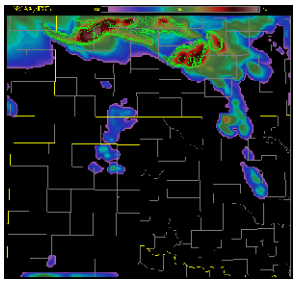

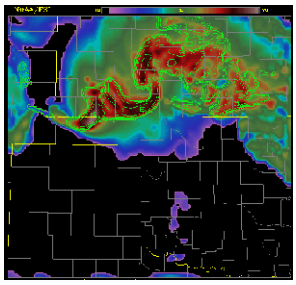

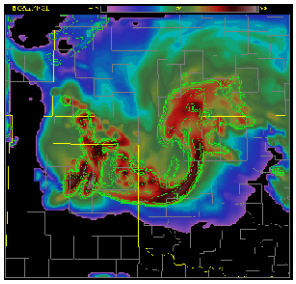

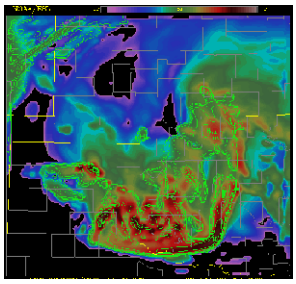

a)

b)

c)

d)

e)

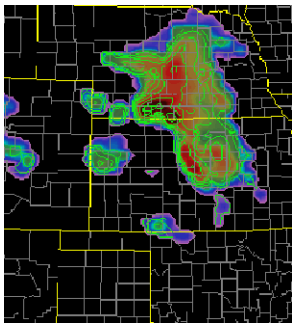

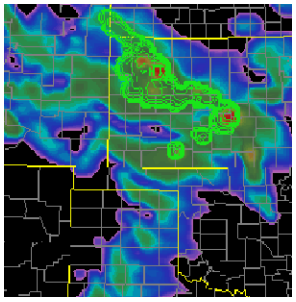

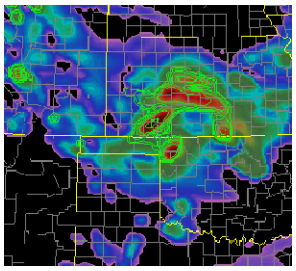

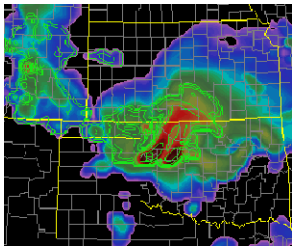

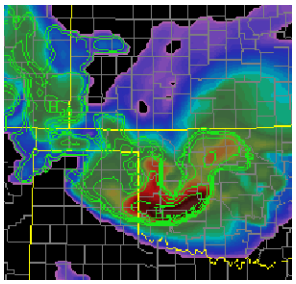

f)

g)

h)

i)

j)

Figure 18 a–j, right. Comparison of MM5 4-km (left column) and MM5 12-km (right) forecasts from the 1800 UTC runs. Reflectivity is shown, as in previous figures. Note that the 11-hour forecast, not the 12-hour, is shown in 18e and 18j.

Evaluating Convective Forecasts During IHOP *(continued)*

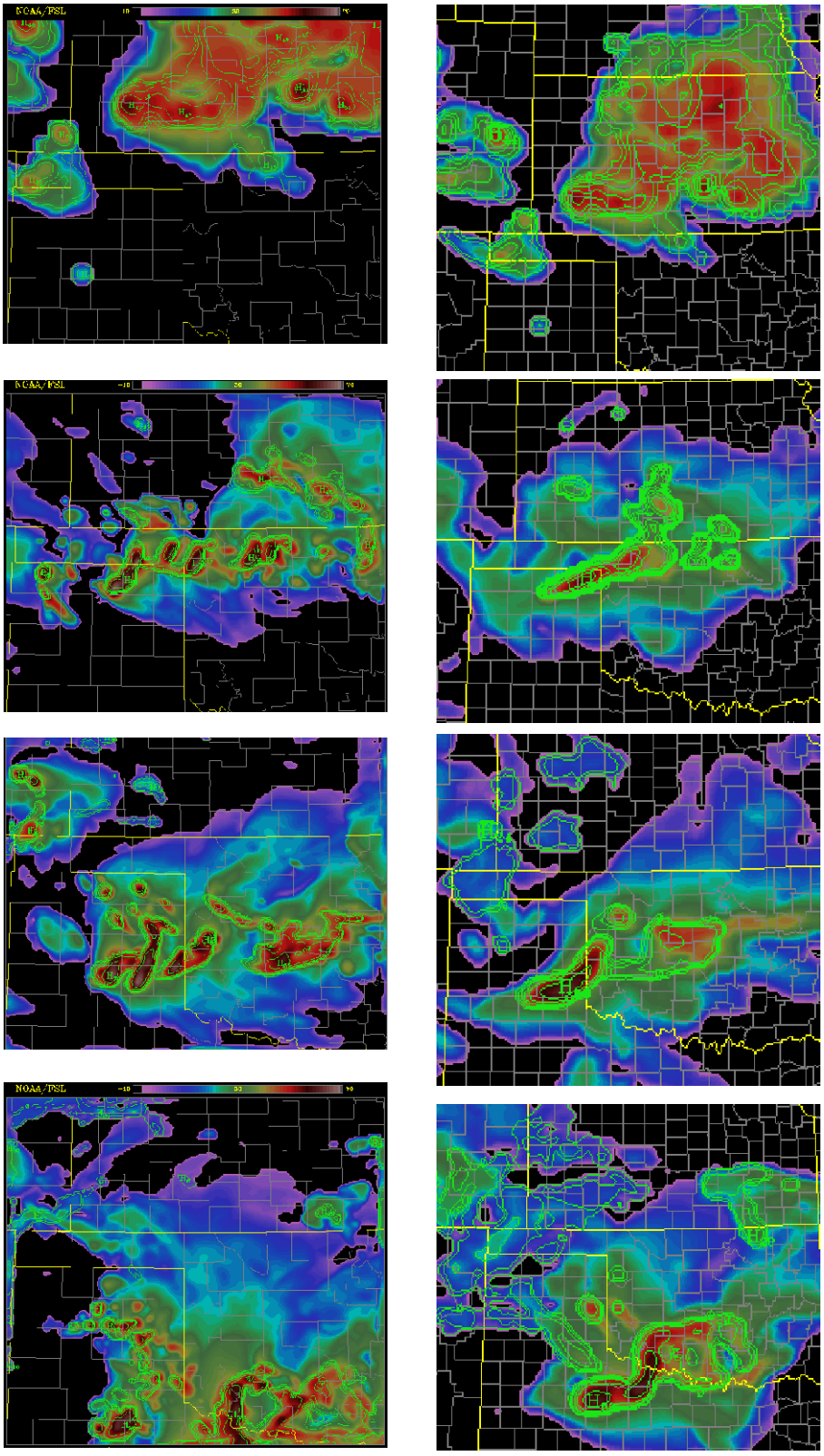

by 0500 UTC is still slower than reality with the position of the line, but not by much. A similar set of model runs for the 2100 UTC initialization, when the convection was beginning to organize more, is shown in Figure 19. Although there is some loss of the system in the first hour of the forecast after a good job of initialization (Figures 19a and 19e), more is retained than in some of the other runs because of the presence of a stronger echo at 2100 UTC. The MM5 12-km run is similar to the run initialized at 1800 UTC, although it develops a line sooner (by 0000 UTC) and ends up with a line position by 0600 UTC closer to reality and similar to the 0600 UTC MM5 rerun shown earlier (Figure 15e). Interestingly, the MM5 4-km run from 2100 UTC does not organize the convection into a line as fast as it did with the 1800 UTC run, and even at 0300 UTC has more of a broken line (not as good a forecast). By 0600 UTC it organizes the line more and accelerates it south of the 4-km domain, similar to the movement that was observed.

Figure 19 a–h (from top left to bottom right). As in Figure 18 except for the runs initialized at 2100 UTC 15 June 2002.

It is apparent that all the models were able to predict the upscale growth and organization of the convection into a line with good location and timing for the most part. There was good agreement between the different models and usually between the different initialization times. A consensus forecast from an ensemble viewpoint of the various runs would have been a good one. The dprog/dt method did not necessarily verify as well, however, especially for the MM5 4-km runs, with the 2100 UTC run not as good a forecast as earlier runs.

Summary and Future Work

The model forecasts examined here from two IHOP days encompass a variety of forecast problems typically encountered especially east of the Rocky Mountains, including convective initiation along a dryline, prediction of supercells, upscale growth and organization of storms into a squall line, and the very tricky forecast of overnight elevated convection. The forecasts presented well represent the behavior of the models used during the IHOP period, and indicate that there is potential for such models to offer forecast guidance that can be valuable to forecasters trying to predict convection. The model was most successful when the convective initiation was forced by a well-defined surface boundary, as in the 2 June 2002 case, and had the most difficult time with storms forced by more subtle boundaries (like the warm front on 15 June) or by no apparent surface boundary, like the elevated storms in the Texas Panhandle on 15 June. Some of the forecasts of supercell formation and movement, as well as upscale growth that occurred on 15 June were impressive, and there was even skill shown for such developments beyond the typical 6–12-hour limit that one might suspect for convective forecasts.

During IHOP, the RUC and MM5 special model runs by FSL were extensively used to help make short-range forecasts, with the models displayed on the FSL FX-Net workstation. Partial examination of an extensive real-time questionnaire completed by the forecasters for as many model runs as possible during IHOP has yielded constructive insight into various model issues that occurred, as well as how much the forecasters trusted some of the predictions.

Often these predictions carried far more detail as well as forecast precipitation (convection) than would be indicated by the operational models (Eta or GFS), and in some cases, some forecasters needed a spin-up time to understand whether the forecasts could be believed and how best to use them. For this study, we will continue completion of the analysis and questionnaires. We also want to examine model performance over a broader spectrum of IHOP days, not in the detail as was done for 15 June but more by phenomenon, such as the different convective types discussed for this same case.

Editor's Note: A complete list of references and more information on this and related topics are available at the main FSL Website www.fsl.noaa.gov, by clicking on "Publications" and "Research Articles."

(Edward Szoke is a meteorologist in the Forecast Research Division headed by Dr. John McGinley. He can be reached at Edward.J. Szoke@noaa.gov, or at 303-497-7395.)

Briefs...

...From the Director's Office

2003 Awards – FSL's greatest asset is its 219 talented and experienced employees. Following is a list of FSL employees who received awards during 2003:

• *Silver Medal*

– Jim Holitza, for leading an effort to procure and implement one of the world's fastest supercomputers, resulting in benefits to U.S trade and to weather hazard mitigation.

• *Bronze Medal*

– Mark Mathewson, Tom LeFebvre, Tracy Hansen, and Mike Romberg, the NOAA GFESuite Team, for leadership in creating software to allow all Weather Service offices to generate high-resolution, digital and graphical forecasts in real-time operations.

• *Tech Museum Award Laureate finalist in the NASDAQ Stock Market Education Award*

– Sandy MacDonald for his idea and creation of Science On a Sphere™.

• *NOAA Team Member of the Month of May 2003*

– Leon Benjamin for his work on the cooperative agency profilers and contribution in the design and implementation of the profiler program's centralized computer system.

FSL's Leon Benjamin receiving a NOAA Honor Award from Vice Admiral Lautenbacher, Under Secretary of Commerce for Oceans and Atmosphere.

• *Women of Color Science and Technology Award*

– Joanne Edwards

• *2003 CIRA Research Initiative Award Winners*

– ITS Data Systems Group: Chris MacDermaid, Leslie Ewy, Paul Hamer, Bob Lipschutz, Glen Pankow, Richard Ryan, and Amenda Stanley.

• *CIRA Employee of the Month Award*

– Brent Shaw for his role in developing an NWP system for the Space Centers at Vandenberg AFB.

• *FSL Employee of the Month* recipients: Tracy Hansen, Cherie Adams, Joaquin Felix, Barry Schwartz, Lee Cohen, Chris Harrop, Leslie Hart, Forest Hobbs, Keith Holub, Paul Hyder, Chuck Morrision, Ed Moxley, Glen Pankow, Craig Tierney, Steve Weygandt, Julie Singewald, Vivian LeFebvre, Mike Vrencur, Jim Frimel, Patty Miller, and Bob Cinea.

• *FSL Web Awards*

– Steve Koch, Bill Moninger, and Nita Fullerton for best product, the FSL Publications Website.

– Patrice Kucera and Woody Roberts, FSL Evaluation Team, for best internal use of Web Technology to develop and administer technical surveys.

– Beth Sigren for the most improved Website, the Aviation Division Website.

...Forecast Research Activities

Assimilation of Surface Cloud, Visibility, and Current Weather Observations in the RUC model – An important problem for short-range numerical prediction is initialization of cloud and hydrometeor fields. Forecasts of cloud, fog, ceiling/visibility, and stable and convective precipitation are dependent on accurate initial conditions for these fields. Most mesoscale models now parameterize stable cloud processes with some type of bulk microphysics. The stable cloud microphysics parameterization used in the RUC is explicitly mixed-phase, with prediction of mixing ratios of five different hydrometeor types (cloud water, ice, rain, snow, graupel). The problem for cloud/hydrometeor assimilation is the mapping of disparate, one-sided (cloud decks apparent from space or the earth's surface with indeterminate depth) observations onto the 3D multihydrometeor mixing ration field.

The information sources for cloud/hydrometeor initialization include background short-range forecasts, satellite- and radar-based observations, and surface-based observations of cloud, visibility, and current weather. The RUC became the first NCEP operational model to introduce modification of initial cloud fields in its data assimilation in 2002.

Case studies and ongoing cycle (retrospective and real-time) testing will be conducted for assimilation of surface-based cloud observations into the RUC. The technique will be modified during this testing to include assimilation of visibility and current weather, both within the logical cloud variable. The local cloud variable will be subdivided into cloud versus hydrometeor components to allow for clearing or not clearing rain/snow hydrometeors from the cloud base to the surface based on the current weather observation. Most importantly, the assimilation for surface-based cloud observations will be combined with previously developed techniques for assimilation of radar reflectivity into the RUC hydrometeor fields.

A comprehensive RUC cloud/hydrometeor analysis including surface-based cloud observations and radar reflectivity assimilation will result in considerable improvement to RUC aviation-specific forecasts of ceiling and visibility, as well as in forecasts of clouds and precipitation important for all users. Implementation of this combined cloud/hydrometeor assimilation technique will be proposed for implementation into the operational RUC late in 2004.

Dr. Stan Benjamin will present recent results on these studies at the 2004 Annual Meeting of the American Metorological Society in Seattle.

Operational Performance and Recent Improvements of the RUC 3DVAR – The RUC hourly update cycle utilizes a unified analysis framework encompassing data ingest and quality control routines, and interchangeable three-dimensional variational (3DVAR) and optimum interpolation (OI) based analysis solvers. Following several years of research and development, the operational version of the RUC (run at NCEP) switched from the OI analysis to the 3DVAR analysis on 27 May 2003. Several earlier versions of RUC 3DVAR were successfully implemented in FSL in real-time test mode. The 3DVAR-based RUC performs appropriately in operations, but there are several open problems, most of which are related to full variational solutions of moisture/cloud fields. One of them is the assimilation of precipitable water data from satellites and ground-based GPS. An experimental version of the RUC 3DVAR with precipitable water data assimilation is being tested, but it is not ready for operational use. Currently, satellite radiances are not assimilated in the RUC 3DVAR, but development is under way to include the OPTRAN radiative forward and adjoint operators. A bias reduction method is under investigation to provide appropriate satellite radiance information. Development of radar data assimilation procedures is also underway, with a long term goal of utilizing reflectivity and radial velocity information to modify water vapor, hydrometeor, and velocity divergence fields. Initial work has focused on updating hydrometeor and water vapor fields, using a national composite maximum reflectivity product in conjunction with satellite data and surface cloud observations. In the present formulation, the radar-based updates occur within the outer loop of the moisture minimization, allowing for an iterative solution in concert with the in situ moisture observations. Real-time parallel tests at FSL indicate a modest improvement in short-term (3–6 hour) precipitation forecasts from this technique.

Dr. Stephen Weygandt will present a a status report on this research at the 2004 Annual Meeting of the American Metorological Society in Seattle.

Modeling Entrainment and Boundary Layer Growth During a Bore Event – The goal of the International H_2O Project (IHOP) field experiment in the Southern Great Plains of the U.S. was to obtain an improved characterization of the time varying three-dimensional water vapor field and to determine its importance in the understanding and prediction of convective processes. Understanding the role played by bores in initiating and maintaining nocturnal convection was one of the objectives of the project. Ground-based remote sensing instruments at the Homestead site in the Oklahoma Panhandle included the NCAR Integrated Sounding System and Multiple Antenna Profile, an Atmospheric Emitted Radiance Interferometer, FM-CW radar, Scanning Raman Lidar and aerosol backscatter lidar.

Briefs... *(continued)*

...Forecast Research Activities *(continued)*

These instruments were complemented by the polarimetric SPOL and Dodge City WSR-88D radars and two research aircrafts equipped with the water vapor differential absorption lidar and surface mesonetwork recording temperature, dewpoint, and wind at 5-minute intervals. The most comprehensive set of observations ever collected on structure and dynamics of bores was probably gathered during IHOP. On 4 June 2002, two bores were observed at Homestead. FSL researchers analyzed the "second" bore which developed in the early morning on this day as a result of an interaction of a cold front with a stable boundary layer. This bore was well documented by the IHOP measurements. Numerical simulations with MM5 reproduced the event quite accurately and are used to study turbulence and boundary layer growth in the wake of the bore. This ongoing research will use the Center for Analysis and Prediction of Storms (CAPS) ARPS model at resolutions of the order of tens of meters to evaluate turbulence parameterizations versus simulations with explicitly resolved eddies.

Dr. Mariusz Pagowski will present a paper on this topic at the 2004 Annual Meeting of the American Meteorological Society in Seattle.

RUC Short-Range Ensemble Forecast System – Because of uncertainties in atmospheric model dynamics, physical parameterizations, and initial and boundary conditions, a single deterministic forecast has some degree of error. In this sense, a deterministic forecast is used merely as a reference to the forecast of the true atmospheric states. Therefore, statistical analysis of a sample of forecasts becomes a plausible approach for the improvement of numerical weather prediction. The task of finding the best way to generate such a sample of forecasts poses an important area of scientific challenge and development.

In collaboration with NCEP's multimodel Short-Range Ensemble Forecast (SREF) initiative, FSL has developed a SREF system based on the Rapid Update Cycle (RUC) model, targeting both operations and research needs. The RUC forecast system is a NOAA operational weather prediction system. One of the unique features of the RUC is that its dynamical core is based on a hybrid potential temperature/sigma vertical coordinate. This feature will certainly add to the model diversity as far as a multi-model ensemble is concerned, and thus possibly increase the ensemble spread. The RUC SREF now runs twice daily with a total of 10 members. The SREF domain encompasses the entire North America including Alaska, Central America including the Caribbean Sea, the western Pacific including the Hawaiian Islands, and the western Atlantic. The forecast is run out to 60 hours with output every 3 hours.

The statistical verification scores show the RUC SREF forecasts compare well against Eta analysis and Eta 12-km operational runs, and yet the forecast spread calculations show that there is significant variability among the forecast members. Future development of RUC SREF is still in order. We plan to experiment with various initial perturbation methods while still using the Eta regional breeding method, and continue to develop posterior analysis, verification schemes, and probability forecast products. The development of an upgrade version for higher horizontal resolution and some research applications are also planned. FSL will work with NCEP/EMC in running the RUC SREF as part of a retrospective test of current and prospective members of the NCEP SREF.

Dr. Chungu Lu will present this research at the 2004 Annual Meeting of the AMS in Seattle.

A Graphical User Interface to Prepare the Standard Initialization for the WRF Model – FSL has created a graphical user interface capable of accommodating researcher needs when using the Standard Initialization (SI). Since the SI is a necessary first step when using the WRF model, the GUI provides an easy method to prepare an otherwise quite complicated system. More than 100 users have so far downloaded the latest SI version 1.3.2 containing the GUI. These users have provided valuable feedback, which is used in updates. As other researchers use the GUI, we plan to continue requesting their feedback and use it to keep up with user needs and the latest software.

Paula McCaslin will present a paper on this topic at the 2004 Annual Meeting of the American Meteorological Society in Seattle.

Verification of the FSL Ensemble of Mesoscale Models Used for a Winter Weather Application – The LAPS group at FSL has built an ensemble of mesoscale models that runs in real time in support of field projects and demonstrations. One of these projects is sponsored by the Federal Highways Administration (FHWA) and is focused on winter weather. The FHWA Maintenance Decision Support System is an effort to tailor weather forecasts for the purposes of winter road maintenance. FSL generates the mesoscale model forecasts and transmits them to the NCAR/Research Applications Program, where they are used to make point forecasts along roadways. These point forecasts feed pavement temperature and chemical dilution algorithms (developed by the Cold Regions Research and Engineering Laboratory), which are used along with codified rules of practice (developed by MIT/Lincoln Labs) to automatically recommend timing and location for snow plowing and chemical applications. Last winter, the MDSS ensemble consisted of six members: three mesoscale models (MM5, RAMS, and WRF) with two larger-scale models (NCEP's Eta and AVN) providing lateral boundary conditions. The models were run out to 27 hours to provide a 24-hour forecast service. The grid configuration, centered on the state of Iowa, is the same for all models. For this test the grid increment was 12 km, with no convective parameterizations because of the focus on winter weather. The execution schedule was driven by the update frequency of the NCEP models; thus, all six members were run four times per day, upon receipt of the NCEP model grids. All model runs were initialized with the same LAPS "hot start" diabatic initialization grids.

Following statistical evaluation of the models' performance during the 2003 Demo, we have begun experiments with alternate configurations of the ensemble modeling system. The pertinent lessons learned were that the use of two different models (AVN and Eta) for lateral boundary conditions did not provide much diversity, the models did not provide much added value beyond 18 hours, the RAMS model routinely had large errors in precipitation and temperature, and the WRF model generated too much precipitation. In light of this experience, we have developed an alternative strategy to take better advantage of what these models do best, which is exploit more of the available observations (particularly radar and satellite) to improve precipitation forecasts in the range of 1–12 hours. This configuration consists of running MM5 and an improved version of WRF every hour, and using "time-lagged" ensembling techniques. For example, a 6-hour ensemble forecast uses the current 6-hour forecast, the previous 7-hour forecast, and the 8-hour forecast from the cycle before that, all forecasts valid at the same time. It is expected that such practice will reduce the cycle-to-cycle "shock" in the MDSS forecast services that was sometimes caused during the 2003 demo when the models updated.

Paul Schultz will present this research at the 2004 Annual Meeting of the American Meteorological Society in Seattle.

Comparisons Between Observations Made during NEAQS and Air Quality Forecasts from MM5 and WRF Chemistry Models – The 2002 New England Air Quality Study (NEAQS) was an intensive effort to investigate the chemical and meteorological factors that contribute to poor air quality in the New England region. The campaign combined efforts of numerous educational institutions as well as federal, state, and local agencies. Atmospheric chemical forecasts and retrospective simulations have been produced using the MM5/Chem and WRF/Chem numerical models, respectively. The forecasts using MM5/Chem took place between July and August of 2002 and coincided with the New England Air Quality Study. The retrospective simulations using WRF/Chem were conducted for the same region and time period. Initial analysis of the numerical model results indicates that both models are capable of producing the observed chemical structure of the lower troposphere. Differences between the observations and simulation results appear to be a product of the relatively large grid spacing used in the model as well as the surface emissions data. Future simulations using WRF/Chem will examine the use of smaller horizontal grid spacing and improved surface emission data. In addition, the impact of including the feedback between aerosols and shortwave radiation will be examined.

Dr. Steven Peckham will present this research at the 2004 Annual Meeting of the American Meteorological Society in Seattle.

Briefs... *(continued)*

...Forecast Research Division *(continued)*

Fully Coupled "Online" Chemistry within the WRF Model – The simulation and prediction of air quality is a complicated problem, involving both meteorological factors (such as wind speed and direction, turbulence, radiation, clouds, precipitation) and chemical processes (such as emissions, deposition, transformations). In the real atmosphere the chemical and physical processes are coupled. The chemistry can affect the meteorology, for example, through its effect on the radiation budget, as well as the interaction of aerosols with cloud condensation nuclei (CCN). Likewise, clouds and precipitation have a strong influence on chemical transformation and removal processes, and localized changes in the wind or turbulence fields continuously affect the chemical transport.

Until recently, the chemical processes in air quality modeling systems were usually treated independently of the meteorological model (i.e., "*offline*") except that the transport was driven by output from a meteorological model, typically available once or twice per hour. Because of this separation of meteorology and chemistry, there can be a loss of important information about atmospheric processes that quite often have a time scale of much less than the output time of the meteorological model, for example, wind speed and direction, rainfall, and cloud formation. This may be especially important in air quality prediction systems, in which horizontal grid sizes on the order of 1 km may be required. In addition, the feedback from the chemistry to the meteorology – which is neglected in "offline" approaches – may be much more important than previously thought.

Over the past few years, several research institutes have collaborated in the development of a new state-of-the-art Weather Research and Forecast (WRF) model *(http://www.mmm.ucar.edu/wrf/users/document.html)*. WRF is nonhydrostatic, with several dynamic cores as well as many different choices for physical parameterizations to represent processes that cannot be resolved by the model. This allows the model to be applicable on many different scales. The dynamic cores include a fully mass- and scalar-conserving flux-form mass coordinate version, which represents a major improvement over commonly used nonhydrostatic models. Similar approaches have recently been implemented in the Operational Multiscale Environment Model with Grid Adaptivity (OMEGA) as well as the Japanese numerical weather prediction model. A fully conservative flux-form treatment of the equations of motion may be especially important for air quality applications. This makes the WRF model ideally suited to be the cornerstone for a next generation air quality prediction system. Fully coupled, "online" chemistry has been implemented into the WRF model. The resulting WRF/Chem model has been evaluated in comparison to MM5/Chem model with a testbed dataset.

Georg Grell will present a summary of statistical comparisons of atmospheric composition predicted by WRF/Chem and MM5/Chem at the 2004 Annual Meeting of the American Meteorological Society in Seattle.

...Systems Development Activities

MADIS Data Now Available Via OPeNDAP Servers – FSL announces a welcome development related to the Meteorological Assimilation Data Ingest System (MADIS) database, which provides value-added surface and upper-air data for improving weather forecasting and supporting data assimilation, numerical weather prediction, and other applications.

MADIS data are now available via OPeNDAP servers, an Internet-based freeware that simplifies all aspects of scientific data networking. These servers make local data accessible to remote locations regardless of local storage format, and provide tools for transforming existing applications into OPeNDAP clients. This new availability is in addition to the previous forms of data access to the MADIS database, such as FTP and the Unidata LDM.

The availability of OPeNDAP servers to the science community also has important implications for the LEAD (Linked Environments for Environmental Discovery) program. The LEAD concept involves a series of interconnected IT "environments" that provide a complete framework within which users can identify, obtain, and work with observational, computer model, and user-generated information. This is possible in a distributed setting where real-time data streams and decision-making are important, and where both the problem being

addressed and the computational resources can change dynamically with time.

An even more significant aspect for LEAD is that MADIS data files are compatible with the Weather Research and Forecast (WRF) model's Three-Dimensional Variational (3DVAR) Data Assimilation System. The MADIS-WRF 3DVAR interface supports the ingest of a vast number of observation types, such as land surface (including ASOS, other METAR, Canadian SAOs, and many mesonets), maritime, GPSMet Integrated Precipitable Water, NOAA Profiler Network (NPN) winds, Multi-Agency Profiler (MAP) winds, automated aircraft, radiosonde, and GOES satellite winds (operational or experimental). More information is available on the MADIS program (including the MADIS-WRF 3DVAR interface) at *http://jailbird.fsl.noaa.gov/MADIS/*. For more specific information from the MADIS manager, contact *Patricia.A.Miller@noaa.gov.*

...Aviation Activities

Volcanic Ash Coordination Tool – FSL announces the successful delivery of a new realization of the FX-Collaborate (FXC) system, referred to as the Volcanic Ash Coordination Tool (VACT). This valuable technology has been installed at three locations: the Anchorage Center Weather Service Unit (ACWSU), the Alaska Aviation Weather Unit (AAWU), and the Alaska Volcano Observatory at the U.S. Geological Survey. The Aviation Division will work with these organizations as well as the NWS Alaska Region Headquarters to develop and demonstrate the VACT applied to a rules-based approach to collaboration in volcanic ash advisory preparation.

A first step in this multiagency effort was to train nine users of the VACT: three ACWSU forecasters, three AAWU forecasters and the MIC, and two USGS geophysicists at the AVO. Now AD staff will work to enhance and refine the VACT to support collaborative decision-making. A key motivating factor for developing the VACT was an analysis by Simpson et al. (2002) of the operational response to the eruption of Mt. Cleveland, Alaska, in 2001. They found that SIGMETs generated for the Anchorage Oceanic FIR (Forecast Information Region) and the Oakland FIR (which are adjacent) called for ash plume heights that were very different.

Future enhancements to VACT include additional satellite imagery displays including polar orbiters; prototype volcanic ash products developed by the FAA Product Development Team for Oceanic Weather; output generated by volcanic ash dispersion models; and radar observations. A software tool will also be developed that will enable Center Weather Service Units (CWSUs) to efficiently generate Center Weather Advisories for volcanic ash.

This work is funded by the NWS Alaska Region and the FAA Aviation Weather Research Program. For more information, contact Dennis Rodgers at *Dennis.M.Rodgers@noaa.gov,* or 303-497-6933.

...Modernization Activities

Examples of GFE Use in Operations During 2003 – In the last few years, the Graphical Forecast Editor and supporting software (called the GFESuite or GFE) has become the primary tool that operational forecasters at the National Weather Service (NWS) offices use to create and edit their gridded forecast fields. The GFESuite provides a wide range of tools and capabilities for this purpose, but it has been left up to the NWS regions, individual forecast offices, and ultimately individual forecasters to decide what approach to take to generate and maintain these forecast fields. Along with maintaining an internally consistent gridded forecast database, forecasters must also consider the gridded forecasts generated by surrounding offices in order to maintain a level of spatial and temporal consistency over the large national domain.

Over the past several years, the FSL Evaluation Team has evaluated most aspects of the NWS modernization and new operational components including AWIPS. We have developed several evaluation metrics that have been successfully used to evaluate these changes and

Briefs... *(continued)*

help direct future development activities. The goal of this study is to determine how the GFE is currently used operationally at NWS offices. Specific objectives are to find out what GFE components are being used, when the GFE is used, how the grids are initialized and modified, how does the GFE fit into the NWS operational framework, and what is the impact of the GFE on the forecast process?

Operational GFE computer logs have been the primary source of information for this study, along with interviews and observations conducted at some of the NWS offices. A survey has also been developed, but has not been administered at the offices. The GFE logs record status information, which tools and capabilities are used, and a time stamp indicating exactly when tools are used or when specific actions are performed. Week-long log "snapshots" were collected in 2003 from 5 randomly selected forecast offices at varied geographical locations and during a variety of weather conditions. These snapshots were examined in order to see the range and frequency of GFE use by a number of forecasters with a variety of forecast responsibilities.

Woody Roberts will present a summary of these results at the 2004 Annual Meeting of the American Meteorological Society in Seattle.

...Demonstration Activities

GPS Water Vapor Observation Errors – FSL has been carrying out research related to the observation errors associated with retrieving integrated or total atmospheric column precipitable water vapor (IPW) from Global Positioning System (GPS) signal propagation delays caused by the neutral atmosphere. Another aim of the project is to show how occasional discrepancies between operational National Weather Service (NWS) radiosonde soundings and GPS precipitable water estimates impact a numerical weather prediction model assimilating both measurements. Although GPS water vapor-observing systems provide no direct information about the vertical distribution of water vapor in the atmosphere, they have several advantages over other moisture sensing systems. Some of these advantages include high measurement accuracy; arbitrary temporal resolution; all weather operability (i.e. they provide data under conditions when other observations fail or provide degraded data); no requirement for calibration; high reliability; and low acquisition and maintenance costs. FSL has quantifed the observation errors associated with estimating the GPS radio signal propagation delays caused by the neutral atmosphere, and retrieving integrated (total atmospheric column) precipitable water vapor from these delays.

Comparisons of GPS water vapor retrievals with other observing systems, especially radiosondes, have been carried out for 10 years. Though uncertainties exist in the absolute water vapor estimation accuracy of any one system, it is fairly certain that radiosondes and GPS are capable of providing total column precipitable water estimates with 1–2 mm level accuracy under ideal circumstances.

Seth Gutman (*Seth.I.Gutman@noaa.gov*) will present a status report on this research at the 2004 Annual Meeting of the American Meteorological Society in Seattle.

...Technology Outreach Activities

The FX-Net Meteorological Workstation Underpins Fire Weather Operations – The National Weather Service has implemented an All Hazards Onsite Meteorological Support System to support the NWS Incident Meteorologists (IMETS) at remote locations. The core component of the system is NOAA FSL's FX-Net system, which provides AWIPS-like displays on a laptop remote from the data server.

FX-Net has been deployed to many fires during the last two fire weather seasons, and has been used at all fires supported by IMETS during this past season. FX-Net delivers high-resolution satellite, radar, observational, and weather prediction model data from a server in either the Western, Southern, Pacific, or Alaska NWS Regions. Any type of network link can be used to access the server data at speeds ranging from low-bandwidth, 56 kbps to high-speed, two-way satellite-based communications systems. Bandwidth limitations are addressed using an FSL-developed Wavelet Data Compression technique along with multi-threaded client-side processing and communication.

FX-Net has proved to be a critical component for fire management teams struggling to save lives and control the fires in California, for example. Rich Douglas, Chief of Meteorological Services at the NWS Western Region headquarters in Salt Lake City, commented last October that "the FX-Net system is heavily used and has had a huge impact on improving firefighter safety"... in that "it is incredibly critical to the fire management team's efforts to get fire fighters in the right position on the fire line and in moving people out of harm's way."

A unique capability of the FX-Net system allows the deployed forecasters to display high-resolution radar data from any local or remote radar at any location across the country. When the fires shut down a local radar site at the forecasters' home base last year, another regional radar was brought up in a few seconds to provide continuous coverage. Another unique dataset that has aided fire weather forecasters is local Mesowest data provided by the Citizen Weather Network, served from FSL. Most of the systems are communicating with the FX-Net server via a two-way satellite communications link.

"The FX-Net system is the 'backbone' of fire weather forecasting in the field," according to Rob Balfour, a National Weather Service Incident Meteorologist and field manager who supports fire management teams such as those at the Padua, Old, and Grand Prix fires in California. Mr. Balfour says that the FX-Net system is critical for "model guidance and 'right-now' weather information, and the RUC model is essential for hourly soundings to improve short-range wind and atmospheric moisture forecasts." Both parameters are constantly changing and are critical for providing structure protection and guidance to the fighters on the fire line.

FX-Net is the only system in the fire management office that displays 5-minute Doppler radar velocity data, critical to keeping track of rapidly changing wind conditions. Mr. Balfour also points out that FX-Net provides rapid updates on weather conditions, unlike the Internet, which is "too slow and the data can't be overlaid, animated, or found all in one place."

For more information on the FX-Net system and Wavelet Compression, see FSL Website *http://www.id.fsl.noaa.gov/fxnet.html*, or contact *Sher.Schranz@noaa.gov* or (303-497-7254).

Application of the SCIT Algorithm to South Korea Storm Data – There are numerous reasons why severe weather detection is a key element of the weather radar system. One severe weather detection algorithm is the Storm Cell Identification and Tracking (SCIT) algorithm, a centroid tracking algorithm included in the Open Radar Product Generator (ORPG) software of the WSR-88D Build. Since 2000, the Korea Meteorological Administration (KMA), in cooperation with FSL, has been developing the Forecaster's Analysis System (FAS), an AWIPS-like forecaster workstation. The System for Convective Analysis and Nowcasting (SCAN) is an integrated suite of multisensor applications that detect, analyze, and monitor convection, and generate short-term probabilistic forecast and warning guidance for severe weather automatically within AWIPS. Basically, SCAN uses composite reflectivity (CZ), vertically integrated liquid (VIL), and SCIT information as its input data.

During 2003, efforts have been made to produce several products for SCAN input data using the ORPG routine with Korean radar data. The data, observed during spring 2003 in southwestern Korea, have been tested using the SCIT algorithm. The lifetime and significant features of these storms will be investigated later, along with the SCIT algorithm's ability to detect and track them. The results also will be compared to improvements in radar data quality.

Dr. Byunghyun Song, visiting scientist at FSL, will present the status of this research at the 2004 Annual Meeting of the American Meteorological Society in Seattle.

Recent Publications – *Nita Fullerton, Editor/Publications Coordinator*

Biere, M., and D.L. Davis, 2003: Multicast data distribution on the AWIPS Local Area Network. *19th Int. Conf. on Interactive Information Processing Systems (IIPS) for Meteorology, Oceanography, and Hydrology*, Long Beach, CA, Amer. Meteor. Soc., CD-ROM, 4.7.

Businger, S., M.E. Adams, S.E. Koch, and M.L. Kaplan, 2003: Reply. *Mon. Wea. Rev.* **131**, 1504–1506.

Devenyi, D., and S.G. Benjamin, 2003: A variational assimilation technique in a hybrid isentropic-sigma coordinate. *Meteor. and Atmospheric Physics* **82**, 245–257.

Flamant, C., S. Koch, T. Weckwerth, J. Wilson, D. Parsons, B. Demoz, B. Gentry, D. Whiteman, G. Schwemmer, F. Fabry, W. Feltz, M. Pagowski, and P. DiGirolamo, 2003: The life cycle of a bore event over the U.S. Southern Great Plains during IHOP-2002. *Sixth Int. Symposium on Tropospheric profiling: Needs and Technologies*, Leipzig, Saxony, Germany, Amer. Meteor. Society, 375–377.

Flamant, C., S. Koch, T. Weckwerth, J. Wilson, D. Parsons, B. Demoz, B. Gentry, D. Whiteman, G. Schwemmer, F. Fabry, W. Feltz, M. Pagowski, P. DiGirolamo, 2003: The life cycle of a bore event over the US Southern Great Plains during IHOP-2002. *10th Conf. on Mesoscale Processes*, Portland, OR, Amer. Meteor. Soc., CD-ROM, P2.14.

Golden, J.H., E.I. Tollerud, A. Negri, and R. Updike, 2003: The hurricane-flood-landslide continuum – Forecasting hurricane effects at landfall. *30th Int. Symposium on Remote Sensing of Environment*, Honolulu, HI, Amer. Meteor. Soc.

Grote, H., and C. Golden, 2003: Enhancements to FX-Collaborate to support operations at NWS, USAF, and NASA. *19th Int. Conf. on Interactive Information Processing Systems (IIPS) for Meteorology, Oceanography, and Hydrology*, Long Beach, CA, Amer. Meteor. Soc., CD-ROM, 12.7.

Gutman, S.I., R. Pursaud, and S.M. Wagoner, 2003: Use of federal and state Departments of Transportation continuously operating GPS reference stations for NOAA weather forecasting. *19th Int. Conf. on Interactive Information Processing Systems (IIPS) for Meteorology, Oceanography, and Hydrology*, Long Beach, CA, Amer. Meteor. Soc., CD-ROM, P1.39.

Gutman, S.I., S. Sahm, J. Stewart, S. Benjamin, T. Smith, and B. Schwartz, 2003: A new composite observing system strategy for ground-based GPS meteorology. *12th Symposium on Meteorological Observations and Instrumentation*, Long Beach, CA, Amer. Meteor. Soc., CD-ROM, 5.2.

Hansen, T., T. Dankers, and C. Paxton, 2003: Text formatting with the Graphical Forecast Editor. *19th Int. Conf. on Interactive Information Processing Systems (IIPS) for Meteorology, Oceanography, and Hydrology*, Long Beach, CA, Amer. Meteor. Soc., CD-ROM, P1.11.

Herzegh, P.H., S.G. Benjamin, R. Rasmussen, T. Tsui, G. Weiner, P. Zwack, 2003: Development of automated analysis and forecast products for adverse ceiling and visibility conditions. *19th Int. Conf. on Interactive Information Processing Systems (IIPS) for Meteorology, Oceanography, and Hydrology*, Long Beach, CA, Amer. Meteor. Soc., CD-ROM, 9.3.

Jones, D.R., C. Bullock, W. Carrigg, C. Dietz, M. desJardin, E. Mandel, D. Rhine, J. Roe, and M.T. Young, 2003: AWIPS Build 5 in review. *19th Int. Conf. on Interactive Information Processing Systems for Meteorology, Oceanography, and Hydrology*, Long Beach, CA, Amer. Meteor. Soc., CD-ROM, 4.1.

Jung, Y.-S., F. Moeng, B.H. Lim, M. Biere, H. Lee, and S.K. Chung, 2003: FAS: An international version of AWIPS. *19th Int. Conf. on Interactive Information Processing Systems for Meteorology, Oceanography, and Hydrology (IIPS)*, Long Beach, CA, Amer. Meteor. Soc., CD-ROM, 4.6.

Kim, D., and S.E. Koch, 2003: Multilevel cloud retrieval from the GOES platform. *12th Conf. on Satellite Meteorology and Oceanography*, Long Beach, CA, Amer. Meteor. Soc., CD-ROM, P1.20.

Koch, S.E., 2003: A structure process for prediction of convection associated with split cold fronts. *Bull. Amer. Meteor. Soc.*, 174–179.

Koch, S.E., B. Demoz, F. Fabry, W. Feltz, B. Geerts, B. Gentry, D. Parsons, G. Schwemmer, T.M. Weckwerth, D. Whiteman, and J.W. Wilson, 2003: Multisensor study of a dual bore event observed during IHOP. *10th Conf. on Mesoscale Processes*, Portland, OR, Amer. Meteor. Soc., CD-ROM, 14.3.

Koch, S.E., M. Pagowski, F. Fabry, W. Feltz, G. Schwemmer, B. Geerts, B. Demoz, B. Gentry, D. Parsons, T. Weckwerth, and J. Wilson, 2003: Structure and dynamics of a dual bore event during IHOP as revealed by remote sensing and numerical simulation. *Sixth Int. Symposium on Tropospheric profiling: Needs and Technologies*, Leipzig, Saxony, Germany, Amer. Meteor. Soc., 378–380.

Koch, S.E., B. Jamison, T.L. Smith, E. Tollerud, C. Lu, N. Wang, M.A. Shapiro, C. Parrish, and O. Cooper, 2003: Field observations and RUC model simulations of turbulence and gravity waves. *10th Conf. on Mesoscale Processes*, Portland, OR, Amer. Meteor. Soc., CD-ROM, P2.24.

LeFebvre, T., M. Mathewson, and T. Hansen, 2003: The Rapid Prototype Project. *19th Int. Conf. on Interactive Information Processing Systems (IIPS) for Meteorology, Oceanography, and Hydrology*, Long Beach, CA, Amer. Meteor. Soc., CD-ROM, 12.4.

Luo, A., Robock, K.Y. Vinnikov, C.A. Schlosser, A.G. Slater, N.A. Speranskaya, A. Boone, H. Braden, F. Chen, P. Cox, P. Rosnay, C.E. Desborough, R.E. Dickinson, Y.-J. Dai, Q. Duan, J. Entin, P. Etchevers, A. Henderson-Sellers, N. Gedney, Y.M. Gusev, F. Habets, J. Kim, V. Koren, E. Kowalczyk, K. Mitchell, O.N. Nasonova, J. Noilhan, A.J. Pitman, J. Schaake, A.B. Shmakin, T.G. Smirnova, D. Verseghy, P. Wetzel, Y. Xue, Z.-L. Yang, and Q. Zeng, 2003: Effects of frozen soil on soil temperature, spring infiltration, and runoff: Results from the PILPS 2(d) Experiment at Valdai, Russia. *J. Hydrometeor*. **4**, 334–351.

Mahoney, J.L., B.G. Brown, J.E. Hart, and J. Henderson, 2003: A statistical evaluation of the Collaborative Convective Forecast Product (CCFP) and the Convective Significant Weather Advisories (C-SIGMET): 1 April–31 October 2001 and 1 April–31 July 2002. *NOAA Technical Memorandum*, Forecast Systems Laboratory, Boulder, CO.

Miller, P.A., M.F. Barth, and A.E. MacDonald, 2003: Ingest, integration, quality control, and distribution of observations from state transportation departments using MADIS. *19th Int. Conf. on Interactive Information Processing Systems (IIPS) for Meteorology, Oceanography, and Hydrology*, Long Beach, CA, Amer. Meteor. Soc., CD-ROM, 10.11.

Moninger, W.R., R.D. Mamrosh, and P.M. Pauley, 2003: Automated meteorological reports from commercial aircraft. *Bull. Amer. Meteor. Soc.* **84**, 203–216.

Poulos, G.S., D.A. Wesley, M.P. Meyers, E.J. Szoke, J.S. Snook, and G. P. Byrd, 2003: Exceptional mesoscale features of the great western storm of 16–20 March 2003. *10th Conf. on Mesoscale Processes*, Portland, OR, Amer. Meteor. Soc., CD-ROM, 6.6A.

Shieh, S.-L, G.-J. Jian, and J.A. McGinley, 2003: Precipitation simulation associated with Typhoon Sinlaku (2002) in the Taiwan area using the LAPS diabatic initialization for MM5. *NOAA Technical Memorandum* , Forecast Systems Laboratory, Boulder, CO.

Smith, T.L., S.G. Benjamin, S.I. Gutman, and B.E. Schwartz, 2003: Impact of GPS-IPW data on RUC forecasts. *Seventh Symposium on the Water Cycle*, Long Beach, CA, Amer. Meteor. Soc., CD-ROM, 3.2.

Steffen, C.E., and N. Wang, 2003: Weather data compression. *19th Int. Conf. on Interactive Information Processing Systems (IIPS) for Meteorology, Oceanography, and Hydrology*, Long Beach, CA, Amer. Meteor. Soc., CD-ROM, 4.9.

Szoke, E., U.H. Grote, P.T. McCaslin, and P.A. McDonald, 2003: D3D update: Is it being used?. *19th Int. Conf. on Interactive Information Processing Systems (IIPS) for Meteorology, Oceanography, and Hydrology*, Long Beach, CA, Amer. Meteor. Soc., CD-ROM, P1.10.

Wang, N., and R. Brummer, 2003: Experiment of a wavelet-based data compression technique with precision control. *19th Int. Conf. on Interactive Information Processing Systems (IIPS) for Meteorology, Oceanography, and Hydrology*, Long Beach, CA, Amer. Meteor. Soc., CD-ROM, 4.8.

(Editor's Note: These and 2004 publications (to date) are listed in the FSL Publications Database. Go to our main Website www.fsl.noaa.gov, click on "Publications" and "Research Articles.")